EKSTERN RAPPORT

Nr. 17/2021

Fyllingsdammer – nedstrøms plastring og damtå
Rockfill dams – downstream riprap and dam toe

FoU-project 80409

NTNU

NVE Ekstern rapport nr. 17/2021
Fyllingsdammer – nedstrøms plastring og damtå
Rockfill dams – downstream riprap and dam toe : FoU-project 80409

Published by: Norwegian Water Resources and Energy Directorate

Authors: Ganesh H.R. Ravindra and Fjóla G. Sigtryggsdóttir/NTNU

Cover photo: Ganesh H.R. Ravindra

ISBN: 978-82-410-2162-6
ISSN: 2535-8235
Case number: 201914006

Abstract: The Norwegian regulations for dam safety and the guidelines on embankment dams include requirements for erosion protection of upstream and downstream slopes of embankment dams. Two recent PhD-studies at NTNU have focused on riprap design on rockfill dams (Hiller, 2017) and rockfill dam behaviour at throughflow and overtopping scenarios (Ravindra, 2020). The studies include experimental and analytical studies, and the findings are summarized in the present report. Focus has been on the erosion protection of the downstream slope and dam toe. A comparative study has also been conducted to investigate the correspondence between the NVE design guidelines and model results. The report can therefore give valuable input to the Norwegian guidelines.

Keywords: Dam safety, rockfill dams, erosion protection, riprap, dam toe

Norwegian Water Resources and Energy
Directorate Middelthuns gate 29
P.O. Box 5091 Majorstuen
N-0301 Oslo
Norway

Telephone: +47 22 95 95 95
E-mail: nve@nve.no
Internet: www.nve.no

October, 2021

FORORD

NVE har en rekke veiledere og retningslinjer som utdyper bestemmelser i forskrift om sikkerhet ved vassdragsanlegg (damsikkerhetsforskriften). Veilederne bygger på forskning og kunnskap som er utviklet over tid. I noen tilfeller er dette forskning og kunnskap som er utviklet i andre land, med sammenliknbare forhold og teknologi, men som likevel kan avvike noe fra norsk dambyggingsteknologi og norske forhold. Det er derfor stadig behov for å oppdatere og utvikle kunnskapsgrunnlaget for veilederne.

De seinere årene har det vært gjennomført to PhD prosjekter på NTNU i Trondheim som er spesielt relevante for NVEs veileder for fyllingsdammer. Prosjektene har inkludert studier på hhv nedstrøms skråning og damtå på norske fyllingsdammer. FOU-prosjekt (80409) oppsummerer resultatene fra disse prosjektene, og gir i tillegg en vurdering av hvordan resultatene fra disse to prosjektene harmonerer med designkriterier gitt i veileder for fyllingsdammer. Prosjektet bidrar dermed til økt kunnskap om sikkerheten ved norske fyllingsdammer, som vil være nyttig ved framtidig revisjon av veileder for fyllingsdammer. Prosjektet bidrar også til å oppfylle NVEs strategi for 2017-2021 innen hovedmål 1
(Bidra til en helhetlig og miljøvennlig forvaltning av vassdragene), og fokusområde F2 som sier at NVE skal arbeide for å sikre samfunnskritisk infrastruktur og forebygge skade på liv, helse og verdier som følge av brudd i energiforsyningen, dambrudd, flom og skred.

Oslo 08.10.2021

Lars Grøttå
Seksjonssjef
Damsikkerhetsseksjonen

Dokumentet sendes uten underskrift. Det er godkjent i henhold til interne rutiner.

Sammendrag

Prosjekt 80409 har hatt som mål å få mer kunnskap om designkriterier som gjelder for utforming av nedstrøms plastring og damtå på norske fyllingsdammer.

Fyllingsdammer er sårbare for ekstreme hendelser som kan føre til økt gjennomstrømning og/eller overtopping. Nedstrøms skråninger på fyllingsdammer i Norge er generelt beskyttet mot disse hendelsene med et lag plastring bestående av stein plassert i forband, dvs. at steinene låser hverandre fast, samt med en spesial utformet tåseksjon. Tåseksjonen regnes som kritisk punkt for igangsetting av progressivt dambrudd. Disse konstruksjonene, nedstrøms plastring og damtå, har derfor stor betydning for totalstabiliteten til fyllingsdammer. Dette har nylig vært undersøkt gjennom to doktorsprosjekter på Institutt for bygg- og miljøteknikk NTNU, Trondheim, samt tilknyttede masteroppgaver. Forskningen har omfattet modell- og feltforsøk, teoretiske studier og undersøkelser av eksisterende dammer for å finne ut hvor stor betydning tilstedeværelse og utforming av nedstrøms plastring og damtå har for sikkerheten av tradisjonelle norske steinfyllingsdammer.

Rapporten oppsummerer nylig funn fra disse forskningsprosjektene og et litteraturstudium. Utfra resultatene beskrives oppførsel av steinfyllingsdammer under gjennomstrømnings- eller overtoppingssituasjoner. Dette inkluderer definisjon av feilmekanismer og stabilitet av nedstrøms plastring under overtopping. Resultater fra kartlegging av nedstrøms plastring og damtå er beskrevet, også i sammenheng med eksperimentelle resultater. Videre er oppførselen av steinfyllingsdammer med forskjellig utforming av tåseksjonen studert og beskrevet basert på eksperimentelle modellstudier.

Det er gjort en omfattende sammenligning og evaluering på tvers av alle modellene som er testet i forskningsprosjektene. Dette for å forklare viktige parametere med hensyn til den totale sikkerheten av plastring, damtå og dermed fyllingsdammer som helhet. Det er også utført en sammenlignende studie for å undersøke samsvaret mellom NVE sine retningslinjer og modellresultatene.

Riprap erosion protection on downstream rockfill dam shoulder and dam toe

NVE Project nr. 80409

Ganesh H.R. Ravindra
Fjóla G. Sigtryggsdóttir

Department of Civil and Environmental Engineering
Norwegian University of Science and Technology
Trondheim

2020 (published in 2021)

Abstract

Dams are vulnerable to extreme flood events in turn leading to accidental overtopping. This in particular applies to rockfill dams comprised of pervious and erodible material. Within a Norwegian context, several large rockfill dams are poised to be upgraded in the near future as a response to enforcing of more stringent dam safety regulations and to counteract the effects of climate change on regional hydrology. Hence, obtaining better understanding of behavior of rockfill dams under extreme loading conditions is of significance from stability and economic standpoints.

The present technical report has been aimed at summarizing recent findings from experimental and analytical studies conducted at the Department of Civil and Environmental Engineering, NTNU, Trondheim. The study outcomes describe hydraulic and structural behaviors of rockfill dams under throughflow and or overtopping scenarios. Research findings outlining failure mechanisms and stability aspects of ripraps under overtopping scenarios. Results from field surveys conducted to investigate construction aspects of placed ripraps constructed on rockfill dams are described. Further, experimental results demonstrating the hydraulic response of rockfill dam structures exposed to overtopping conditions are provided. Furthermore, behavior of rockfill dam structures coupled with disparate toe configurations subjected to throughflows are described based on experimental model studies.

The technical report also brings out the significance of key parameters influencing the overall stability of ripraps and rockfill dams. This is achieved through a comprehensive comparative evaluation of riprap stability across all the models tested as part of the research program. A comparative study has also been conducted to investigate the correspondence between the NVE design guidelines and model results.

Furthermore, the present report also outlines planned research activities to be conducted NTNU, Trondheim. The overarching focus of the research will be to obtain holistic evaluation of rockfill dam behavior when subjected to extreme loading conditions. This in turn is intended at improving the state of the art in design and construction of these structures.

Contents

List of papers published as part of the research projects at NTNU

A. 2018-2020

1. **Buckling analogy for 2D deformation of placed ripraps exposed to overtopping.**
   Ravindra, G.H.R., Sigtryggsdottir, F.G and Lia, L (2020).
   Journal of Hydraulic Research,
   DOI: https://doi.org/10.1080/00221686.2020.1744745.
2. **Toe support conditions for placed ripraps on rockfill dams- A field survey.**
   Ravindra, G.H.R., Sigtryggsdottir, F.G., Asbølmo, M.F and Lia, L (2019).
   Vann 2019 (3), pp. 185- 199.
   Retrieval link: https://vannforeningen.no/dokumentarkiv/toe-support-conditions-for-placed-ripraps-on-rockfill-dams-a-field-survey/
3. **Failure mechanism in placed riprap on steep slope with unsupported toe.**
   Ravindra, G.H.R., Gronz, O., Dost, B and Sigtryggsdottir, F.G.
   Engineering Structures 2020, Volume 221.
   DOI: https://doi.org/10.1016/j.engstruct.2020.111038
4. **Non-linear flow through rockfill embankments.**
   Ravindra, G.H.R., Sigtryggsdottir, F.G and Høydal, ØA (2019).
   Journal of Applied Water Engineering and Research, 7:4, 247-262.
   DOI: https://doi.org/10.1080/23249676.2019.1683085
5. **Effects of toe configurations on throughflow hydraulic properties of rockfill embankments.**
   Kiplesund, GH., Ravindra, G.H.R., Rokstad, M.M and Sigtryggsdottir, F.G (2021)**.**
   Journal of Applied Water Engineering and Research.
   DOI: https://doi.org/10.1080/23249676.2021.1884615
6. **Evaluation of design criteria for downstream riprap of rockfill dams.**
   Ravindra, G.H.R., Sigtryggsdottir, F.G., Lia, L (2018), Q. 101- R.71, pp. 1195- 1209, Twenty- sixth International Congress on Large Dams, 4th- 6th July, Vienna, Austria, Published by CRC Press, Taylor and Francis Group.
7. **Protection of embankment dam toe and abutments under overtopping conditions.**
   Ravindra, G.H.R., Sigtryggsdottir, F.G., Lia, L (2018), 3rd International Conference on Protection against Overtopping, 6- 8 June, Grange over Sands, UK.

8. **Stability and failure mechanisms of riprap on steep slopes exposed to overtopping**. Hiller, P.H., Ravindra, G.H.R (2020), In: Zhang JM., Zhang L., Wang R. (eds) Dam breach modelling and risk disposal. ICED 2020, Springer series in Geomechanics and Geoengineering. Springer, Cham.

B. 2014-2018

1. **Accumulating stone displacements as failure origin in placed riprap on steep slopes.**
   Priska H. Hiller, Jochen Aberle, *Journal of Hydraulic Research*, 2018, DOI: http://dx.doi.org/ 10.1080/ 00221686.2017.1323806
2. **Field and model tests of riprap on steep slopes exposed to overtopping.** Priska H. Hiller, Leif Lia, Jochen Aberle, *Journal of Applied Water Engineering and Research, 2018*. DOI: https://doi.org/10.1080/23249676.2018.1449675
3. **Smartstones: A small 9-axis sensor implanted in stones to track their movements.** Oliver Gronz, Priska H. Hiller, Stefan Wirtz, Kerstin Becker, Thomas Iserloh, Manuel Seeger, Christine Brings, Jochen Aberle, Markus C. Casper, Johannes B. Ries (2016) *CATENA*: 142, 245-251, Doi: http:// dx.doi.org/ 10.1016/ j.catena.2016.03. 030.
4. **Placed riprap as erosion protection on the downstream slope of rockfill dams exposed to overtopping.**
   Priska H. Hiller, Leif Lia, *25th Congress on Large Dams Stavanger*, Norway, 2015.
5. **Dam Svartevatn - An example of challenging upgrading of a large rockfill dam.** Priska H. Hiller, Leif Lia, Per Magnus Johansen, Rolv Guddal, *ICOLD Annual Meeting and Symposium* Bali, Indonesia, 2014.
6. **Riprap design on the downstream slope of rockfill dams.**
   Priska H. Hiller, Leif Lia, Jochen Aberle, Stefan Wirtz, Markus C. Casper
   Mitteilungen - Leichtweiss-Institut für Wasserbau der Technischen Universität Braunschweig Vol. 161, 39-44, 2014.
7. **Large-scale overtopping tests - Practical challenges and experience**.
   Priska H. Hiller, Leif Lia, *1st International Seminar on Dam Protections against Overtopping and Accidental Leakage*, Madrid, Spain, 2014.
8. **Practical challenges and experience from large-scale overtopping tests with placed riprap.**

Priska H. Hiller, Leif Lia (2015), In M. Á. Toledo, R. Morán, E. Oñate (Eds.*), Dam Protections against Overtopping and Accidental Leakage*, 151-157. London: CRC Press/ Balkema.

9. **Field tests of placed riprap as erosion protection against overtopping and leakage**. Priska H. Hiller, Fredrikke Kjosavik, Leif Lia, Jochen Aberle, *United States Society on Dams - Annual Meeting and Conference Denver* CO, USA, 2016.
10. **Kartlegging av plastring på nedstrøms skråning av fyllingsdammer**. Survey of placed riprap on the downstream slopes of rockfill dams, Priska H. Hiller NTNU Report B1-2016-1, ISBN-10: 978-827598-095-1 Trondheim, Norway, 2016.

PhD thesis that are a part of the research projects at NTNU

Priska H. Hiller (2017). Riprap design on the downstream slopes of rockfill dams,. *Doctoral Thesis, Norwegian University of Science and Technology, Trondheim*.

Ganesh H.R. Ravindra (2020). Hydraulic and structural evaluation of rockfill dam behavior when exposed to throughflow and overtopping scenarios. *Doctoral Thesis, Norwegian University of Science and Technology, Trondheim*.

List of master thesis projects carried out as part of research projects at NTNU

A. 2017- 2020.

Guri Holte Veslegard (2017): *Plastring av fyllingsdammer - Modellforsøk, praktiske forhold og avvik fra regelverk,* (Master project).

Kofi Ntow Opare (2018) *Load measurements at riprap toe* (Master thesis).

Malin Fossum Asbølmo (2019) *Kartlegging av nedstrøms damtå på valgte fyllingsdammer/Field survey of downstream dam toes on selected rockfill dams* (Master project).

Malin Fossum Asbølmo (2019) *Utforming av damtå og betydning for plastring av fyllingsdammer - Kartlegging og modellforsøk/ Significance of toe support conditions on placed riprap stability- Field survey and model studies* (Master thesis).

Nils Solheim Smith (2020) *Physical and numerical modelling of extreme flow through rockfill dams* (Master thesis).

Styrmir Sigurjonsson (2020) *Breaching of rockfill dams* (Master thesis).

Unnar Númi Almarsson (60 ETCS MSc thesis to be completed 2021**)** *Fuse plugs in embankment dams*.

B. 2014-2016.

Ellen Bogfjellmo (2013): *Nedstrøms skråning av steinfyllingsdammer - Analyse av eksisterende plastringer. Development of a method to survey placed riprap on rockfill dams,* (Semester project).

Hans Edward Røer (2014): *Nedstrøms skråning av steinfyllingsdammer - Modellforsøk av plastring under ulike strømningsforhold. Scaled model tests of placed riprap exposed overtopping, through flow and a combination,* (Master thesis).

Ragnhild Sørlie Meaas (2014): *Plastring av elvebunn med sterk strøm. Scaled model tests of placed riprap exposed to supercritical flow,* (Master thesis).

Johannes Kobel (2014): *Smartstones. Testing out the Smartstone sensors and evaluate its application properties,* (Semester project).

Jens Jakobsen (2015): *Plastring av fyllingsdammer - Forskyving i plastring og anvendelse av Smartstone sensorer. Evaluating displacements in placed riprap and test the application of the Smartstone sensors,* (Master thesis).

Eirik Helgetun Pettersen (2015): *Plastring av fyllingsdammer - Effekt av forband på styrken av plastringen. The effect of interlocking placement on the stability of placed riprap,* (Master thesis).

Wiebke Marie Zander (2015): *Untersuchungen zur Genauigkeit von Smartstones - ein auf RFID-Technologie basierendes Tracersystem. Evaluating the accuracy of the Smartstone - a tracer system based on RFID technology,* (Bachelor thesis).

Fredrikke Kjosavik (2015): *Plastring av fyllingsdammer - Forskyvingar i damkrona. Analysis of displacements on the dam crest with large-scale field tests and scaled model tests,* (Master thesis).

Guri Holte Veslegard (2016): *Plastring av fyllingsdammer - Forskyving i plastring. Analysis of displacements within placed riprap,* (Semester project).

List of figures

List of tables

1 Introduction

Embankment dams, constructed with locally excavated earth or rockfill represent 78% of the total number of existing dams worldwide (ICOLD, 2019). Embankment dams comprising of coarse-grained fractional material for over 50% of the dam volume are further classified as rockfill dams, representing 13% of the worldwide dam population (ICOLD, 2019). A constant trend in society comprises an increase in the safety requirements for all critical infrastructure (Toledo & Morera, 2015). During the last decades, there has been a significant increment of the social demand on dam safety standards, especially in the most developed countries. This has led to new and more demanding dam safety regulations and guidelines (Moran, 2015). This trend is also valid as applied to the Norwegian dam infrastructure. The retroactive enforcement of new and more stringent dam safety regulations (OED, 2009) has necessitated rehabilitation of multitudes of large Norwegian rockfill dams.

Dam safety assessment is a complex task as it is influenced by multitudes of internal and external factors (Sigtryggsdóttir et al., 2016). It is essential to determine the most common causes of dam failure incidents over the decades to identify probable factors which contribute to dam instability. ICOLD statistics (ICOLD, 1995) state overtopping as the main cause of embankment dam failure appearing as the primary factor in 31% of the total number of failures, and is further involved in another 18% of failures as a secondary agent. Hence, equipping rockfill dams with defense mechanisms to safeguard the dam structure against unanticipated overtopping or leakage events is of paramount importance from a dam safety perspective.

Under overtopping conditions, the downstream slope of a rockfill dam is subjected to highly destabilizing dynamic forces generated due to turbulent throughflow (overtopping of dam core) and or overflow (overtopping of dam crest). Considering throughflow conditions, turbulent flow with high seepage velocities within the embankment structure can result in internal erosion and also destabilize the downstream embankment due to pore pressure build up (Figure 1). Further, under overflow conditions, the downstream slope is inundated with highly turbulent surface flow resulting in preogressive external erosion leading to dam breach.

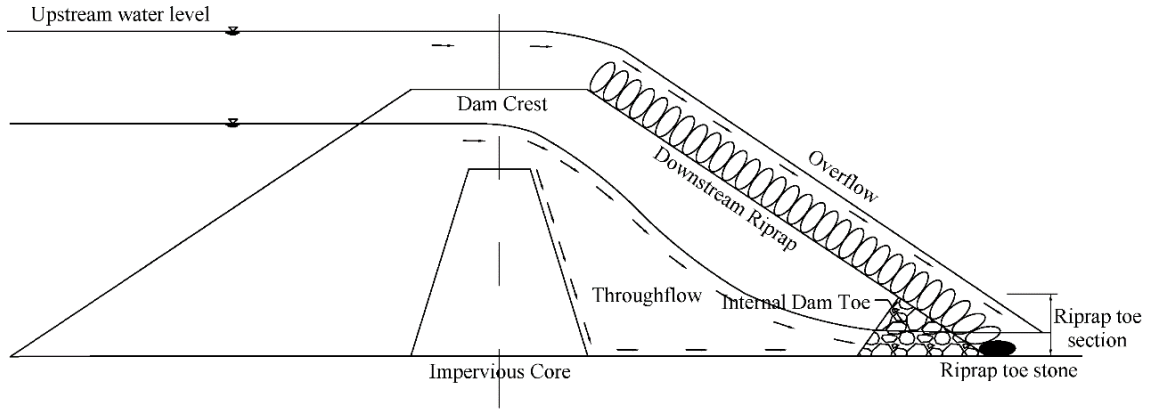

Figure 1. Description of throughflow and overflow scenarios in rockfill dams (Adopted from Ravindra et al. (2019a)).

Ripraps and rockfill dam toes are extensively employed in embankment dam engineering as key components of the overtopping protection system. The Rockfill dam toe comprising of coarser material as compared with the shoulder material is constructed in tandem with the downstream rockfill dam shoulder either as an internal or an external structure. This structure facilitates efficient expulsion of seepage and accidental leakage flows from within the dam structures. This helps in preventing buildup of excess pore pressures leading to slope instability and also assists in minimizing internal erosion due to particle dragging. Hence, the rockfill dam toe is constructed to assure enhanced stability of the downstream shoulder under extremely high through-flow conditions (Moran et al., 2019).

Ripraps are one of the most widely used erosion protection measures for various in-stream hydraulic structures such as embankment dams, spillways, streambeds, river banks, bridge piers and abutments (e.g. Hiller et al., 2019; Thornton et al., 2014; Abt et al., 2013; Khan & Ahmad, 2011; Siebel, 2007). Ripraps are also used in coastal protection structures such as dikes, embankments and jetties against wave action (Kobayashi & Jacobs, 1985). As applied to rockfill dam engineering, ripraps are constructed on the upstream embankment to protect against erosion resulting because of wave impacts and ice induced forces. Further, ripraps constructed on the downstream slope to protect against erosion due to accidental leakage or overtopping events (Figure 2).

Figure 2. Placed riprap constructed on the downstream slope of dam Oddatjørn, which is a 142 m high rockfill dam constructed in Suldal, Norway (Photo: GHR Ravindra, NTNU).

Obtaining a better understanding of stability aspects of these rockfill dam components under extreme loading conditions is vital for the rockfill dam construction industry. From dam safety and economical standpoints, accumulating technical knowledge on the hydraulic and structural behavior of these structures can lead to safe and economical design, construction and rehabilitation of rockfill dams.

1.1 Research at NTNU and present report for NVE

Recent experimental and analytical studies conducted at the Department of Civil and Environmental Engineering at NTNU, Trondheim have been directed towards investigating failure mechanisms in rockfill dam models subjected to throughflow and or overtopping conditions. The present technical report aims at presenting a brief summary of key findings from these investigations. Furthermore, research activities to be conducted as part of potential future research project are also outlined.

The present report is prepared in compliance with a contract between NVE and NTNU on project nr. 80409 in NVE registry, with the Norwegian title “Plastring av nedstrøms damskråning og damtå” or “Riprap erosion protection on downstream rockfill dam shoulder and dam toe”. The report reviews the literature on the topic and summarize two research projects at NTNU conducted within the project PlaF and WP1.2 HydroCen. The associated master theses and PhD theses are listed on page 4 to 8, along with journal publications and conference articles. The PhD thesis within these research projects are those of Priska H. Hiller

in PlaF and Ganesh H.R. Ravindra in WP1.2 HydroCen (A1.2.1). Professor Leif Lia was Priska H. Hillers supervisor, and Professor Jochen Aberle was her co-supervisor. Fjóla G. Sigtryggsdóttir was Ganesh H.R. Ravindra's main supervisor and Prof. Leif Lia his co-supervisor. Fjóla G. Sigtryggsdóttir is the project manager for project WP1.2 Hydrocen.

The project WP1.2 HydroCen (A1.2.1) is referred to as the HydroCen study in the following.

2 Objectives and scope

The overarching theme of the research presented in this technical report is to contribute to the field of rockfill dam engineering through generation of new knowledge aimed at improving dam safety. The investigations are in particular, focused on achieving better understanding of hydraulic and structural response of rockfill dams or dam components under extreme loading circumstances. The research efforts under this theme are directed at conduction of experimental studies aimed at achieving the following research objectives:

***Objective 1*:** Analyzing failure mechanisms and key factors affecting stability of ripraps constructed on the downstream slopes of rockfill dams under overtopping conditions.

Objective 2: Evaluating the hydraulic response of rockfill dams exposed to throughflow scenarios and studying the effects of rockfill toes on throughflow hydraulic properties of rockfill dams.

The study scope is limited to investigating hydraulic and structural behavior of rockfill dam components coupled with the downstream slopes of rockfill dams under throughflow or overflow scenarios.

3 State of the art

A detailed literature review of the state of the art in a research discipline enables formulation of pertinent research questions by providing valuable insights into the historical development of research methodologies and experimental tools and techniques which have been previously adopted by past research works. The following discussions are aimed at summarizing the state of the art on stability of placed ripraps and on the hydraulic response of rockfill dams under overtopping conditions.

3.1 Placed riprap stability under overtopping conditions

Riprap is defined as an erosion resistant surface cover of large elements such as natural rocks or artificial elements to secure subjacent layers against the impact of hydrodynamic forces due to currents and waves and due to ice induced forces. Riprap on the upstream dam slope is exposed to wave action or currents either perpendicular or parallel to the slope. On the downstream slope, the primary function of riprap is to provide erosion resistance under throughflow and/or overflow conditions. Ripraps can be broadly classified into two categories based on the method of construction; Dumped ripraps comprise of randomly placed stones while placed ripraps are characterized by stones arranged in a specific interlocking pattern. Although dumped ripraps could be considered as a more viable alternative from an economic standpoint, placed ripraps with toe supports have been found to offer higher degree of stability against overtopping in comparison with dumped ripraps (Hiller et al., 2018). This is attributed to the formation of a bearing structure due to interlocking of stones, which results in increased stability compared to randomly dumped stones.

The stone density (ρ_s), stone size (d), grain size distribution and the embankment slope (S) parameterize the surface layer of dumped ripraps as these parameters in general govern the hydraulic behavior of dumped ripraps. For placed ripraps, an additional parameter needs to be evaluated to discern the overall stability of the riprap structure. The packing factor (P_c) is a generally employed parameters to evaluate the quality of placement of placed ripraps. It should be noted that these parameters are not the commonly used indicators of stability from a structural or geotechnical standpoint. However, these are considered as bridge parameters for correlating the hydraulic and structural stability of ripraps.

The packing factor P_c is adopted to obtain a quantitative measure of density of riprap stone placement as this can have an impact on overall riprap stability. The term packing factor was defined as Equation (1) by Olivier (1967).

$$P_c = \frac{1}{N.{d_{50}}^2} \tag{1}$$

where N represents the number of stones per m^2 surface area of the riprap and d_{50} signifies the median stone size. The median stone size is computed as $d_{50} = (abc)^{1/3}$ averaged over a sample set, where a, b and c represent the longest, intermediate and shortest stone axis respectively. P_c is lower for a densely placed riprap compared to a loosely packed riprap (Hiller et al., 2018).

The research discipline of dumped riprap design under overtopping conditions has advanced since its inception with the classic study of Isbash (1936). Since this early effort to determine the size and thickness of a resistant stone layer, more than 21 stone-sizing relationships for overtopping have been developed (Abt & Thornton, 2014) with major contributions from Chang (1998), Frizell et al. (1998), Abt et al. (1991), Olivier (1967) and others. These studies have been dedicated towards investigating stability of dumped ripraps on moderately steep slopes complying with international construction practice.

Available literature describing the stability aspects of placed ripraps under overtopping conditions is rather limited as compared with the extensive research database available with respect to design and construction of dumped ripraps. Notable contributors to the research area of placed riprap design are Peirson et al. (2008), Dornack (2001), Sommer (1997) and Larsen et al. (1986). These past experimental model studies have been aimed at comprehending the underlying 1D failure mechanism in placed ripraps with fixed toe supports exposed to overtopping flows on mild to steep slopes (S = 0.125 to 0.67 with S being the ratio of the vertical to the horizontal slope dimensions). Some of these investigations have also made attempts at juxtaposing stability aspects of placed and dumped ripraps to better understand the fundamental differences in behavior of these structures under overtopping conditions. Within this doctoral study, primary emphasis is laid on better understanding stability of placed ripraps constructed on steep slopes subjected to overtopping flows.

The experimental study conducted by Larsen et al. (1986) was primarily aimed at comprehending the 1D underlying failure mechanisms of placed ripraps exposed to overtopping flows on mild to moderately steep slopes (S = 0.125 to 0.40; S is the ratio of the

vertical to the horizontal slope dimensions). Larsen et al. (1986) found that the successive overtopping of the riprap with increasing discharges resulted in a compaction of the downstream part of the placed riprap (Hiller et al., 2018). A new technique for quantification of the compaction process along the chute length was introduced by Larsen et al. (1986) wherein relative stone displacements were monitored as a function of overtopping magnitude. Relative displacements ($\Delta x\ L_i^{-1}$) of select riprap stones were computed as the ratio of stone displacements along the flow direction (Δx) and the distance between the select stone and the downstream fixed toe structure (L_i). A similar study was later carried out by Sommer (1997) on placed riprap models constructed on slopes S = 0.25 to 0.50. Based on experimental test results, a three step design methodology for placed ripraps was developed by Sommer (1997) taking into account stone displacements. Further, the recent study conducted by Hiller et al. (2018) adopted the technique of relative stone displacement monitoring to analyse the 1D failure mechanism in placed ripraps with fixed toe supports constructed on steep slopes of S = 0.67. Hiller et al. (2018) (Figure 3 left) concluded that unidirectional stone displacements along the chute direction leading to formation of a gap at the upstream section of the riprap was the underlying 1D failure mechanism in placed riprap supported at the toe. Further, to evaluate laboratory and scaling effects and for further validation of the physical modeling test results, overtopping tests on placed and dumped ripraps at prototype scale were conducted by (Hiller et al., 2019) (Figure 3 right).

Figure 3. (Left) Sideview of the model setup in the laboratory with placed riprap (Photo: NTNU). (Right) Test with full-scale riprap stones in 2015 (in the Stavanger ICOLD Congress Technical tour).

Also, several past experimental studies have documented considerable stability gain for placed ripraps as compared with dumped ripraps. This was quantified to approximately 30% in Peirson

et al. (2008) and 80% in Larsen et al. (1986). Hiller et al. (2018) state that placing riprap stones in an interlocking pattern resulted in on an average five times higher stability as characterized by critical overtopping flow magnitude as compared to randomly dumped riprap. This effect has generally been attributed to generation of interlocking forces within the placed riprap structure which offers higher resistance against flow forces, especially at steep slopes.

As an illustration of large-scale application of placed ripraps on rockfill dams, the case of Norwegian rockfill dams can be considered. The Norwegian Water Resources and Energy Directorate (NVE) is responsible for the development of guidelines for construction and monitoring of Norwegian rockfill dams. In order to safeguard dams against accidental overtopping events, dam safety regulations in Norway prescribe construction of single-layered placed ripraps on the downstream slopes of rockfill dams. The individual riprap stones are to be placed in an interlocking pattern with their longest axis inclined towards the dam (OED, 2009; NVE, 2012). The dams are generally classified into four different consequence classes (class 1 through 4). The criteria for the classes reflect the consequences that a possible failure may have for people, the environment and property with Class 4 designating dams with a very high potential for damage in case of dam failure, Class 3 indicating dams with high damage potential and Class 2 signifying dams with medium damage potential (Midttømme et al., 2012).

As per the recommendations of NVE dam safety guidelines of 2012 (NVE, 2012), placed ripraps need to be constructed on rockfill dam slopes with stones of volume of minimum 0.15 m^3 for dams classified within consequence class 4. To determine the stone size for dams in class 3 and 2, Equation (2) can be used assuming a minimum unit discharge 'q_f' of 0.5 m^3/s for Class 3 and 0.3 m^3/s for Class 2.

$$D_{min} = 1.0 \; S^{0.43} \; q_f^{\;0.78} \tag{2}$$

The proposed design criteria by the NVE is based on large scale field tests and physical modelling investigations carried out by EBL Kompetanse AS (EBL Kompetanse, 2006). Investigations into breach formation mechanisms of rockfill dams subjected to throughflow and overflow conditions were carried out through construction of large-scale rockfill dam structures in an open channel at Rossvatn, Norway and also by conducting overtopping tests on model rockfill structures in a flume (Kjellesvig, 2002 and Sand, 2002). The accumulated data from the tests were employed to arrive at a best-fit design criterion for the design of ripraps of rockfill dams presented as Equation (3).

$$D_{min}=0.43\ S^{0.43}\ q_f^{\ 0.78} \tag{3}$$

The large scale rockfill dams were constructed of coarse rockfill, however, without riprap. The coarse rockfill can at best be considered comparable to dumped ripraps. Application of Equation (2) for the design of placed ripraps was based on the assumption that for a particular size of riprap stones, the stability of placed ripraps would be higher compared to dumped ripraps. Although Equation (2) includes a slope parameter '*S*', it was originally developed with data sets obtained from experimental investigation conducted on large scale rockfill dams with downstream embankment slope of S = 0.67 in accordance with Norwegian construction practice. Furthermore, a safety factor of 2.3 is incorporated within Equation (2) over the best-fit Equation (3) proposed by EBL Kompetanse (2006) (Ravindra et al., 2018a).

A literature review into the international state of the art in placed riprap design and construction reveals that description of 2D failure mechanism in placed ripraps under overtopping scenarios is currently not available. Furthermore, all these past studies investigating stability aspects of placed riprap under overtopping conditions have been carried out with ripraps constrained at the toe section with fixed toe support structures. This entails enhanced resistance against sliding at the riprap toe section. However, several past studies investigating rockfill dam stability aspects under overtopping conditions such as Moran et al. (2019), Javadi and Mahdi (2014) and Moran and Toledo (2011) have demonstrated toe section of rockfill dams as a critical location for initiation of progressive dam failure. Also considering the guidelines offered by the NVE for placed riprap design and construction, protocols addressing specifics on the design aspects of toe support for the riprap structures are currently unavailable.

Thus, this discussion helps in identification of important parameters which could potentially be of significance for placed riprap stability. Since all past experimental research has focused on analyzing 1D failure mechanism in placed ripraps, extension of the findings to 2D could lead to findings which can lead to more effective design of these structures. Further, A large-scale field study documenting existing state of riprap toe construction on rockfill dams is currently unavailable. Furthermore, carrying out experimental overtopping investigations on model placed ripraps with realistic toe support conditions is of significance to obtain representative findings concerning the stability aspects of placed ripraps exposed to overtopping flows. This would also facilitate evaluation of the validity of findings from past research works describing stability of placed ripraps under overtopping conditions.

3.2 Flow through rockfill medium

Under overtopping scenarios, highly turbulent flow through the downstream embankment structure of rockfill dams can result in internal erosion and also destabilize the downstream slope due to dynamic pore pressure generation. Several instances of embankment dam failures resulting as a consequence of flow through the embankment structure are documented in international literature (e.g. Leps, 1975; Cruz et al., 2010 and Foster et al., 2000). Comprehending turbulent throughflow hydraulic properties of rockfill dams facilitates effective safety assessment (e.g. Moran and Toledo., 2011 and Siddiqua et al., 2011; Ferdos and Dargahi., 2016a and Ferdos and Dargahi., 2016b). Furthermore, it is also of relevance for development of numerical models predicting rockfill dam breach process as this can assist in effective design of components of rockfill dam overtopping protection system such as the dam toe resulting in reduced risk of dam failure.

Flow through porous media is generally characterized as either Darcy or non-Darcy type based on confirmation of flow properties with the linear Darcy flow theory (Equation 4) widely implemented in soil mechanics. Deviations from the linear trend requires the flow to be classified as non-Darcian type.

$$V = K\ i \tag{4}$$

where, V = Bulk flow velocity, K = Coefficient of permeability and i = hydraulic gradient.

Darcian or linear flow through rockfill is seldom encountered in practical applications (Leps, 1975). Wilkins (1955) states that applicability of the linear Darcy flow theory is limited to flow through small grains of the order of 0.5 mm. Flow in rockfill structures depart from the linear flow regime because of the highly porous characteristic of rockfill material resulting in large interconnected void spaces leading to high velocity flows (Siddiqua et al. 2011). Hence, it can be concluded that Darcy's law does not adequately describe throughflow hydraulics in coarse-grained porous media especially at high velocities (e.g. Hansen et al. (1995), Venkataraman and Rama Mohan Rao (1998), Siddiqua et al. (2011) and Ferdos and Dargahi (2016a)).

Pertaining to throughflow hydraulic characteristics of rockfill dams, flow through the core as well as through the sand filter can be considered to be laminar confirming with the linear Darcy flow theory owing to considerably low permeability. However, these low velocity and low magnitude flows do not generally pose considerable threat to the integrity of the rockfill embankment as long as internal erosion is not an issue. But, flow through the transition zone

and the supporting fill is more problematic as the state of flow is highly turbulent as a consequence of large permeability resulting in generation of highly destabilizing forces with high internal erosion potential (e.g. Solvik, 1991 and Cruz et al., 2010). Hence, it is of importance to better understand turbulent throughflow hydraulics in rockfill embankments as this can facilitate effective design of rockfill slopes and components of rockfill dam overtopping protection system such as the dam toe.

Description of non-Darcian or turbulent flow through porous media is generally represented as a power-law function (Equation 5), as demonstrated by past investigations such as Izbash (1931), Escande (1953), Wilkins (1955), Scheidegger (1963), Parkins (1966) and Siddiqua et al. (2011).

$$V = a\ i^b \tag{5}$$

where, a and b are empirical coefficients to be determined experimentally. Coefficient a depends on the properties of fluid and porous media such as porosity, particle shape, particle size, roughness, tortuosity of void structure and viscosity of fluid. Parameter b *is* dependent upon the state of flow or the level of flow turbulence (Siddiqua et al. 2011).

Much literature is available in the study discipline of non-linear flow through rockfill as several past studies have investigated non-Darcian throughflow aspects of rockfill medium adopting theoretical approaches and also through experimental throughflow tests conducting in varying sizes of permeameters. In depth reviews of the available literature within this research discipline are available in studies such as Leps (1975), Venkataraman and Rama Mohan Rao (1998), Sidiropoulou (2007), Cruz et al. (2010) and Salahi et al. (2015). These past research works have resulted in accumulation of various empirical equations describing the non-linear relationship between velocity and gradient of flow through rockfill. Some of the well-established empirical criteria describing non-linear flow through rockfill such as Wilkins (1955) and Engelund (1953) are presented in Table 1.

Table 1. Description of well-known empirical relationships describing non-linear flow through porous media.

Research work	Empirical relationship	Remarks
Engelund (1953)(Escande, 1953)(Escande, 1953)(Escande, 1953)(Escande, 1953)	$i = \frac{V^2}{k_t}$ (6) $k_t = \frac{n^3 g d_i}{\beta_o (1-n)}$ (7)	k_t = turbulent permeability β_o = particle shape coefficient (3.6 for blasted or crushed rock) d_i = characteristic dimension or the representative particle size of the porous medium* n = porosity of the medium
Wilkins (1955)	$V = W\, n\, m^{0.50}\, i^{0.54}$ (8)	n = porosity of the medium m = hydraulic mean radius defined as the ratio of the void ratio (e) to the specific surface area of the stones (S_o) W = material dependent coefficient with a value of 5.243 for crushed rocks**

* A relationship for d_i is presented in publications such as Solvik (1991) and Cruz et al. (2010) as $d_i = 1.7\, d_{10}$. However, some recent studies such as EBL Kompetanse (2006) and Siddiqua et al. (2011) argue on behalf of a different relationship $d_i = 1.22\, d_{20}$.

**Wilkins (1963) based on additional experimental data proposed a revised version of Equation 2.8 with $W = 6.693$.

Wilkins (1955) noted measurement of the surface area of irregular stones (S_o) as a difficult problem. To address this concern, Leps (1975) carried out an investigation to obtain a general empirical relationship to relate parameter m with the median stone size (d_{50}) of the rockfill material. Leps (1975) tabulated the values of parameter m for rock particles of median diameter ranging over a broad interval of d_{50} = 19 mm to 1220 mm which in turn translates to equation 9 (Cruz et al., 2010).

$$m = \frac{d_{50}}{8} \quad (9)$$

Further, several studies have conducted experimental testing programs in permeameters for further validation of performance of the Engelund (1953) approach (Equations 6 and 7) and the Wilkins (1955, 1963) approach (Equation 8). Parkins (1963, 1966) performed tests on d_{50} = 10 mm to 20 mm homogenous angular gravel and concluded that the performance of the Wilkins (1955) approach was satisfactory in predicting the experimental results. Further, a recent study conducted by Siddiqua et al. (2011) on rockfill material with median particle size ranging over d_{50} = 10 mm to 150 mm in a large scale permeameter (D = 0.76 m and L = 2.7 m) further corroborated the performance of the Wilkins (1955, 1963) and the Engelund (1953) approaches in describing non-linear flow through coarse rockfill. The ability of the Engelund (1953) and the Wilkins (1955, 1963) approaches in describing the non-linear throughflow characteristics of rockfill embankments is further evaluated in this article as these are widely implemented in practical applications concerning throughflow hydraulics of rockfill material.

Furthermore, most past studies have not assessed throughflow hydraulic properties in sufficiently coarse rockfill material of sizes commonly employed in dam construction especially at extremely high turbulence levels. To address this concern, recent studies conducted by Ferdos et al. (2015), Ferdos and Dargahi (2016a) and Ferdos and Dargahi (2016b) have focused on investigating flow through properties in large rockfill with d_{50} = 100 mm to 240 mm at high turbulence levels. Large-scale field studies (in injection wells) and permeameter studies in laboratory settings were undertaken in this regard, aimed at calibration and validation of numerical simulation tools.

Although these different permeameter studies have provided valuable insight into throughflow hydraulics in rockfill material, research into quantitative physical validation of these relationships in actual rockfill dams is currently unavailable in international literature. This is considering the fact that any findings originating from theoretical studies or from experimental investigations conducted in permeameters inevitably require validation within actual rockfill dam models at laboratory and large scales to enhance confidence in the findings for practical implementation. This has been a missing link in the process of development of a sophisticated numerical model simulating rockfill dam breach (Figure 4).

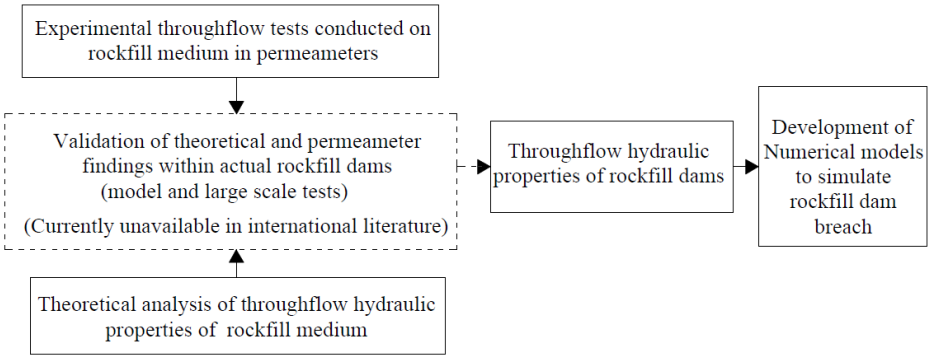

Figure 4. Illustration of processes involved in the development of a numerical rockfill dam breach model and the missing link currently unavailable in international literature (Adopted from Ravindra et al. (2019b)).

Due to the resource intensive nature of experimental testing on rockfill dam models, especially at large scales, research in this area has seldom been conducted in the past. Hence, a comprehensive experimental investigation aimed at providing a realistic description of non-linear flow through homogenous rockfill embankments is required. This would also address scaling concerns with regards to flow through rockfill dams and also facilitate further development of numerical dam breach models.

3.3 Flow through rockfill embankments

Under extreme throughflow or overtopping scenarios, rockfill dam failure could result as a consequence of primarily three failure modes, (a) internal erosion, (b) surface erosion and (c) mass slope instability (Moran, 2015). Under throughflow scenarios, highly turbulent flow entering the downstream embankment structure may develop high seepage velocities leading to transport of fine material downstream leading to internal erosion (e.g. Ravindra et al., 2018 and Moran, 2015). Further, overtopping of the dam crest leading to skimming flow on the downstream slope could lead to progressive surface erosion (e.g. Hiller et al., 2018 and Abt et al., 1991). Furthermore, internal buildup of dynamic pore pressures under such extreme scenarios could lead to significant reduction in the geotechnical stability of the dam and in turn lead to mass slope instability and sliding (Moran, 2015 and Moran and Toledo, 2011).

A prerequisite for effective design of safe rockfill dam structures is having a good understanding of behavior of rockfill dams exposed to throughflow and overflow scenarios. Ability to predict and model flow through rockfill dams can facilitate effective design and dam safety assessment. Numerous past theoretical, numerical and experimental studies have made

attempts at quantitatively describing flow through and stability aspects of rockfill dams exposed to extreme scenarios.

Studies such as Javadi and Mahdi (2014), Siddiqua et al. (2013), Garga et al. (1995), Hansen et al. (1995) have conducted experimental investigations on model rockfill dams subjected to throughflow and overflow conditions. The underlying study objective has been to quantitatively describe and in turn predict initiation and progression of failure in rockfill dams from hydraulic and geotechnical standpoints. Further, several past numerical and theoretical investigations such as Larese et al. (2015), Hansen and Roshanfekr (2012), Hansen et al. (2005), Worman (1993), Townsend et al. (1991) and so on have made attempts at development and validation of empirical methodologies and numerical tools for modelling behavior of rockfill embankments subjected to extreme throughflow and or overtopping conditions.

Furthermore, numerous past studies such as Moran et al. (2019), Javadi and Mahdi (2014), Siddiqua et al. (2013), Cruz et al. (2010), Marulanda and Pinto (2000) and Leps (1973) have stated that the toe section of rockfill dams could be a critical location for failure initiation under throughflow scenarios. Rockfill dam toes are commonly coupled with the downstream rockfill dam structure to counter the destabilizing effects of seepage flows entering the downstream dam structure and to stabilize the toe section under extreme situations. Although numerous past studies have investigated rockfill dam behavior when exposed to throughflow and overtopping scenarios, experimental model studies investigating performance of rockfill dams coupled with toe structures are scarce. In this regard, recent studies such as Moran et al. (2019) and Moran and Toledo (2011) have conducted experimental studies on rockfill dam models with external rockfill toes. This was to document the hydraulic and geotechnical effects of an external toe on the performance of rockfill dams under extreme situations. This research also led to the development and further validation of a design methodology for external toes for rockfill dams.

Apart from the HydroCen study looking at the efficacy of external toes, experimental studies focusing on investigating the behavior of rockfill dams constructed with disparate toe configurations is currently unavailable in international literature. From a dam safety standpoint, it is of significance to comprehend the effects of various toe configurations on throughflow properties and in turn, stability aspects of rockfill dams under extreme loading scenarios. Arriving at new knowledge in this regard can facilitate effective design and construction of these structures. This could also enable development and validation of numerical design tools and dam breach models which can further streamline the rockfill dam design process.

4 Research Methods

The overarching objective of the research has been the holistic evaluation of behavior of downstream section of rockfill dams exposed to accidental leakage and or overtopping events. To achieve the study objective, several laboratory experimental testing programs and large-scale field studies have been conducted (Figure 5). Each of these model studies build on knowledge and insights generated during the preceding investigations. The investigation aims presented under were oriented towards addressing fill several knowledge gaps in international literature and fall within the preview of the two principal research objectives presented.

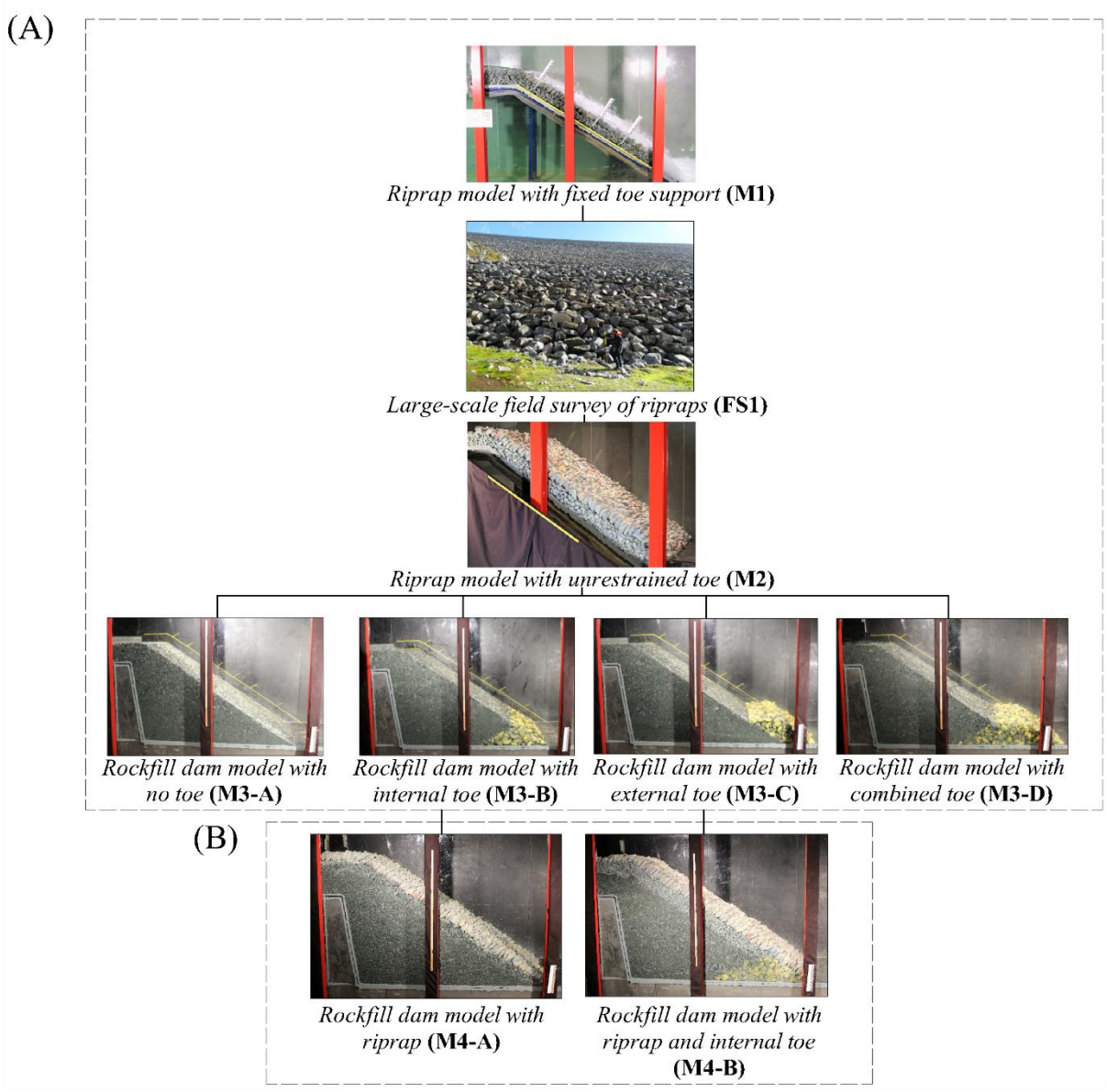

Figure 5. Overview of model tests and field studies conducted as part of the research program.

4.1 Research activities

As part of the research project, several experimental model studies, field surveys and statistical evaluations were carried out. A brief overview of the research activities carried out are presented herein.

Activity 1: **Model 1 *(M1)*- Riprap model with fixed toe support**

1D and 2D descriptions of failure mechanisms in placed ripraps.

Activity 2: **Field survey 1 *(FS1)*- Large-scale field study of ripraps**

Documentation of existing state of riprap toe construction on Norwegian rockfill dams.

Activity 3: **Model 2 *(M2)*- Riprap model with unrestrained toe**

Riprap stability investigations with realistic toe support conditions**.**

Activity 4: **Model 3 *(M3)*- Rockfill dam models with disparate toe configurations**

Presenting quantitative descriptions of effects of toe configurations on throughflow hydraulic properties of rockfill dams.

Activity 5: **Model 4 *(M4)*- Rockfill dam models coupled with riprap and toe structures**

Evaluation of holistic stability aspects of rockfill dam structure coupled with riprap and internal toe.

In addition to these experimental studies, results from a statistical analysis conducted on experimental data from throughflow investigations conducted on rockfill dam models are presented in this report. Research objective was to provide a realistic description of flow through homogenous rockfill dams through derivation of a general non-Darcy type power-law describing the non-linear throughflow hydraulic response of rockfill embankments subjected to throughflow.

Furthermore, as part of the experimental testing program, a series of overtopping tests were conducted on placed riprap models provided with load measuring pressure cells at the toe section. The underlying study objective was to obtain better understanding of the dynamic load generation processes at the toe sections of placed ripraps. This can be considered a major factor influencing placed riprap stability. Ability to quantitatively predict the forces generated at the toe sections of placed ripraps could also facilitate design of efficient toe support measures. The accumulated data is yet to be analyzed as part of future research activities.

5 Brief descriptions of testing methodologies and key findings from PhD studies

This section provides descriptions of the various model setups and testing methodologies implemented in the research programs presented as part of the present report. Further, strategies adopted for conducting the field survey are also presented. Key findings from the conducted investigations are also briefly summarized.

5.1 Riprap model with fixed toe support *(M1)*

The research on placed riprap stability was initiated at NTNU, Trondheim in 2014 with the *PLaF* (PLastring av Fyllingsdammer / placed ripraps constructed on rockfill dams) research project. The *PLaF* study was funded by EnergiNorge with research emphasis placed on experimental investigation of stability aspects of placed ripraps exposed to overtopping flows (Hiller, 2017). All tests were conducted with ripraps provided with fixed toe supports. Further following the *PLaF* study, a research project was initiated by Hydrocen, Norway in 2017 to further develop on the findings from previous studies and also to generate new knowledge regarding stability of rockfill dams and dam toes. Hiller et al. (2018) designed and tested a placed riprap model supported at the tor section in the hydraulic laboratory of NTNU, Trondheim. The model was subjected to overtopping scenarios and the accumulated data sets were used by Hiller et al. (2018) to arrive at a description of 1D failure mechanism in placed ripraps. Further, Ravindra et al. (2020) further analyzed the data sets gathered by Hiller et al. (2018) to extend the previous findings to 2D.

As part of the *PLaF* research project, experimental overtopping tests were conducted by Hiller et al. (2018) on model ripraps constructed in a flume (25 m long, 2 m high and 1 m wide) at the hydraulic laboratory at NTNU (Hiller, 2017). Discharge to the flume was supplied by pumps with a combined capacity of q = 0.4 m^2 s^{-1}. A conceptual 1:10 model setup consisting of a single-layered placed riprap section of width 1 m and chute length of L_S = 1.8 m constructed over a base frame inclined at 1:1.5 (S = 0.67) (Figure 6) was designed by Hiller et al. (2018). The test setup was designed assuming Froude similarity. Quarry stones of rhyolite with median diameter of d_{50} = 0.057 m and density of ρ_s = 2710 kg m^{-3} were used as riprap stones. The stones could be considered angular to sub-angular (average $a\ b^{-1}$ = 1.7) and uniformly graded ($C_u = d_{60}\ d_{10}^{-1}$ = 1.17). Test ripraps were placed on a 0.1 m thick filter layer comprised of geotextile and angular stones of size $d_{50,F}$ = 0.025 m and density $\rho_{s,F}$ = 3050 kg m^{-3}. The

dimensions of the filter and the riprap were chosen in accordance with guidelines offered by the Norwegian Water Resources and Energy Directorate (NVE, 2012).

Placed ripraps were constructed by manual placement of stones in an interlocking pattern commencing at the toe progressing upstream to the crest. The test setup required 1200 stones on average. Riprap stones on the slope were deliberately placed with the longest axis (*a*-axis) inclined at $\beta \approx 60^{o}$ with respect to the chute bottom and with an inclination of $\beta \approx 90^{o}$ for stones placed on the horizontal crest to account for practical considerations (Figure 6) (Lia et al., 2013). The ripraps were supported at the toe section with a metallic support structure and the entire test setup was elevated from the flume bottom to avoid backwater effects (Figure 5). The experimental setup was situated sufficiently downstream of the inflow section to achieve calm flow upstream of the test ripraps.

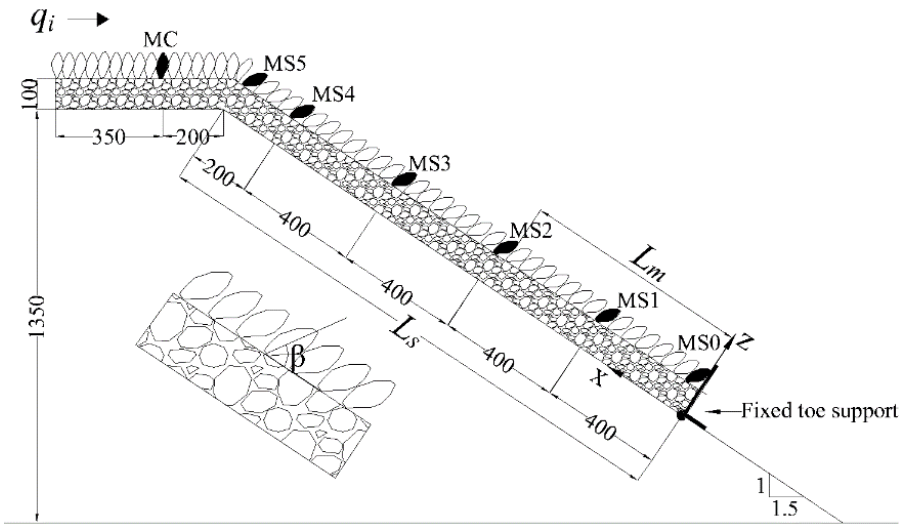

Figure 6. Depiction of experimental setup of model placed riprap supported at the toe. This depiction of the experimental setup is a modified form of Figure 3 from Hiller et al. (2018).

The location co-ordinates of select riprap stones were measured using a laser traverse system in a 3D Cartesian coordinate system with its origin situated at the fixed toe support (Figure 6). The *x*-axis was aligned in a direction parallel to the chute (33.7º to the flume bottom) pointing in the upstream direction and the *z*-axis was set perpendicular to the chute. Location coordinates could be measured to an accuracy of ± 0.1 mm in the *x*-direction and ± 1 mm in the *z*-direction. The selected stones were located along the centerline of the flume ($y = 0.5$) at specific positions of $x = 0$, 0.4, 0.8, 1.2, 1.6 and 1.8 m. The chosen riprap stones were identified as MS*m* (Figure 6), with $m = 0$, 1, 2, 3, 4 and 5 for stones located at $x = 0$, 0.4, 0.8, 1.2, 1.6 and 1.8 m respectively. The marked stone placed on the horizontal crest of the model was labelled MC

(Figure 6). Stone displacements were considered only along the *x* and *z*-directions as any possibility of encountering lateral flows prompting stone displacements in the *y*-direction was ruled out.

5.1.1 Testing methodology

Discharge was supplied to the flume in stepwise increments of q_i = 0.02 - 0.05 m^2 s^{-1} for a specific time interval Δt. 3D location co-ordinates of selected stones were measured prior to and after exposure every discharge step. This procedure was repeated until total failure of the riprap structure was achieved. The overtopping discharge magnitude at which complete collapse or bulk erosion of the riprap occurred was defined as the critical unit discharge (q_c) in this experimental study. Continuous monitoring of erosion of individual stones was not possible due to highly aerated and turbulent flow over the riprap surface.

5.1.2 1D description of failure mechanism in placed ripraps on steep slopes provided with toe support

As part of *PLaF* research published as Hiller et al. (2018), a total of 10 overtopping tests were conducted at the hydraulic laboratory in NTNU, Trondheim. Eight of these tests were on placed ripraps and two of them were on dumped ripraps. The results from the model tests demonstrated that the stability in terms of the stone related Froude number:

$$Fs, c = \frac{q_c}{\sqrt{g d^3}} \tag{10}$$

was on average five times higher for placed ripraps with diameter (d) in comparison with dumped ripraps. The observations revealed furthermore that the chute length covered with riprap L_S, see Figure 6 and the packing factor:

$$P_c = \frac{1}{N d_s^2} \tag{11}$$

where N is the amount of stones per m^2, influence the stone displacements and in turn stability of placed ripraps. Lower values for chute length and packing factors resulted in stability gain for the placed ripraps.

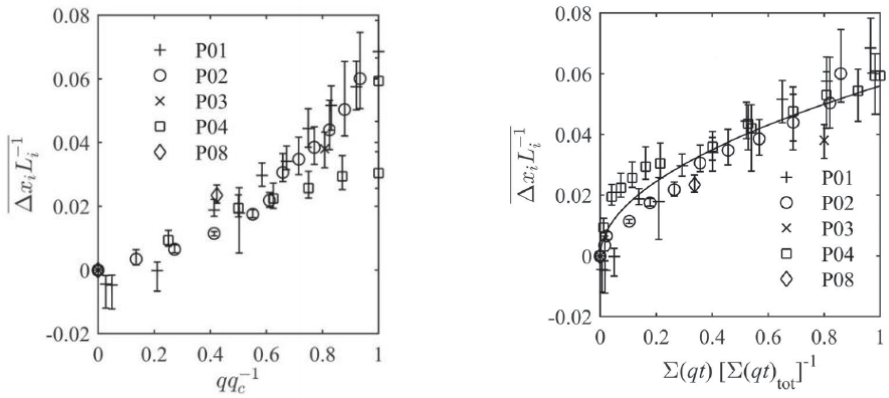

Figure 7: (Left) Averaged dimensionless displacements over MS0 to MS1400 compared to the relative discharge and (Right) compared to the volume of water passed over the riprap, Hiller et.al. (2018)

*P01-P08 represent test numbers 1 to 8 conducted on placed ripraps.

The main finding of the project was that accumulating stone displacements have to be considered as potential failure mechanism for placed riprap on steep slopes exposed to overtopping. During the tests with placed riprap, a developing gap was observed on the downstream edge of the dam crest. The overtopping flow compacted the placed riprap on the downstream part of the chute during the tests, resulting in loosening further upstream. Stones adjacent to the gap gradually lost their interlocking leading to overall riprap failure. The stone displacements were proportional to the distance between the stone location and the downstream fixed end. This was a deduction made from Figure 7 (Left) which clearly pointed out the fact that the relative stone displacements ($\Delta x_i L_i^{-1}$) were similar for all of the marked stones. It was also an important observation that the maximum absolute displacements were observed at MS0 (transition point from horizontal crest to inclined riprap) where L_i was maximum ($L_i \approx 1.8$ m).

A statistical analysis to comprehend the combined effect of loading period and discharge on stone displacements resulted in a plot presented in Figure 7 (Right). The data was fitted by a power law with a coefficient of determination $R^2 = 0.85$ presented in the equation below and further investigations revealed the possibility that the riprap became unstable when the maximum stone displacements exceeded the size of the longest axes of the riprap stones.

$$\Delta x_i L_i^{-1} = 0.056 \left(\frac{\Sigma(qt)}{\Sigma(qt)_{tot}} \right)^{0.51} \quad (12)$$

5.1.3 Buckling of placed ripraps with toe supports

As previously stated in section 3.1, all past experimental research on placed ripraps has focused on analyzing the 1D failure mechanism in toe supported placed ripraps on steep slopes exposed to overtopping. Consequently, 2D description of the same was unavailable in international literature. To address this concern, Experimental data sets accumulated by Hiller et al. (2018) through physical modelling investigation conducted on model ripraps with fixed toe supports constructed with angular stones on a steep slope of S = 0.67 were further analyzed along with additional experimental data from tests carried out within the HydroCen project.

3D location co-ordinates of selected placed riprap stones were measured as part of the experimental testing program (Figure 6) prior to and after exposure to incremental overtopping magnitudes (q_i). Data sets from seven overtopping tests were analyzed as part of the study to describe 2D displacements of placed riprap stones exposed to overtopping flows. Table 2 presents a brief overview of the testing procedure and critical unit discharges. Data sets for tests 5 to 7 were obtained from Hiller et al. (2018) with the addition of data sets from four new tests (tests 1 to 4) (Ravindra et al., 2020a). Tests 5, 6 and 7 were referred to as P01, P02 and P04 respectively within the article Hiller et al. (2018).

Table 2. Testing procedure for the documented tests incorporating the discharge q_i given as range, number of discharge steps N, time intervals Δt, initial packing factor P_c and the critical unit discharge q_c representing loading condition at total riprap failure (Ravindra et al., 2020a).

Test	q_i (m^2 s^{-1})	N (-)	Δt (s)	P_c (-)	q_c (m^2 s^{-1})
1	0.05-0.30	9	1800	0.58	0.30
2	0.05-0.20	7	1800	0.56	0.20
3	0.05-0.12	3	1800	0.57	0.12
4	0.05-0.15	4	1800	0.54	0.15
5 (P01*)	0.05-0.24	9	1800	0.56	0.24
6 (P02*)	0.05-0.36	11	3600	0.55	0.36
7 (P04*)	0.10-0.40, 0.35, 0.40	6	3600, 17h	0.53	0.40

*Original labels for the respective tests as employed within Hiller et al. (2018).

As can be inferred from Table 2, the critical unit discharges for the tested ripraps varied over the range q_c = 0.12 m^2 s^{-1} to 0.4 m^2 s^{-1}. Variability in stability of placed ripraps against overtopping has been described by Hiller et al. (2018) as dependent on factors such as the packing density of placement and skill level of labor. All tests were conducted by exposing the

ripraps to incremental overtopping in regular discharge and time steps. Test 7 from Table 4 is a special case as riprap failure could not be achieved even after application of the maximum possible unit discharge.

Figure 8 illustrates 2D displacements analysis results from a single test, test 1 presented in Table 4. The plot depicts development of 2D stone displacements as a function of applied overtopping discharge magnitudes ($q_i\, q_c^{-1}$). The horizontal axis of the plot ($L_m\, L_s^{-1}$) represents the distance to the respective selected riprap stones from the riprap stone placed adjacent to the fixed toe structure along the x-axis ($L_m = x_m - x_0$) (Figure 6) normalized over the total riprap length ($L_s = x_5 - x_0$ at $q_i\, q_c^{-1} = 0$). Stone displacements were computed with respect to the position of selected riprap stone adjacent to the fixed toe structure as the displacement of the stone identified as MS0 were moderate in comparison with the displacements measured for the other stones. The vertical axis of the plot represents the progressive stone displacements along the z-axis normalized over the median riprap stone diameter ($\Delta z_m\, d_{50}^{-1}$).

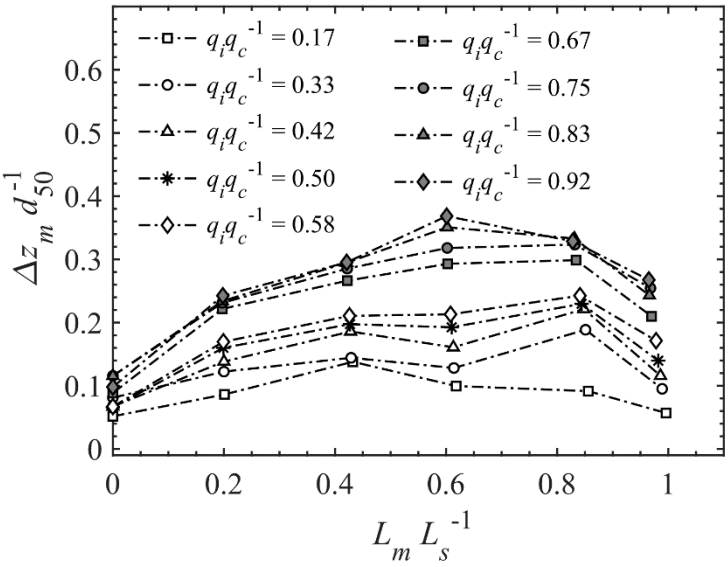

Figure 8. Depiction of 2D displacements of selected riprap stones for test 1 from Table 5 (Adopted from Ravindra et al., 2020a).

From Figure 8, it can be observed that the selected riprap stones underwent progressive displacements in the x-z plane with incremental overtopping. The displacements along the x-axis can be seen as gradual translation of selected riprap stones in the downstream direction. The magnitude of displacements along the x-axis are proportional to the magnitude of overtopping discharge and the distance of the respective stones from the downstream toe, further validating the findings of Hiller et al. (2018). Further, riprap stones undergo progressive

displacements along the *z*-direction in a manner directly proportional to the applied overtopping flow magnitude. Also, magnitude of displacements in the *z*-direction are dependent on the distance of the respective selected stones from the toe support as depicted in Figure 8.

Figure 9 presents results from the cumulative statistical analysis carried out with data sets obtained from all the seven tests presented in Table 2. Similar methodology as outlined for test 1 (Figure 8) has been adopted to compute the 2D stone displacements for the remainder of the tests. Figure 8 depicts the mean trends of 2D stone displacements for all the tests represented by average values of $\Delta z_m\, d_{50}^{-1}$ and $L_m\, L_s^{-1}$ computed for the seven tests at uniform intervals of overtopping ($q_i\ q_c^{-1}$ = 0.20). Variability in test results are presented as 95% confidence intervals.

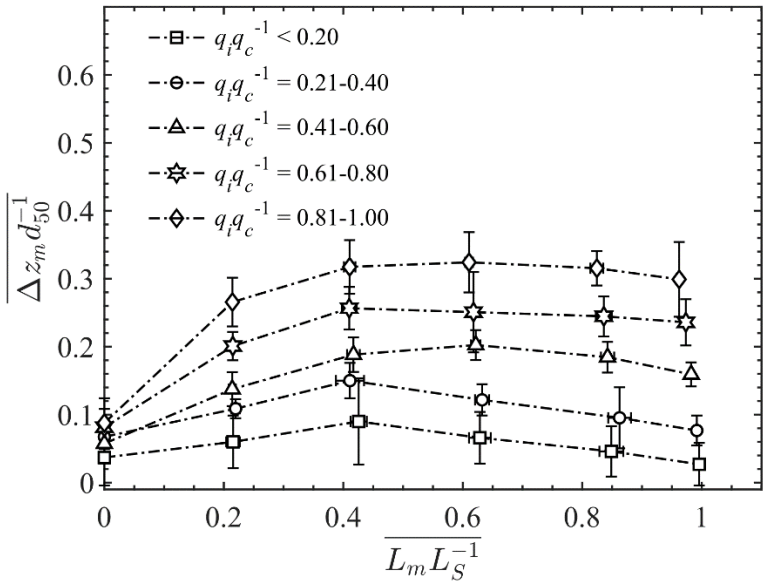

Figure 9: Results from the cumulative analysis carried out on data sets from seven tests representing average stone displacements in 2D. Uncertainty in displacements shown as 95% confidence intervals (Adopted from Ravindra et al., 2020a).

The process of 2D displacements of selected stones previously demonstrated by Figure 8 for test 1 was observed for all seven tests. Cumulative analysis results presented in Figure 9 further corroborate the observations made from Figure 8 of progressive 2D displacements of selected riprap stones as a function of both the overtopping flow magnitude and distance of the respective stones from the fixed toe structure. Total riprap failure defined as the ultimate collapse of the entire riprap structure in the conducted tests was found to be initiated at the upstream section of the riprap when the maximum displacement of riprap stones along the *x*-axis exceeded the size of the longest axes of the riprap stones at MS5 ($\Delta x_5 \approx a \approx 1.6\ d_{50}$) (Hiller

et al., 2018). This further corresponds to displacement of 0.3 - 0.35 times the median stone diameter of riprap stones at MS5 ($\Delta z_5 \approx 0.3\ d_{50}$ to $0.35\ d_{50}$) along the *z*-axis (Figure 9).

The mechanism of progressive 2D deformation of placed riprap stones discussed herein can be thought as being comparable to the mechanism of buckling observed in a slender-long column, pinned at one end and free at the other. A statistical analysis was conducted to demonstrate the similarities between the two mechanisms in the simplest possible manner by implementing the well-established Euler's theory for column buckling.

A non-dimensional equation was derived based on the methodology described within Wang and Wang (2004) with an intention of quantitatively illustrating the buckling modes of placed ripraps by considering a conceptual column with lateral deformations defined as $\Delta z_m\ d_{50}^{-1}$ at a distance of L_m from the pinned end (Equation 13).

$$\left(\frac{\Delta z_m}{d_{50}}\right)_i = A\ \frac{q_i}{q_c}\ \sin\left[k \cdot \pi \cdot \left(\frac{L_m}{L_s}\right)_i \cdot f\right] \tag{13}$$

where the term $L_m\ L_s^{-1}$ represents the column length ratio, A is a dimensionless numeric constant, obtained through calibration, $q_i\ q_c^{-1}$ denoting the applied hydraulic load, k denotes the buckling mode (k = 0, 1, 2, ...) and *f is a* numeric constant. It should be noted that $L_m\ L_s^{-1}$ is incorporated in Equation 4.1 as a function of $q_i\ q_c^{-1}$ to account for riprap stone displacements along the *x*-axis with incremental overtopping where the iterative variable i denotes a discharge step (i = 0 for $q_i\ q_c^{-1} = 0$ and $i = n$ for $q_i\ q_c^{-1} = 1$). The term $(L_m\ L_s^{-1})_{i=0}$ represents the original positions of the selected riprap stones prior to being exposed to overtopping.

The term $(L_m\ L_s^{-1})_i$ in Equation 13 can be computed employing Equation 14. The variable $(\Delta x_m\ L_s^{-1})_i$ for a particular overtopping flow can be obtained with the help of the statistically derived Equation 14. Equation 13 is valid for i = 0 to $i = n$ whereas Equation 13 is valid for $i > 0$ and $(L_m\ L_s^{-1})_{i=0}$ represents the initial positions of the riprap stones prior to overtopping exposure and $(\Delta x_m\ L_s^{-1})_{i=0} = 0$ for all stones.

$$\left(\frac{L_m}{L_S}\right)_{i+1} = \left(\frac{L_m}{L_S}\right)_i - \left(\frac{\Delta x_m}{L_S}\right)_{i+1} \tag{14}$$

$$\left(\frac{\Delta x_m}{L_S}\right)_i = \left(\frac{L_m}{L_S}\right)_{i=0} 0.0035 \cdot e^{\left(2.97 \cdot \frac{q_i}{q_c}\right)} \tag{15}$$

Equation 13 was calibrated against experimental data sets to obtain values for the numerical constants A and f. The calibration resulted in Figure 10 with values for calibration constants as A = 0.38 and f = 0.70 for the first buckling mode (k = 1). This corresponded to correlation

between the observed and the predicted displacements of $R^2 = 0.89$ and $R^2 = 0.99$ for $\Delta z_m \, d_{50}^{-1}$ and $L_m \, L_s^{-1}$ respectively. Further, Equation 13 with $A = 0.38$, $f = 0.70$ and $k = 1$, was used to compute the continuous profiles of the buckling progression also presented in Figure 10.

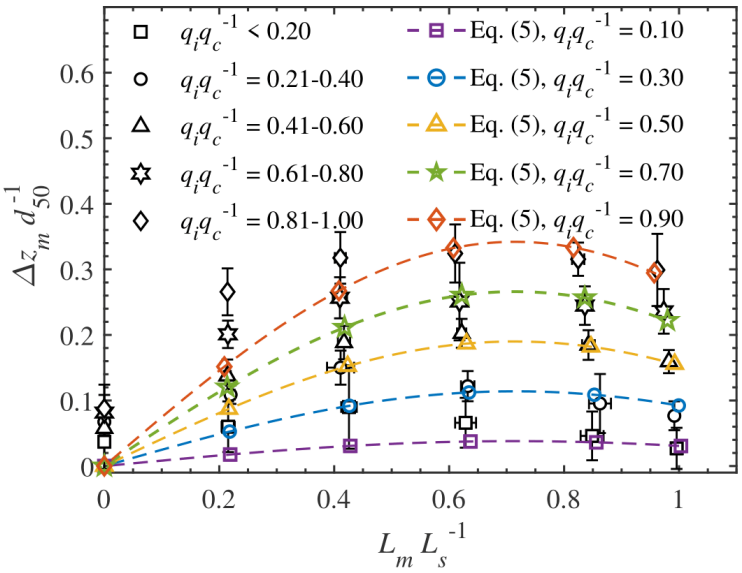

Figure 10. Observed 2D stone displacements from Figure 9 juxtaposed with predicted values from Equation 13 (Adopted from Ravindra et al., 2020a).

5.2 Field survey of ripraps *(FS1)*

The field survey within the HydroCen study was intended at investigating toe structures and construction aspects of placed ripraps and riprap toe conditions of existing rockfill dams. To achieve this goal, placed ripraps constructed on nine different Norwegian rockfill dams were surveyed. Key parameters describing quality of placement of riprap and toe stones such as size, shape and inclination were recorded and these were further analyzed and discussed. Further, conformity of placed riprap toe construction with official dam safety guidelines were evaluated as part of the study. Observations from the field survey (see Table 3) concerning existing toe conditions for placed ripraps were also recorded.

Table 3. Details of the dams surveyed as part of the study (Ravindra et al., 2019a).

Dam Index	Dam name	Location	Consequence class	Dam height (*H*) (m)	Dam length (*L*) (m)
1	Vessingsjø Secondary dam	Tydal, Trøndelag	2	5	70
2	Skjerjevatnet Secondary dam 1	Masfjord, Hordaland*	2	18.7	101.2
3	Skjerjevatnet main dam	Masfjord, Hordaland*	3	29.5	251
4	Nesjø main dam	Tydal, Trøndelag	4	45	1030
5	Fjellhaugvatn dam	Kvinnherad, Hordaland*	2	52	72.8
6	Akersvass dam	Rana, Nordland	4	53	485
7	Førreskar dam	Suldal, Rogaland	3	81	640
8	Storvass dam	Suldal, Rogaland	4	90	1400
9	Oddatjørn dam	Suldal, Rogaland	3	142	466

*Presently known as Vestland.

A field survey of placed ripraps on 33 different Norwegian rockfill dams was conducted by Hiller (2016). Findings from the HydroCen study add to the findings of Hiller (2016) through investigation conducted to study details concerning toe construction of placed ripraps on nine rockfill dams. Details regarding the dam location, consequence classification, height and length are presented in Table 3. The rockfill dams chosen for the field surveys consisted of varying

sizes of dams from 5 m up to 142 m in height (H) and from 70 m to 1400 m in length (L). The criteria for dam selection was presence of well-defined toe structures within the dam structure. The selections included Oddatjørndammen (H = 142 m and L = 466 m) which is the highest rockfill dam in Norway and Storvassdammen (H = 90 m and L = 1400 m) which is the largest Norwegian rockfill dam by volume. Further, the selection also comprised of dams belonging to different dam safety consequence classes (2 to 4). The variability in dam sizes was considered as an important parameter in order to obtain a representative picture of placed riprap toe construction in rockfill dams.

The nominal stone size (d_n) was employed to quantify sizing of the riprap stones as this can be considered as the representative size of individual riprap stones (Equation 16). Computation of d_n requires measurements of the longest, intermediate and the shortest axes dimensions of the riprap stones (a, b and c stone axes dimensions). The median stone size (d_{50}) for the stones was further computed as the average of individual nominal stone sizes. Furthermore, the placement angle of the riprap stones with respect to the downstream dam slope was characterized through the parameter (α) (Figure 11), which is the sum of the downstream embankment slope (θ) and the inclination of the longest stone axis with respect to the horizontal (β) (Equation 17).

$$d_n = (abc)^{1/3} \tag{16}$$

$$\alpha = \beta + \theta \tag{17}$$

The field measurements were subdivided into two different measurement phases. The first phase included measurements conducted to study the properties of the riprap section and the second phase was primarily intended at investigating properties of the toe stones and the toe support conditions. During the first phase of measurements, sizing of the riprap stones (a, b and c) and the inclination of the stones with respect to the horizontal (β) were measured for individual stones lying within a random 5 m x 5 m strip of the riprap. The stone dimensions were measured employing standard rulers and the inclinations were measured using a digital inclinometer. During the second phase of the survey, the dimensioning and the placement inclination of toe stones placed along the length of the dam toe were measured at regular distance intervals dependent on the dam length. Also, details regarding existing support conditions for the toe stones were recorded during this phase of the survey.

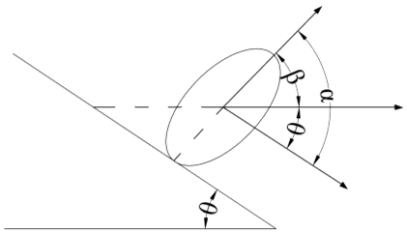

Figure 11. Portrayal of stone inclination with respect to the dam slope (α) as sum of inclination with respect to the horizontal (β) and embankment slope (θ) (Ravindra et al., 2019a).

5.2.1. Toe support conditions for placed ripraps on rockfill dams - A field survey

The data sets accumulated as part of the field survey of placed ripraps were subjected to a statistical evaluation. Measurements of stone sizes (*a*, *b* and *c*) were used to analyze the size distribution and angularity of the riprap and the toe stones. Further, measurements of inclination of the stones with respect to the horizontal (β) were employed to compute the angle of placement of the stones with respect to the downstream slope (α).

It was of importance to establish a technical background for the analysis. Comparison of the outcomes from the data analysis with design methodologies for placed ripraps would help bring out the technical significance of the findings. As discussed in Section 3.1, availability of technical literature describing design of placed ripraps is limited. The guidelines available within the Norwegian dam safety regulations and the recommendations of the NVE are some of the very few available official design procedures. Hence, to bring forth the practical relevance of the study findings, the results from the statistical investigation have further been subjected to a comparative evaluation with Norwegian dam safety requirements and recommendations. This would also further help in obtaining a better understanding of compatibility between construction practices and official guidelines. However, it is conveyed that the findings in general would be relevant and applicable for international interpretation.

Table 4 briefly summarizes the official regulations and recommendations concerning design and construction of placed ripraps. Furthermore, main findings from the statistical evaluation regarding conformity of riprap and toe construction practices with official guidelines and recommendations are also presented. To summarize, study findings suggest that construction

practices adopted for placed ripraps in general meet the requirements of Norwegian dam safety regulations with regards to sizing and placement of the stones. However, investigation outcomes also show that construction practices adopted at present do not prioritize on addressing additional recommendations put forward by the dam safety authorities with regards to uniformity and angularity of stones used for construction.

Table 4. Summary of official regulations and recommendations with respect to placed ripraps

Parameter	OED (2009) regulations	Additional NVE recommendations	Riprap stones	Toe stones
Minimum stone size (d_{min})	The downstream slope should have slope protection which ensures that the dam can withstand large overtopping due to accidental loads or damage to the dam. Stones within the riprap must have satisfactory size and quality and be arranged in a stable manner.	$d_{min} = 1.0\ S^{0.43}\ {q_f}^{0.78}$ (2) *	All surveyed dams meet requirements of OED and the NVE	All surveyed dams meet requirements of OED and the NVE
Uniformity of stone size (d_{max} /d_{min})		d_{max} / d_{min} < 1.7 *	None of the dams meet the recommendation of the NVE	Vessingsjø secondary dam and Fjellhaugvatn dam meet the NVE recommendation
Angularity		The stones be situated within the bladed to rod shape regimes within the Zingg diagram (Zingg, 1935). This is to ensure optimum interlocking with minimal void formation. **	Majority of the measured riprap stones (67 %) lie outside the NVE specified region within the Zingg diagram	Majority of the measured riprap stones (69 %) lie outside the NVE specified region within the Zingg diagram
Stone placement	The individual riprap stones are to be placed in an interlocking pattern with their longest axis inclined towards the dam.	As stated in the OED (2009) regulations.	Generally in agreement with the regulation	Generally in agreement with the regulation

*Obtained from NVE (2012) and ** from the presentation Hyllestad (2007). The parameters d_{min} and d_{max} denote the minimum and maximum riprap stone sizes; S stands for the downstream embankment slope (S is the ratio of the vertical to the horizontal slope dimensions) and q_f represents recommended minimum design discharge value for the respective dam consequence classifications.

5.2.2 Toe classification

Based on observations from the field study, toe conditions for the surveyed dams were classified into five different categories (Table 5 and Figure 12). The first category of riprap toe construction includes ripraps built with no toe support. This entails that the toe stones were either lying on bare rock surfaces or buried underneath moderate amounts of soil cover. All the surveyed ripraps could be classified under this category as majority of the toe sections were resting on bare rock surfaces or buried with moderate amount of soil cover.

Illustrations of ripraps built with no toe support conditions are presented for dams Fjellhaugvatn, Oddatjørn and Skjerjevatnet main dam in Figure 12(a), 12(b) and 12(c) respectively. Toe stones at Fjellhaugvatn dam and Skerjavatnet main dam were found to be resting on rock surfaces whereas toe stones at Oddatjørn dam were buried under moderate soil cover. The second category of observed riprap toe conditions at the surveyed dams consists of submerged riprap toe sections. This was the case at certain reaches of riprap toe sections of Skjerjevatnet main dam and Skerjevatnet secondary dam 1. An illustration of the scenario at Skjerjevatnet main dam is depicted in Figure 12(d).

Further, the third classification of riprap toe conditions observed was the placement of larger sized stones at the toe section of the riprap. Fjellhaugvatn dam and Storvass dam fall under this category as larger size stones ($d_{50,\,T}$ / $d_{50,\,RR}$ = 1.53 and 1.45 respectively) were found to be placed at the toe sections of these dams. For the rest of the surveyed dams, stone sizing at the toe and the riprap were found to be comparable. The fourth category of riprap toe construction observed was the use of steel bars for stabilization of the toe stones. A small section of the riprap toe at Storvass dam was observed to be tentatively supported using reinforcing steel bars (Figure 12(e)) measuring 25 mm in diameter with average outcrop length of 0.3 m. Although majority of the riprap toe sections of Storvass dam were observed to be unsupported, the reinforcing bars were used to tentatively stabilize toe sections of the riprap close to the right abutment where the foundation was observed to be at a steep inclination. The steel rebars were most likely used to facilitate placement of toe stones on the steep foundation.

At Akersvass dam, a small stretch of the riprap toe section was seen to be supported with a concrete wall (Figure 12(f)) and this is classified as the fifth riprap toe state observed as part of this field study. The concrete wall was constructed in tandem with a leakage measuring station and hence, it was evident that riprap toe stabilization was not the primary intention of constructing the structure but rather to facilitate leakage measurements from the dam.

Table 5. Classification of different riprap toe conditions (Adopted from Ravindra et al., 2019a)

Category	Description of toe condition	Dam name
1	No toe support	All surveyed dams (Table 2)
2	Submerged toe	Skjerjevatnet main dam Skjerjevatnet secondary dam 1 (e.g. Figure 15(d))
3	Larger stones at the toe	Fjellhaugvatn dam Storvass dam (Figures 15(a) and (e))
4	Steel rebars	Storvass dam (Figure 15(e))
5	Concrete wall	Akersvass dam (Figure 15(f))

Figure 12. Depiction of existing conditions of placed riprap toe sections. Category 1 at dams **(a)** Fjellhaugvatn dam **(b)** Oddatjørn dam and **(c)** Skjerjevatnet main dam. Category 2 at **(d)** Skjerjevatnet main dam. Category 4 at **(e)** Storvass dam. Category 5 at **(f)** Akersvass dam (Adopted from Ravindra et al., 2019a).

5.3 Riprap model with unrestrained toe *(M2)*

The study described herein was aimed at investigating the influence of toe support conditions on stability aspects of ripraps on steep slopes exposed to overtopping flows. A modified version of the experimental setup introduced in Section 5.1 (M1) was put into use to investigate stability and failure mechanism of model placed and dumped ripraps unsupported at the toe section.

As previously stated, the original model designed by Hiller et al. (2018) consisted of a fixed metallic toe support structure fastened to the base frame at the downstream end of the riprap chute providing resistance against sliding of the riprap structure. A modified version of the model setup was used in the HydroCen study, wherein the fixed toe support structure was replaced with a horizontal platform at the downstream extremity of the riprap chute to facilitate construction of placed riprap models with unrestrained toes (Figure 13). The modifications to the experimental rig were so designed as to maintain the original dimensioning of the riprap structure as employed in the preceding investigations to enable comparison of experimental findings. The surface of the horizontal platform was covered with a layer of geotextile to provide realistic friction for the toe stones.

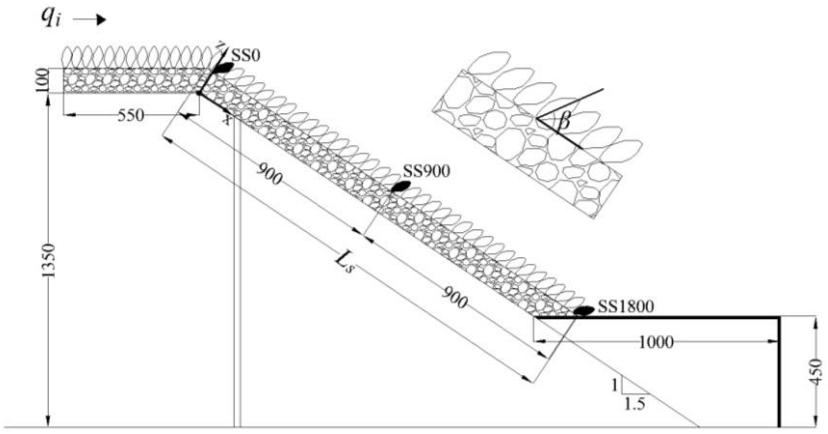

Figure 13. Illustration of experimental setup of model placed riprap with unsupported toe (Adopted from Ravindra et al. (2020b)).

Overtopping tests were carried out with both placed and dumped ripraps to better understand the fundamental differences and similarities in failure mechanisms between the two structures. Placed riprap models were constructed by manual placement of stones in an interlocking pattern commencing at the toe, progressing upstream to the crest. The individual riprap stones were deliberately placed with the longest axis (a-axis) inclined at $\beta \approx 60^{o}$ with respect to the chute bottom and at an inclination of $\beta \approx 90^{o}$ on the horizontal crest to account for practical

considerations (Lia et al., 2013). It should be noted that the last row of riprap stones, which constitute the toe of the riprap were placed flat on the horizontal platform ($\beta \approx 0^{o}$) (Figure 13). Subsequent rows of stones were placed at incremental inclinations to attain the required stone inclinations of $\beta \approx 60^{o}$. This was also in alignment with the findings from field surveys of riprap toes presented in *FS1*, wherein mean placement inclinations (β) for the toe stones were found to be much lower in comparison with those for the riprap stones. Further, single layer dumped ripraps were constructed by randomly dumping the riprap stones on the slope with arbitrary orientations and without any interlocking pattern.

Due to flow aeration in the model and the sudden nature of riprap collapse, conventional stone displacement measurement techniques could not be used for monitoring stone motions during these tests. To obtain quantitative descriptions of stone displacement in the tested riprap structures prior to and during riprap failure, new technology in stone displacement monitoring named as Smartstone probes (*Smartstone probe v2.1*), developed at the University of Trier, Germany was adopted within the HydroCen study. Further, for validation of results obtained by the smartstone sensors, particle image velocimetry (PIV) technique was implemented as part of the investigation in collaboration with University of Trier.

5.3.1 Smartstones

Smartstone sensors are accelerometers designed to be implanted in stones for tracking of parameters describing stone displacements such as accelerations and rotations in time. The module comprises of a triaxial acceleration sensor, a triaxial gyroscope and a geomagnetic sensor (Figure 14). Owing to their non-intrusive nature of operation and flexibility for applicability in various engineering and research disciplines, Smartstone technology was found to be an ideal technique for implementation within the present experimental program.

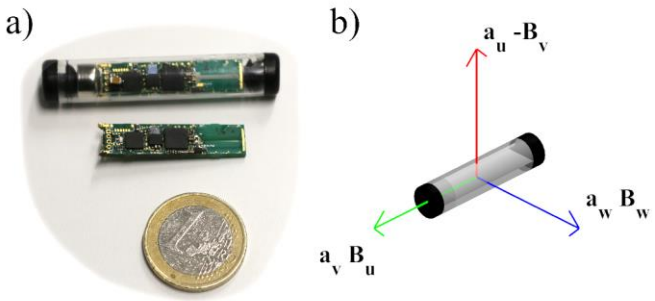

Figure 14. (a) The Smartstone probe in a plastic tube with button cell on the left end and the circuit board with sensors underneath. **(b)** The probe's coordinate system (Adopted from Ravindra et al. (2020b)).

The current version of the smartstone sensor is covered by a 50 mm long and 10 mm wide plastic tube that is closed with two plastic plugs. Energy for recording and data exchange is supplied by a standard 1.5 V button cell (type AG5). The memory size allows for up to 8 minutes of constant movement with 100 Hz sampling rate. Commencement of data acquisition is marked by exceedance of stone movements over a user-defined threshold.

In order to equip select riprap stones with Smartstone probes within the HydroCen study, cylindrical holes of diameter 10 mm and length 50 mm were drilled within the stones. The probes were encased in watertight rubber envelopes and mounted within the cylindrical drill holes. The openings were further sealed using sealing agents. Three riprap stones were mounted with Smartstone probes and placed within the test ripraps at the crown, the center and at the toe sections of the riprap structure for all the tests. This was to monitor stone movements at these locations as this could provide details regarding initiation and progression of riprap failure. The respective stones were identified as SS_0, SS_{900} and SS_{1800} (Figure 13) respectively with the indices representing the distance to the respective stones from the origin along the *x*-direction. The selected stones were located along the centerline of the flume ($y = 0.5$) to address concerns of wall effects.

5.3.2 Particle Image Velocimetry (PIV)

High-speed video footages of the overtopping tests were recorded over the course of the experimental testing program for all the tests. The video footages were in turn subjected to Particle Image Velocimetry (PIV) analysis to enable cross corroboration of investigation results. PIV analysis allows for estimation of the velocity distribution in image pairs. The direction and the velocity of particles in image pairs result from cross-correlation functions. The tool *PIVlab* (Thielicke and Stamhuis, 2014a; Thielicke and Stamhuis, 2014b; Thielicke, 2014; Garcia, 2011), which is available for MATLAB was used to carry out the analysis.

5.3.3 Testing methodology

Due to limitations with the Smartstone probes with respect to battery life and inbuilt memory, adoption of similar testing methodology as adopted within previous investigations to conduct extended overtopping tests was not possible within the HydroCen study. Hence, testing methodology was modified to accommodate the limitations of the probes. This was done also considering changes in the behavior of placed riprap models with unsupported toes concerning deformations and critical discharges.

To begin with, several pilot overtopping tests with placed and dumped ripraps were conducted without incorporation of the Smartstone probes. The pilot tests on model ripraps were carried out by exposing the riprap structures to incremental overtopping with discharge steps of Δq = 0.02 $m^2 s^{-1}$. The discharge levels were maintained constant over regular time intervals of Δt = 1800 s. The 3D location co-ordinates of several marked stones were measured in between overtopping steps employing the 3D laser traverse system. This procedure was further repeated over N discharge steps until ultimate riprap collapse was achieved (q_c). Further, for tests conducted with placed and dumped ripraps implanted with Smartstone probes, the riprap structures were directly exposed to the critical discharge (q_c) levels obtained from the pilot tests in order to achieve riprap failure in the shortest possible time. This was to obtain measurements regarding the motion of riprap stones during riprap collapse, also accommodating limitations of the Smartstone probes. In essence, the adopted testing procedure results in measurements describing motion of the riprap stones prior to and during riprap collapse thereby providing a comprehensive description of the underlying failure mechanisms in the tested placed and dumped ripraps.

5.3.4 Failure mechanism in placed riprap on steep slope with unsupported toe

Details regarding the experimental testing program are presented within Table 7. The table also presents particulars regarding construction and testing procedures adopted for experiments conducted on placed (P01 - P06) and dumped (D01 - D03) ripraps. The critical overtopping discharge levels for initiation of irreversible riprap failure (q_c) were found to be higher for placed ripraps as compared with dumped ripraps. Unraveling riprap failures were found to be initiated at overtopping discharge magnitudes of q_c = 0.06 $m^2 s^{-1}$ and 0.04 $m^2 s^{-1}$ respectively for placed and dumped riprap (Table 6). This ratio of critical discharge values between placed and dumped ripraps was hence found to be 1.5.

Table 6. Description of the experimental testing procedure (Ravindra et al., 2020b).

Test	P_c (-)	q_i (m^2 s^{-1})	n (-)	Δt (s)	q_c (m^2 s^{-1})
P01*	0.53	0.02 - 0.06	3	1800	0.06
P02	0.53	0.06	1	-	0.06
P03	0.54	0.06	1	-	0.06
P04	0.48	0.06	1	-	0.06
P05	0.49	0.06	1	-	0.06
P06	0.52	0.06	1	-	0.06
D01*	0.91	0.02 – 0.04	2	1800	0.04
D02	0.83	0.04	1	-	0.04
D03	0.74	0.04	1	-	0.04

*Pilot tests conducted without incorporation of the Smartstone probes

Further, the 2D deformations within placed riprap structures were analyzed with respect to incremental overtopping discharge magnitudes using laser measurements of location co-ordinates of six marked stones collected during the pilot tests. Reference is made to *Section 5.1* (Ravindra et al., 2020) for further details regarding the analysis procedure. Analysis results revealed that the marked riprap stones placed on the riprap chute underwent only minor displacements along and normal to the chute direction (*x* and *z* axes respectively) prior to initiation of progressive riprap failure. Further, the toe stones placed on the horizontal platform experienced insignificant downstream displacements along the platform surface. Furthermore, no definite correlations were found between the stone displacements and the overtopping discharge magnitudes.

5.3.5 Initiation and progression of placed riprap failure

The Smartstone probes were adopted within the HydroCen study to better understand the mechanisms of failure initiations and progression in placed and dumped ripraps. Also, Particle Image Velocimetry (PIV) analysis using the recorded video footages (provided as a supplementary video file) were also conducted to further validate results derived from measurements obtained from the Smartstones. Cumulative results from analysis conducted implementing these two techniques are presented herein

Detailed analysis of the accelerometer and gyroscope data revealed that riprap failure takes place in uniquely identifiable phases. To illustrate the sequence of events leading up to and

further progressing as total riprap collapse, depictions of stone acceleration and orientation measurements for an overtopping test conducted on a model placed riprap are presented as Figure 15). Recorded measurements from the Smartstone placed at the riprap crest (S_0 from Figure 13) from test P05 are portrayed in Figure 15. Further, the individual phases of stone motions within the time series are labelled with capital letters.

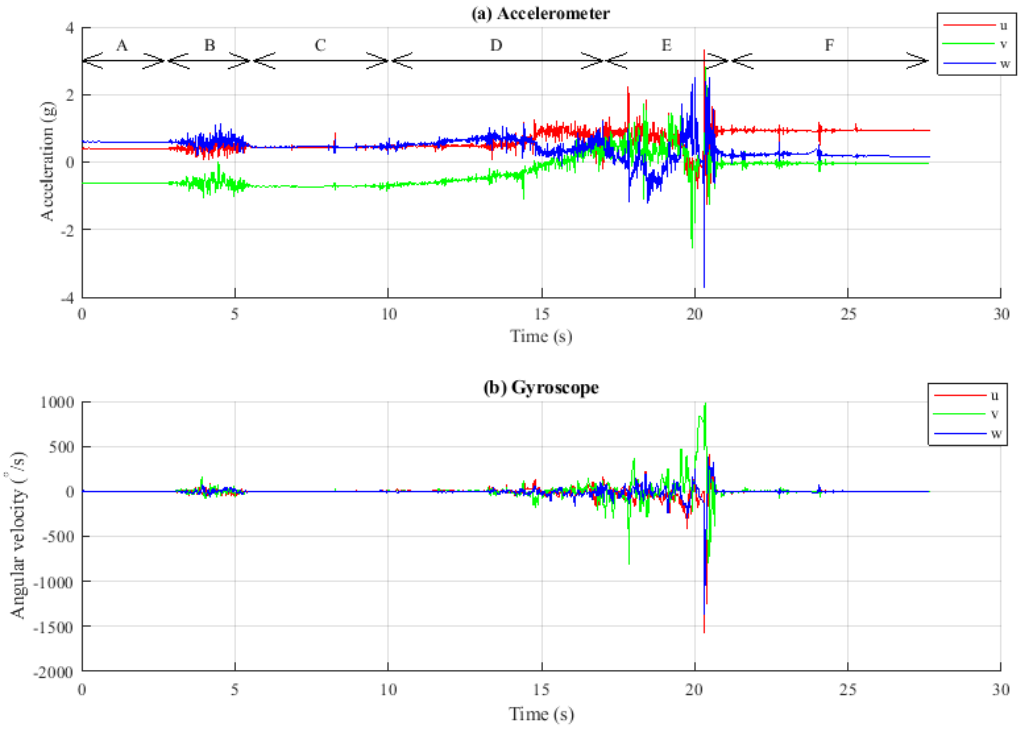

Figure 15. Depictions of **(a)** accelerometer and **(b)** gyroscope measurements from the Smartstone placed at the riprap crest (S_0) from test P05 (Ravindra et al., 2020b).

Phase A: The start of Phase A (t = 0) represents the trigger point of the probe subsequent to which the probe initiates the data recording protocol. That is, at t = 0, the water flow reaches a magnitude that results in accelerations of the sensor-equipped stone that exceed the threshold of 48 mg. This threshold represents the minimum trigger acceleration value to be experienced by the sensor beyond which data acquisition can commence. This can be due to minor changes in stone inclination by fractions of a degree, as a change of inclination changes the fraction of gravity measured along each probe axis. This effect can be considered a consequence of vibrations generated due to initial flow attack on the stone. The stone does not undergo major displacements during the remainder of phase A. Similar observations were made for Smartstones placed at the center (S_{900}) and at the toe of the riprap (S_{1800}).

Phase B: The hydrodynamic drag and lift forces generated by incremental overtopping flows reaches higher magnitudes resulting in strong vibrations as can be seen from the accelerometer plot in Figure 16. The impinging flow forces and the resulting vibrations further lead to small reorganizations of the stones within the riprap structure, as demonstrated by minor changes in stone inclinations. These are visible within the acceleration plots for the *u* and *w* axes (the blue and red lines) presented in Figure 16. These are on different levels prior to phase B and almost on the same level after phase B. This entails that the stone underwent rotation along the *u*-*w* plane to attain a final configuration for Phase C. This conclusion could also be further corroborated through inspection of the video footage that revealed that during phase B, the riprap layer in its entirety undergoes slight compaction and the stones experience changes in orientation, tilting towards the downstream direction. The Smartstone placed at the center (S_{900}) of the riprap displayed similar behavior. However, the stones placed at the toe (S_{1800}) did not appear to experience significant displacements or rotations during this phase.

Phase C: After this initial readjustment phase leading to compaction of the riprap structure, there is a phase of relative rest with only occasional single small spikes in the acceleration data. In this phase, the overtopping flow magnitude is gradually increasing.

Phase D: The failure begins quite slowly during several seconds with a tilting of the stones in the riprap layer. This tilting is visible by the changing levels of the different acceleration time series. It can be observed that the absolute values at the *v* axis (green line) gradually decrease while the *w* axis values increase (blue line). Thus, the sensor's end indicated by the blue *w* axis moves downwards. This effect is also documented in the video as the whole top layer tilts within this phase of failure initiation.

Phase E: Initiation of progressive sliding collapse of the riprap structure. Reference is made to Ravindra et al., (2020b) for detailed description of the sliding process.

Phase F: The riprap stones further collapse to form a pile on top of the horizontal platform. The pile is still overrun by water, resulting in small spikes in measurements. The pile is continually undergoing rearranged as a consequence of flow attack after a pause of several seconds.

Furthermore, dumped ripraps were found to go through a surface erosion process where individual stones were eroded by the action of destabilizing turbulent flow forces. This was in contrast to failure initiation in placed ripraps wherein the riprap structure as a whole was found to undergo a slide.

The acceleration and the gyroscope measurements were subjected to further analysis to derive displacement velocities of the Smartstone during riprap failure. Using integration of the acceleration values, a velocity time series was obtained.

In total, three runs of placed riprap and three runs of dumped riprap were examined. The observations in these two groups are similar within each group and also the differences between the groups are obvious. The general findings are: Placed ripraps collapse were found to occur more abruptly than dumped ripraps. The peak velocities were also found to be higher (between 0.66 and 1.008 m s^{-1}) for placed ripraps as compared with velocities computed for dumped ripraps (between 0.31 and 0.52 m s^{-1}). Also, placed riprap acceleration time series show more frequent and higher magnitude peaks, while the gyroscope time series show less rotations. This in turn entails that placed ripraps are characterized by high degree of vibrations within the riprap structure and that placed ripraps collapse as a unit in the sense that the whole riprap layer slides down the slope as a unified structure. However, for dumped ripraps, less acceleration peaks were visible and significantly higher stone rotations were recorded by the gyroscope. This further suggests that dumped riprap failures entail lower degree of vibrations and that the failure progresses randomly with erosion of individual stones from the slope.

The velocities derived from Smartstone data should be confirmed using different techniques. To accomplish this, Particle Image Velocimetry (PIV) analysis was conducted on the video footage to obtain velocity distributions during the overtopping test. The tool PIVlab (Thielicke and Stamhuis, 2014a; Thielicke and Stamhuis, 2014b; Thielicke, 2014; Garcia, 2011), which is available for MATLAB was employed to carry out the analysis. For each frame, the estimated velocities were stored in a matrix for the horizontal component and a second matrix for the vertical component. The peak of the time series of the PIV-derived velocities in this cell were compared to Smartstone derived velocities. In all runs that were compared, excellent correlation between the Smartstone derived maximum velocities and the PIV derived peak velocities were observed. Deviations between PIV and Smartstone velocities ranged between 0.01 and 0.06 m s^{-1}.

5.4 Rockfill dam models subjected to throughflow

The European research project dubbed IMPACT (Investigation of Extreme Flood Processes and Uncertainties) was undertaken during the period 2001-2004 by a consortium of 11 institutions across Europe. The primary research focus of the project was the assessment and reduction of risks from extreme flooding caused by natural events or the failure of dams and flood defense structures (e.g. Zech and Soares-Frazao, 2007 and Morris and Park, 2007). Several experimental overtopping tests were conducted on earth and rockfill dams of different configurations as part of the research project (Kjetil et al., 2004). Experimental data sets from a single large-scale test conducted on a 6 m high prototype homogenous rockfill dam in Røssvatn, Norway as part of the IMPACT project (EBL Kompetanse, 2003; EBL Kompetanse, 2006; and EBL Kompetanse, 2007) were further analyzed as part of the HydroCen study. Further, in parallel studied conducted by NTNU, Trondheim and SINTEF, Trondheim, model studies on 1:5 and 1:10 scaled models of the large-scale test dam were conducted at the hydraulic testing facility of NTNU, Trondheim (Kjellesvig, 2002 and Sand, 2002). The test dams were composed of uniformly graded rockfill with median particle sizes ranging from d_{50} = 10.2 mm to 350 mm. Experimental data pertaining to throughflow hydraulic behavior of rockfill embankments were accumulated as part of these experimental studies conducted on rockfill embankment models of varying sizes. The data sets were further subjected to a statistical evaluation within the HydroCen study in collaboration with the Norwegian Geotechnical Institute (NGI), Oslo. This was to better understand non-linear flow through actual rockfill embankments.

5.4.1 Large-scale field test experimental setup

The 6 m high homogenous rockfill embankment was constructed in a channel with mean top width of 42.8 m as part of the IMPACT project (EBL Kompetanse, 2006). The cross-sectional geometric outline consisted of crest and bottom widths of 2 m and 20 m respectively with upstream and downstream inclinations of S = 1:1.5 (V: H). The inclination of the embankment side slope was chosen in accordance with Norwegian rockfill dam construction practice (e.g. NVE, 2012). The abutment profiles at the test location were steep resulting in a trapezoidal channel cross-section. The rockfill embankment of volume $V_E \approx 2000$ m^3 was constructed of uniformly graded rockfill material with median stone size of d_{50} = 350 mm. During embankment construction, a set of four piezometers (P_1 to P_4) were installed within the downstream embankment structure at an elevation of 2 m from the channel bottom at a spacing

of 4 m along the flow direction for throughflow depth measurements. Images from the test site depicting the test embankment prior to and during testing are presented in Figures 16(a) and 16(b) respectively.

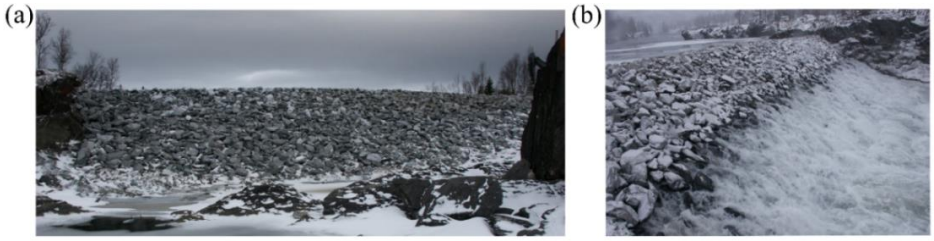

Figure 16. (a) Image of the test rockfill embankment (M1) from the test site downstream of Røssvatn, southern Norway prior to testing; **(b)** Image of the test dam during testing (Image courtesy: EBL Kompetanse (2006) and published in Ravindra et al., 2019b).

5.4.2 Model tests experimental setup

The 1:10 and 1:5 scale models of the large-scale test dam were constructed in flumes available at the hydraulic testing facilities of NTNU, Trondheim (Kjellesvig, 2002 and Sand, 2002). The 0.6 m high dams were constructed in a 2.2 m wide and 10 m long stepped flume and the 1.2 m high dams were constructed in a 4 m wide and 10 m long flume. The top and bottom cross-sectional widths of the 0.6 m high dam were 0.4 m and 2.2 m respectively. Further, top and bottom cross-sectional widths of the 1.2 m high dam were 1.0 m and 2.8 m respectively. All test dams for the 1.2 m high dam models were built with upstream and downstream inclinations of 1:1.5. However, due to limited availability of space within the flume, test dams for model setup were constructed as partial dam structures with only the downstream embankment built with an inclination of 1:1.5. From a dam safety standpoint, it is of importance to comprehend the throughflow properties within the downstream shoulder of a rockfill dam in comparison with the upstream embankment as the downstream slope of rockfill embankments are exposed to higher degree of destabilizing forces under turbulent throughflow conditions. Also, the large-scale field test model consisted of piezometers installed at the center and within the downstream half of the embankment. Hence, model setups for the 1.2 m high dam, influenced by limited availability of space in the flume, were constructed as half dams with only the downstream half of the embankment structure.

Further, the flume sidewalls for both setups were sloped at 1:1 transforming the flume cross-section to a trapezoidal profile. This was done to account for the steep abutment profile

observed at the large-scale dam test location (Figure 16) which resulted in a trapezoidal channel cross-section. For the 0.6 m high dam models, a total of seven piezometers were positioned along the centerline of the dam sections with uniform spacing of 0.3 m for throughflow depth measurements and two piezometers were placed upstream of the test dam sections for water level measurements. For the 1.2 m high dam models, five piezometers with even spacing of 0.5 m were installed within the embankment structures of the test dams and a single piezometer was installed upstream of the test embankments. Reference is made to reports EBL Kompetanse (2006), Kjellesvig (2002) and Sand (2002) for detailed information regarding the model dam experimental setups.

5.4.3 Testing methodology and material properties

A series of seven tests were conducted on the model dams described in earlier discussions. A single throughflow test was conducted on the 6 m high rockfill embankment. Further, a set of six throughflow tests were carried out on the 1:10 and 1:5 models. Technical details regarding the material properties employed for construction of the models are presented in Table 7. Parameters H and W_{cr} represent the height and crest width of the rockfill embankments respectively. S denotes the upstream and downstream embankment slope values. For tests conducted with the 1.2 m high model dams, S represents only the downstream slope as the embankments were constructed as partial dams incorporating only the downstream embankment structures. Details regarding rockfill material properties such as the specific gravity (SG), median stone diameter (d_{50}), coefficient of uniformity (C_u) and porosity are also presented in Table 7. The testing procedures are described through the parameter ΔQ symbolizing the throughflow discharge intervals.

The test embankments were exposed to incremental throughflow discharges in steps of ΔQ (Table 7). The discharge levels were maintained constant over regular time intervals of 10 minutes to ensure attainment of steady state flow within the dam structure. The process was repeated until the development of total embankment breach characterized by the breach discharge represented as Q_b. However, for the tested dams constructed with large size rockfill with $d_{50} > 87.5$ mm, ultimate dam breach could not be achieved even with application of maximum flow (Q_{max}) considering capacity of the channel for the large-scale test and the capacities of the flumes for the model tests. The piezometric pressure head measurements at the individual piezometers located within the dam structure were recorded for the corresponding throughflow magnitudes.

Table 7. Details of embankment construction aspects, rockfill material properties and testing procedures (Ravindra et al., 2019b).

Test No.	H (m)	S (-)	W_{cr} (m)	SG (-)	d_{50} (mm)	C_u (-)	n (-)	ΔQ ($m^3 s^{-1}$)	Q_b ($m^3 s^{-1}$)	Q_{max} ($m^3 s^{-1}$)
1	6	1: 1.5	2	2.7	350	1.2	0.40	5	-	30.5
2	0.6	1: 1.5	0.4	3.0	51.4	1.8	0.44	0.005	0.10	0.10
3	0.6	1: 1.5	0.4	3.0	10.8	2.0	0.45	0.005	0.025	0.025
4	0.6	1: 1.5	0.4	3.0	18.5	1.3	0.45	0.005	0.045	0.045
5	0.6	1: 1.5	0.4	3.0	87.6	1.4	0.49	0.01	-	0.15
6	1.2	1: 1.5	1.0	3.0	87.6	1.4	0.49	0.025	-	0.30
7	1.2	1: 1.5	1.0	3.0	203.7	1.7	0.52	0.05	-	0.50

5.4.4 Non-linear flow through rockfill embankments

The recorded piezometer data from the tests (Table 7) were employed to compute hydraulic gradients and the corresponding void velocities within the test dams at incremental throughflow magnitudes. Further analysis of the i-V_n trends within the different test dams were conducted over the range of applied through flows for which the test dams were stable. The computed i-V_n trends for the tests are presented in Figure 17(a) and 17(b) for the 0.6 m and 1.2 m high model setups respectively and in Figure 17(c) for the 6 m high large-scale field setup. It can be inferred from the depictions that the computed i-V_n trends for the tests followed non-linear trends in general. Although some degree of variability in the i-V_n trends were observed at different locations within the tested dam structures, the trends in general were in good agreement with each other. The observed variability could be explained as a consequence of local variations in porosity or packing density of rockfill medium at the different piezometric locations due to disparities in manual construction efficiency. The i-V_n trends are presented over a broad range of hydraulic gradients (i = 0.01 to 0.5) for tests conducted with the 0.6 m and the 1.2 m high dam models. But, for the 6 m high rockfill dam (Figure 16), i-V_n trends are presented over a narrower hydraulic gradient range of i = 0.24 to 0.40 as a consequence of unavailable measurements of flow depths for lower throughflow magnitudes as the piezometers were located at 2 m elevation from the dam bottom.

Trend lines of the form $y = a\,x^b$ were added to the individual i-V_n plots demonstrating excellent correlation. Further, values for parameters a and b for the respective tests were extracted as part of the analysis. It was observed that the parameter b for all the tests was consistently placed within the range of 0.48 to 0.55 except for Test 7 (Table 7), wherein a lower value of parameter

b = 0.41 was found. The average of the obtained b values was found to be b = 0.51. As stated earlier, parameter b within the power-law (Equation 5) represents the degree of flow turbulence. The obtained average value of parameter b = 0.51 signifies fully developed turbulent flow regime. This finding is in line with conclusions of several past studies such as Escande (1953), Soni et al. (1978) and Siddiqua et al. (2011) with regards to parameter b that $b \approx 0.5$ represents post-linear or non-Darcian flow regime. Furthermore, correlation between material properties such as C_u and n and parameter b were evaluated and no definitive relationships could be observed in this regard between the parameters. Considering the anomalous value of b = 0.41 for test 7, although the exact reason for the observation is not apparent, the large size of the rockfill particles used for the test (d_{50} = 0.203 m) could offer a possible explanation in this regard as the mean stone diameter for this particular test was oversized considering the dam height (H = 1.2 m). This could inhibit complete development of flow turbulence resulting in a lower value of b. Furthermore, the porosity of the dam material for test 7, n = 0.52 was slightly higher in comparison with other materials which fall within a range of 0.40 – 0.49 and this could also influence flow turbulence levels within the test dam.

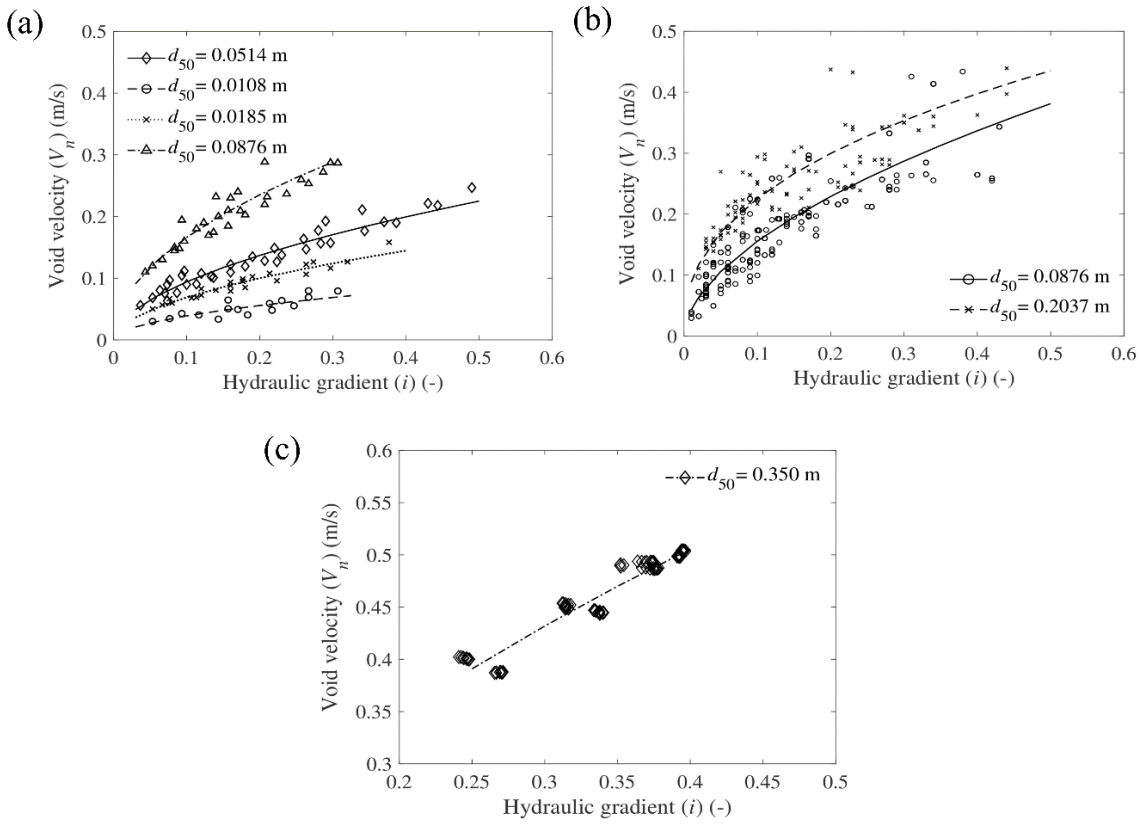

Figure 17. Computed i-V_n trends for **(a)** 0.6 m high dam model **(b)** 1.2 m high dam model and **(c)** 6 m high large-scale dam (Ravindra et al, 2019b).

Further, Figure 18 represents the correlation between parameters a and d_{50} for the respective tests. A clear exponential trend can be observed in this regard quantitatively described by a symmetrical sigmoidal trend line represented as Equation (18). The trend line demonstrated good correlation with the parent dataset with an $R^2 = 0.95$.

$$a = \left(72.987 - \frac{73.613}{\left(1+\left(\frac{d_{50}}{1.136\ .\ 10^{9}}\right)^{0.179}\right.}\right) \tag{18}$$

To obtain a general power-law describing the non-linear i-V_n trend for throughflow in rockfill embankments, the experimentally derived results for parameters a and b were further used to arrive at Equation (19). The value for parameter b is adopted as 0.51 as this represents the average for all tests.

$$V_n = \left(72.987 - \frac{73.613}{\left(1+\left(\frac{d_{50}}{1.136\ .\ 10^{9}}\right)^{0.179}\right.}\right) i^{0.51} \tag{19}$$

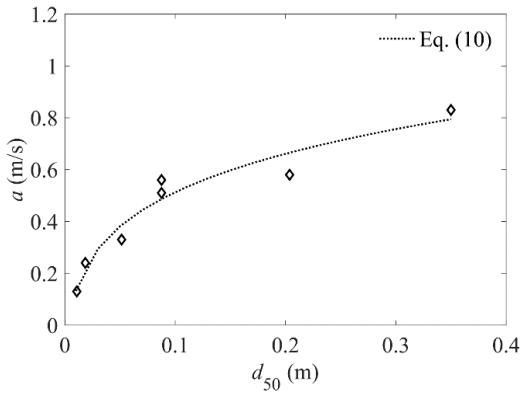

Figure 18. Relationship between parameter a and the mean rockfill particle sizes (d_{50}) (Ravindra et al, 2019b).

The proposed power-law relationship describing the correlation between hydraulic gradient and void-velocity of flow through rockfill embankments (Equation (18)) was further subjected to a comparative performance-based evaluation along with some well-establish power-law relationships from international literature. The Engelund (1953) (Equations (6) and (7)) and the Wilkins (1955, 1963) (Equation (8)) power-law relationships obtained from experimental studies conducted in permeameters, describing non-linear flow through rockfill medium are widely implemented in various disciplines of hydraulic engineering. These criteria have been included in the HydroCen study to investigate their validity in describing throughflow properties in actual rockfill embankments.

5.5 Rockfill dam models with disparate toe configurations *(M3)*

The HydroCen study described was aimed at investigating the effects of toe configurations on the hydraulic response of rockfill dam exposed to throughflow scenarios. The model studies were conducted within the same flume settings detailed in the previous sections. The basic model setup comprised of the downstream half of a 1:10 scale rockfill dam structure of height H_d = 1 m, bottom width B_b = 1.8 m, top width B_t = 0.3 m (Figure 19(a)) and transverse length L_d = 1 m. The downstream embankment slope was chosen to be S = 1 : 1.5 (H : V) complying with Norwegian rockfill dam construction practice (NVE, 2012). The impervious steel element incorporated in the model setup encompassed the dimensioning of the central core and the adjacent filter zones (Zone (B), Figure 19(a)). This is because, flow through the core, as well as the adjacent sand filter zone can always be considered to be laminar. Even for large rockfill dams, flow through these regions under throughflow conditions is unlikely to affect the stability of the downstream structure (Solvik, 1991). Since the objective of the experimental study was to investigate the behavior of downstream structure of rockfill dams simulating overtopping of the dam core, an impervious element representing the central core and filter zones was incorporated to simplify model design. All model dimensions were detailed following the guidelines offered by the Norwegian dam safety authorities (NVE, 2012).

Basing on a study of design and constructional aspects of several Norwegian rockfill dams, three discreet rockfill dam toe structures designs were identified, namely the external, internal and combined toe configurations. The external toe configuration represents a trapezoidal rockfill structure constructed on the downstream slope covering the toe region (Zone (F), Figure 19(b)). The internal toe configuration is characterized by a triangular region within the downstream embankment structure comprising of coarse rockfill material (Zone (E), Figure 10(b)). The combined toe configuration represents a coupling of the internal and external toe configurations (Zones (E) + (F), Figure 19(b)). The height of the toe structures were chosen as H_t = 0.25 m basing on a literature review of design of several existing Norwegian rockfill dams. The internal toe represents an equilateral triangle with altitude H_t. The external toe dimensions were so chosen as to achieve similar volume of construction as compared to the internal toe and to allow for sufficient length downstream of the dam structure to allow for complete flow development.

The rockfill dam models were constructed on a horizontal support platform of length L_p = 3 m, width W_p = 1 m and height H_p = 0.35 m. This was to elevate the entire test setup from the flume

bottom in order to avoid backwater effects (Figure 19). The experimental setup was situated sufficiently downstream of the inflow section of the flume to achieve calm flow upstream of the test models. A series of 10 pressure sensors (P1-P10) were coupled with the experimental setup for measurements of internal pore pressure developments at different locations within the dam structure as shown in Figure 19(a) and also for monitoring of the upstream/downstream water levels during the overtopping tests. The pressure sensors were connected to the platform through a pipe network linked to an array of holes as depicted in Figure 19(c). A series of four holes were provided along the width of the platform at each pressure measurement location for measurement of the average pressure levels and also as a safety precaution against blockage.

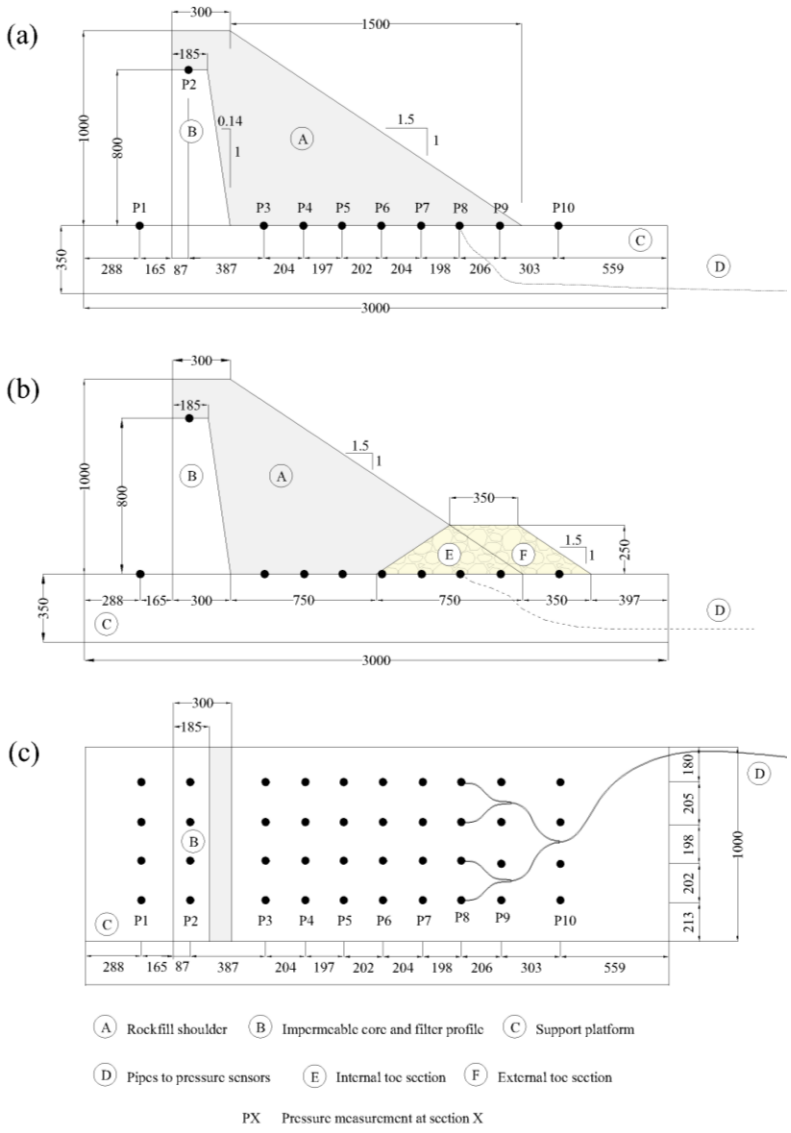

Figure 19. Depictions of the experimental setup with **(a)** planar view of the horizontal platform **(b)** sectional view of the rockfill dam model and **(c)** details regarding the disparate toe configurations.

Two SIEMENS SITRANS P210 sensors with pressure ratings of 0 to 2.5 m water column were employed at locations P1 and P2 and eight SIEMENS SITRANS P210 sensors with pressure ratings of 0 to 1.6 m water column were used at locations P3 to P10. These sensors provide reliable performance with high accuracy of 0.25% of the full-scale value. The sensors were in turn coupled with a data logging system to enable automatic data registration.

The dam shoulder comprised of well-graded rockfill material of density ρ_S = 2720 kg m^{-3}, median particle size $d_{50,S}$ = 0.0065 m and coefficient of uniformity of $C_{u,S}$ = 7.5. The toe sections were constructed employing uniformly graded coarse rockfill of density ρ_T = 2860 kg m^{-3}, median stone size $d_{50,T}$ = 0.052 m and coefficient of uniformity $C_{u,T}$ = 1.42. The material gradations were scaled down from a data base of gradation curves from large-scale rockfill dam constructions with a scaling ratio of 1:10. However, the gradation was biased towards the coarser range of the database. This was due to restrictions with the pumping systems installed in the laboratory, inclusion of very fine particles < 0.5 mm was not possible in the model. Hence, the gradation was carried out with 0.5 mm as the minimum allowed particle size.

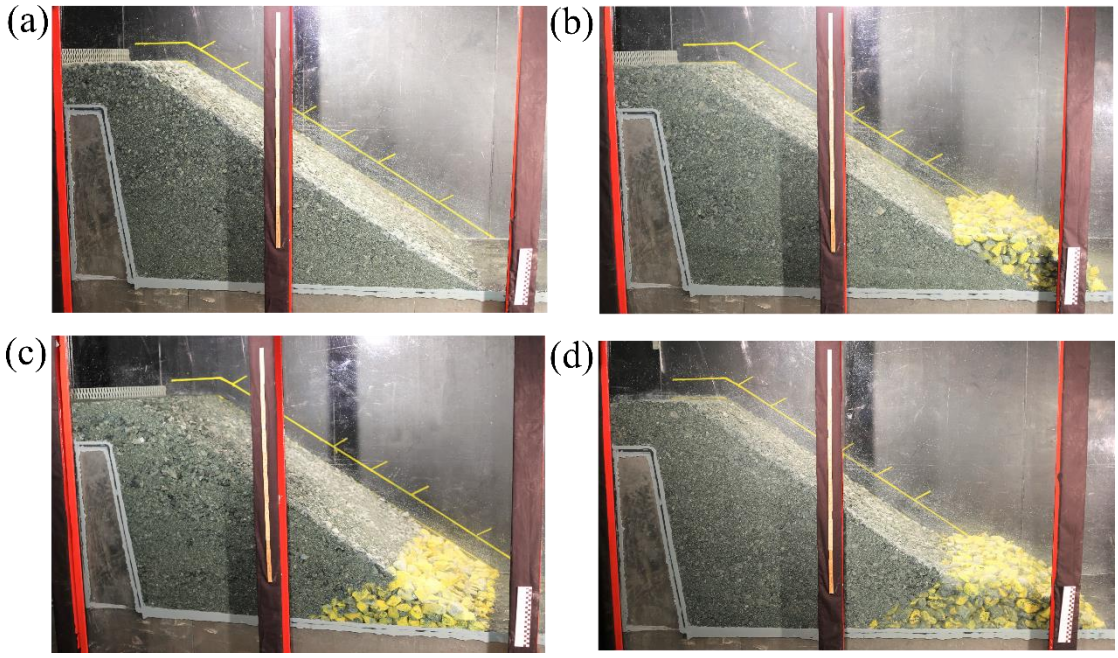

Figure 20. Depictions of the rockfill dams with (a) no toe, (b) external toe, (c) internal toe and (d) combined toe configurations.

The rockfill dam shoulder was built in layers of 0.1 m and were hand compacted using a 0.2 m x 0.2 m tamper weighing 4.54 kg (Figure 20). As a standard method of construction, the tamper was dropped free from a vertical distance of 0.1 m for 10 tampings at each location to achieve

uniform energy of compaction over the entire experimental testing program. The toe sections were constructed by manual placement of stones and were further hand compacted to avoid large voids in the structure.

5.5.1 Testing methodology

The study objective was to provide qualitative and quantitative descriptions of hydraulic responses of the dam structures exposed to incremental throughflow levels and to further evaluate and juxtapose the effects of disparate toe configurations on throughflow development. To accomplish these tasks, A total of twelve throughflow tests were conducted on model rockfill dam structures. A set of three tests were carried out with rockfill dam models without any form of toe. Further, a series of nine tests were conducted on rockfill dams provided with three different toe configurations, three tests per configuration for external, internal and combined toe geometries (Table 8).

Table 8. Descriptions of toe configurations, testing methodology and critical discharges.

Test no.	Toe configuration	q_i (. 10^{-3} m^3 s^{-1})	N (-)	Δt (s)	q_c (. 10^{-3} m^3 s^{-1})
1	No toe	1.0 - 3.5	6	1800	3.5
2	No toe	1.0 - 3.0	5	1800	3.0
3	No toe	1.0 - 5.0	9	1800	5.0
4	External	1.0 - 3.5	6	1800	3.5
5	External	1.0 - 5.5	10	1800	5.5
6	External	1.0 - 5.0	9	1800	5.0
7	Internal	1.0 - 4.0	7	1800	4.0
8	Internal	1.0 – 5.0	9	1800	5.0
9	Internal	1.0 - 4.5	8	1800	4.5
10	Combined	1.0 - 4.0	7	1800	4.0
11	Combined	1.0 - 3.0	5	1800	3.0
12	Combined	1.0 - 3.0	5	1800	3.0

The rockfill dam models were subjected to incremental levels of overtopping in regular discharge intervals of $\Delta q = 0.5 \cdot 10^{-3}$ m^3 s^{-1} commencing at $q_i = 1 \cdot 10^{-3}$ m^3 s^{-1}. The discharge levels were maintained constant over regular time periods of Δt = 1800 s to allow for flow stabilization at each overtopping interval. To analyze the development of throughflow patterns,

the pore pressure levels within the dam structure were recorded at various locations employing the pressure sensor- data logger setup at an acquisition rate of 100 Hz. Further, high quality images and videos of the tests were acquired. The procedure was repeated until complete erosion of the dam profile was achieved.

5.5.2 Effects of toe configuration on throughflow hydraulic properties of rockfill embankments

As described previously, pore pressures were measured at different locations within the dam structures (P2-P10) during the tests (Figure 20). In addition, the corresponding upstream water levels (P1) were recorded. The raw pore pressure datasets were subjected to a change point based statistical analysis to obtain representative pore pressure magnitudes at different discharge levels (q_i). The pore-pressure development patterns at different locations within the dam structure for Test 1 conducted with no toe (Table 8) are depicted in Figure 21. The pore pressure values depicted for each of the discharge intervals represent the stable values attained after maintaining the discharge magnitude at the respective levels over time periods of Δt = 1800 s. As can be observed, the individual pore-pressure levels within the rockfill shoulder were found to undergo non-linear increments as functions of the applied throughflow magnitudes for Test 1. The non-linear trends in pore-pressure developments were found to be less pronounced at the downstream section of the dam structure. Similar trends were observed for all the tests.

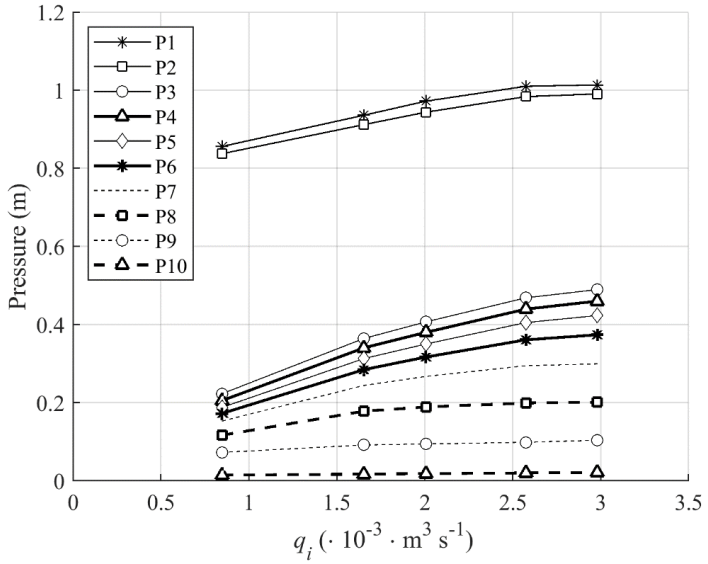

Figure 21. Pore pressure development profiles at different locations within the dam structure for Test 1 from Table 8.

The effects of different toe geometries on phreatic surface developments within the rockfill dam structures were investigated. Figure 22 depicts the positions of the phreatic surfaces within the model dams coupled with different toe configuration as derived from pore pressures measured at the ten pressure sensor locations (P1-P10, Figure 20). As can be observed from Figure 22, the flow patterns upstream of sensor location P3 were found to be consistent across models. During the tests, the water surface profiles upstream of the dam crest section (P1) were observed to be horizontal in nature as they entered the crest. Hence in Figure 22, the water surface profiles are shown as extensions of pressure measurements from P1 onto the entry surface of the crest using horizontal lines. Further, the drops in pressure from the entry location to P2 were used to plot flow lines with mild gradients over the core-filter element. Furthermore, the flow underwent transitions over the core-filter element and in turn plunged into the downstream dam structure towards P3. The plunge patterns were visually observed to be near vertical drops. This could be explained as a consequence of the steep slope of the core-filter element. A milder slope would lead to more moderate flow patterns.

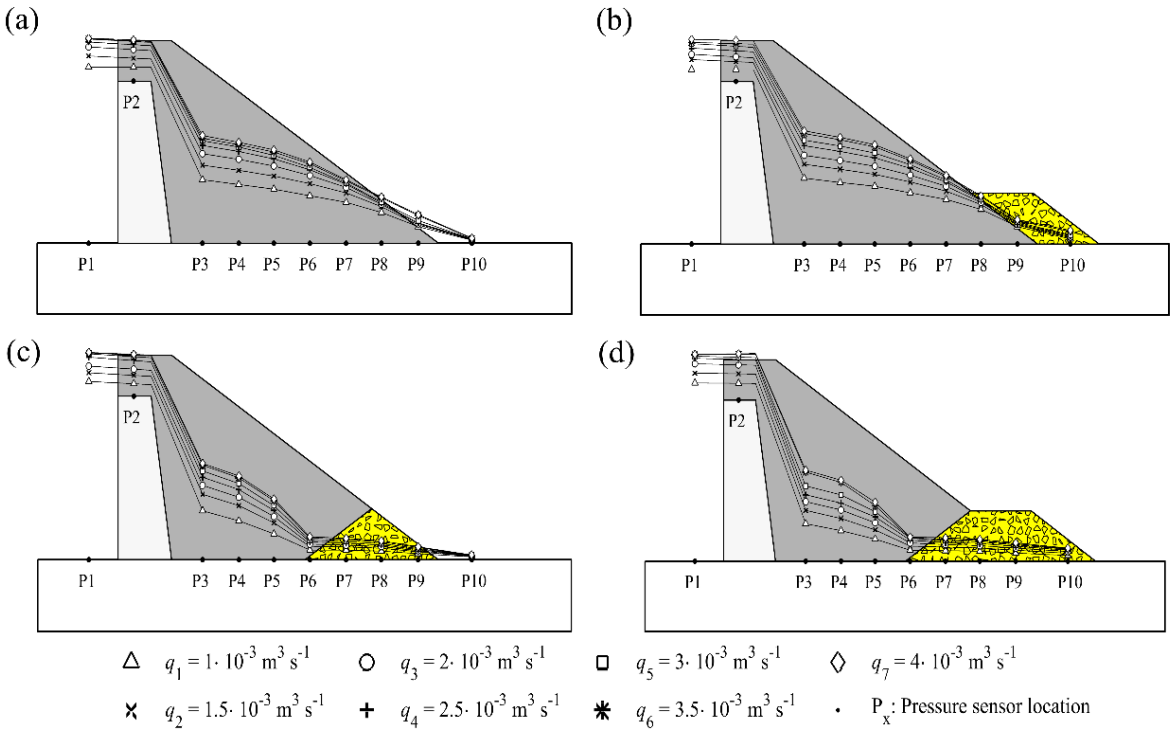

Figure 22. Phreatic surface depictions within model rockfill dams with **(a)** No toe, **(b)** external toe, **(c)** internal toe and **(d)** combined toe configurations as functions of applied throughflow magnitudes (q_i).

Further, for rockfill dam structures with no toe (Figure 22(a)) and with external toe (Figure 22(b)), closely resembling smooth non-linear phreatic surface profiles were observed within the rockfill shoulders. The pore-pressure development was found to be correlated to the applied throughflow magnitudes (q_i). The spacing between the phreatic surfaces were found to undergo decrements with incremental overtopping, owing to the non-linear nature of pore-pressure developments at each of the sensor locations (Figure 21). From visual observations of Figure 22, the external toe was found to have minor impact on throughflow development within the rockfill shoulder. Results from further quantitative analysis show that adding an external toe introduces friction losses within the toe structure. This results in minor elevations of the phreatic surfaces within the supporting fill, especially towards the downstream section. This in turn leads to reductions in total flow length along the phreatic surfaces. Further, due to the highly porous nature of the toe material, the flow downstream of the shoulder were found to be affected to a minor degree by the external toe configuration. The primary difference in behavior of the two structures was the additional protection offered by the external toe against scouring and erosion at the seepage exit face. Significant damages were observed at the toe sections of the rockfill shoulders for models constructed without toes. This was due to surface erosion resulting as a consequence of the drag forces generated over the seepage exit face and due to occurrence of occasional slides leading to scouring. However, no such damages were observed for dams constructed with external toes.

For dam models built with internal and combined toe configurations, significantly different pore pressure development profiles were obtained as juxtaposed with the dam models built with external toe and with no toe. The phreatic surfaces were found to be located at significantly lower elevations within the shoulders downstream of P3 entailing marked reduction in internal pore pressures. The phreatic surfaces experienced much steeper drops from P3 moving downstream towards P6 (Figure 22) resulting as a consequence of high permeability of the internal toe reaches. The pore-pressure magnitudes downstream of P6 were further seen to experience mild progressive reductions within the toe structures finally exiting the dam structure. The throughflow development patterns within the dam structures constructed with internal and combined toes closely resembled each other. The internal reaches of the high permeability zone give rise to disparate throughflow profiles. The external portion of the combined toe configuration from a theoretical standpoint result in marginal raising of internal pore pressures as described earlier. However, this was not seen from the recorded data, potentially due to variability in permeability of the shoulder material. No damage to the toe

sections were observed for either of the toe configurations even at maximum throughflow magnitude.

To further quantitatively describe the previously presented observations, several parameters were quantitatively analyzed. Percentage differences in pore-pressure magnitudes, differences in percentage areas of the dam structures exposed to pore pressure and the length of the phreatic surface profiles within the dam structures for different toe configurations were analyzed and compared. Reference is made to Kiplesund et al. (2020) for in depth discussions in this regard.

5.5.3 Failure initiation

Discharge levels for initiation of dam breach were recorded as part of the experimental testing program. As a key finding, critical locations for breach initiation were always found to be situated over the upstream crest of the dam structures being independent of the flow conditions in the lower reach of the dams. In essence, none of the tested dams experienced irreversible dam breach at the toe section even with the application of maximum throughflow magnitude which could be accommodated through the crest. Significant damage to the toe sections were observed for dams constructed with no toe. However, ultimate breach initiation leading to erosion of the dam structure were always found to be initiated at the overtopped upstream crest section.

Furthermore, no clear correlations were found between the magnitude of maximum throughflow required for initiation of dam breach and the toe configurations employed (Table 8). This in turn suggests that the amount of throughflow entering the dam structure is primarily dependent on properties of the dam crest such as the dimensioning and the permeability rather than on the downstream flow conditions. This also suggests that stability of rockfill dams under overtopping situations with unprotected downstream slopes is determined by features of the dam crest. However, during piping scenarios leading to entry of highly turbulent, large magnitude pressure flows into the dam structure, the rockfill dam toe could greatly help stabilize the dam structure. Further investigations in this regard are highly recommended.

5.6 Rockfill dam models with riprap (M4-A) and internal toe (M4-B)

As described in Section 4 of this report, the overarching research objective of the project has been to obtain a holistic evaluation of rockfill dam stability when exposed to extreme throughflow and/ overtopping situations. Hence, the next progression of the research was the inclusion of ripraps and rockfill toes with the parent dam structure. This would help obtain details regarding the interactions between the different dam components and ultimately help in identifying the critical component and location for initiation of dam failure.

Rockfill dam model presented as M3 (Figures 19 and 20) was further used as part of M4. For the model setup M4-A, the 1.8 m long downstream slope of the downstream dam slope was used for construction of ripraps with unrestrained toes (Figure 23 (a)). The same ripraps stones as used within M1 and M2 were further utilized. For the construction of ripraps with unrestrained toes, the methodology detailed within Section 5.3 for M2 was further adopted. The riprap model was built on a 0.1 m thick filter layer following the norm adopted within M1 and M2. The filter sections uniformly graded coarse rockfill of density ρ_F = 2900 kg m^{-3}, median stone size $d_{50,F}$ = 0.022 m with coefficient of uniformity $C_{u,F}$ = 1.2.

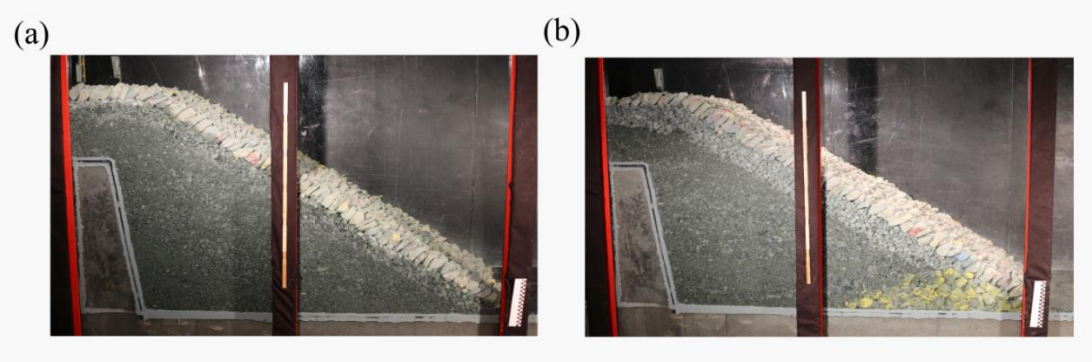

Figure 23. Rockfill dam model coupled with (a) riprap on the downstream slope and (b) with riprap and internal dam toe section.

Further within model setup M4-B, an internal toe section of dimensioning as depicted in Figure 19 was incorporated within the dam structure along with the overlying filter and riprap layers. This was to investigate the impact of rockfill dam toe on overall stability of the structure. The internal toe configuration was chosen as a result of the study outcomes from M3. The internal toe configuration demonstrated significant reductions in internal pore pressures as compared with the other configurations. Although the combined configuration also demonstrated similar performance as compared with the internal configuration, adoption of the external

configuration would lead to considerable increase in length of the riprap structure. To enable comparison with model setup M4-A, a decision was taken to include the internal dam toe within the model.

Furthermore, both model setups M4-A and B were further tested with incorporations of dumped ripraps to comprehend the difference in stability aspects between the two methods of construction. The construction methodology as detailed within Section 5.3 for dumped ripraps was further adopted.

5.6.1 Stability of rockfill dam structures exposed to overtopping

A total of 8 tests with different riprap and toe configurations were conducted. The details of the test setups and the testing methodology adopted are presented in Table 9. Upon construction of the dam models, the dam structures were exposed to low magnitude throughflows with regular discharge increments as presented in Table 9. The respective throughflow discharge magnitudes were maintained over a duration of 1800 s. This was done to achieve complete saturation of the dam structure with throughflow prior to being exposed to overflow conditions. Subsequent to complete saturation of the dam structure, overtopping flows were applied commencing at $q_i = 5.\ 10^{-3}\ m^3\ s^{-1}$ progressing in incremental discharge intervals of $\Delta q = 5.\ 10^{-3}\ m^3\ s^{-1}$ maintained over 1800 s intervals until complete failure of the dam structures were achieved (q_c).

From Table 9, it can be inferred that rockfill dam models provided with placed ripraps on the downstream slopes failed at an overtopping discharge magnitude of $q_i = 30.\ 10^{-3}\ m^3\ s^{-1}$. Visual observations of the failure process suggested sliding failure of the riprap structure in the same manner as described within Section 5.3.4 of this technical report concerning sliding failure of placed ripraps with unsupported toes. The riprap structures were found to undergo minor degree of initial compaction when applied to low magnitude overtopping flows. This was described previously as rearrangements taking place within the riprap structure due to voids present in the structure during construction. It should also be noted that no major movements of the riprap stones or the toe stones were observed when exposed to throughflows. Further, after these initial rearrangements, no further deformations within the riprap structures were observed with incremental overtopping exposure. This was also an observation from Section 5.3.4.

Table 9. Details of test setups and testing methodologies

Test no.	Riprap configuration	Toe configuration	q_i (. 10^{-3} m^3 s^{-1})	N (-)	Δt (s)	q_c (. 10^{-3} m^3 s^{-1})
1	Placed	No toe	1, 1.5, 3, 5-30	3,6	1800	30
2	Placed	No toe	1, 1.5, 3, 5-30	3,6	1800	30
3	Placed	Internal	1.5, 3 5-45	2,9	1800	45
4	Placed	Internal	1.5, 3 5-45	2,9	1800	45
5	Dumped	No toe	1, 1.5, 3 5-15	3,3	1800	15
6	Dumped	No toe	1, 1.5, 3 5-20	3,4	1800	20
7	Dumped	Internal	1, 1.5, 3 5-30	2,6	1800	30
8	Dumped	Internal	1, 1.5, 3 5-25	2,5	1800	25

Dam failure commenced at an overtopping discharge magnitude of q_c = 30. 10^{-3} m^3 s^{-1}. The failure was observed to commence at the riprap layer when the riprap structure as a whole was found to undergo sliding commencing at the toe section. The underlying rockfill shoulder was observed to be stable at this time period in turn suggesting the overlying riprap layer as the critical component as far as failure initiation under overtopping conditions are considered. The failure in essence commences as further progresses from the toe section as the riprap layer slides down as a unified member upon toe yield. The term toe yield refers to the point in time at which the applied hydrodynamic forces exceed the frictional forces at the contact points between the toe stones and the horizontal platform with geotextile.

Further considering rockfill dam models coupled with dumped ripraps, the average failure discharges were found to be reduced to q_c = 17.5. 10^{-3} m^3 s^{-1}. This was a 42% reduction in the critical discharge magnitude as compared with dams protected with placed ripraps. This suggested that placed ripraps on the downstream slopes of rockfill dams offer significantly higher degree of stability as compared with dumped ripraps. Also, following the findings from Section 5.3.4, failure of dumped ripraps could be attributed to random dislodgements of individual riprap elements.

For reference, tests conducted with dams with unprotected slopes (Table 8) can be considered. From Table 8, it could be noticed that average failure discharge for dams with unprotected downstream slopes was $q_c = 4.\ 10^{-3}\ m^3\ s^{-1}$. This entails that a dam protected with dumped riprap on the downstream slope results in about 3-4 times more stable dam profile as compared with an unprotected dam. Furthermore, a dam protected with placed ripraps could result in 7-8 times higher stability when compared with an unprotected dam.

Inclusion of an internal toe within the dam structure resulted in stability gains for both placed and dumped ripraps. For placed ripraps, critical failure discharge magnitudes were found to undergo increments from $q_c = 30.\ 10^{-3}\ m^3\ s^{-1}$ to $q_c = 45.\ 10^{-3}\ m^3\ s^{-1}$, which is a 50% increment. Further for dumped ripraps, the average critical failure discharge magnitudes were found to undergo increments from $q_c = 17.5.\ 10^{-3}\ m^3\ s^{-1}$ to $q_c = 27.5.\ 10^{-3}\ m^3\ s^{-1}$, which is a 36% increment in stability. The reasoning behind this increment could be derived considering findings from M3. Rockfill dam models coupled with internal toes were found to result in significant reductions in internal pore-pressures. This suggests that under throughflow conditions, inclusion of an internal toe leads to lower degree of exposure of the downstream slope at a particular overtopping magnitude as compared with a dam without an internal toe. This suggests that complete submergence of the riprap structure happens at a higher discharge level as compared with a dam without a toe structure. Findings from Section 5.5.3 suggest that the magnitude of throughflow entering the downstream shoulder is controlled by the dimensioning and the material properties of the crest. However, for a given throughflow magnitude, it was also evident from Section 5.5.2 that the internal toe yields the lowest pore pressure magnitudes as compared with a dam provided with no toe or an external toe. This also further entails that inclusion of internal toe would lead to significant delays in complete submergence of the riprap and hence, delayed failure.

Further, due to the coarse nature of the material used for the construction of the internal toe, the exit throughflow would have much higher velocities as compared to a dam without internal toe. This could lead to crossing of high velocity flow velocity vectors between the exit throughflow forces and the overflow forces leading to attenuation of flow forces and in turn, lower degree of resultant forces on the riprap toe stones (Figure 24).

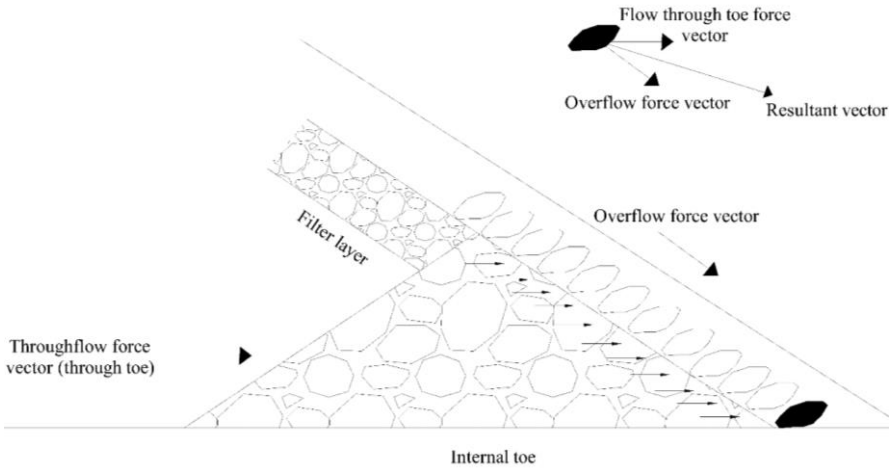

Figure 24. Flow force vectors depiction.

Although the described effect is challenging to discern visually at high discharges, it is clearly evident at low discharges. Figure 25 presents a snapshot from Test 3 (Table 9). Overflow in the model was generally found to be characterized by white water (highly aerated) flow. As can be seen from Figure 25, the upper reaches of the riprap is covered with aerated flow. However, the flow over the riprap section covering the exit face of the internal toe does not have any white-water flow over it. This can be explained as due to the effect brought to light earlier. The overflow gains high velocities under the influence of gravity as it skims over the riprap. As the flow reaches the toe section, the flow vector is disrupted by the throughflow vector exiting the toe section which leads to rapid reductions in the flow velocities and in turn, flow forces on the riprap stones at the toe section.

Figure 25. Snapshot from Test 3 (Table 9) depicting overflow.

6 Holistic evaluation of research findings

Two principle research objectives were defined earlier within the report. **Objective 1** was oriented towards obtaining a holistic description of stability and failure mechanisms in ripraps exposed to overtopping. Further, **Objective 2** was focused on evaluating the hydraulic response of rockfill embankments subjected to throughflow scenarios. The present section is aimed at providing overarching interpretations of key research findings from the different studies with emphasis on addressing the laid-out objectives.

6.1 Holistic evaluation of riprap stability under overtopping conditions (*Objective 1*)

The main research outcomes from model studies M1, M2 and M4 are discussed within the present sub-section. The objective of these discussions is to bring out the significance of the research on ripraps and to provide an overarching evaluation of the relationship between the different studies. These are in turn intended at presenting a holistic evaluation of the research program on ripraps as a whole.

6.1.1 2D deformation behavior in toe supported placed ripraps on steep slopes (*M1*)

Several past research works such as Hiller et al. (2018), Dornack (2001), Sommer (1997), Larsen et al. (1986) and Siebel (2007) have described 1D failure mechanism in placed riprap provided with toe support exposed to overtopping flows. These studies have introduced novel techniques and methodologies for detection of riprap stone displacements. These have also provided valuable insight into the longitudinal compaction process occurring within the riprap structure. Findings related to 2D deformations in placed ripraps with toe support (***M1***) under overtopping conditions obtained from the present research work add to the available international literature on the research topic. The results obtained from the study demonstrate that toe supported placed ripraps constructed on steep slopes exposed to overtopping flows undergo a 2D buckling process analogous to the buckling profile of a long-slender column under compression pinned at one end and free at the other end (Figures 9 and 10). This can be explained as a direct consequence of the interlocking forces generated between the individual riprap stones forming a bearing structure capable of withstanding certain degree of deformations. Placed ripraps supported at the toe exposed to overtopping undergo initial

compaction to form a unified riprap structure. Further increment in the applied hydraulic loading which in turn results in higher drag and lift forces on the riprap structure. The drag forces lead to compaction of the riprap along the chute length and a combined effect of the bending moments and in part, the hydraulic lift forces generated within the riprap structure lead to out of plane deformations. This process eventually leads to ultimate structural collapse of the riprap structure.

Numerous past studies investigating placed riprap stability have concluded that the erosion of single stones in a placed riprap does not necessarily result in the loss of the structural integrity of the placed riprap structure (Hiller et al., 2018; Dornack, 2001; Sommer, 1997; Larsen et al., 1986). The findings of the HydroCen study provide evidence in support of this statement. Since placed ripraps exposed to overtopping loads form a unified structure as a consequence of the generated interlocking effect, detachment of a single loosely placed stone from the structure does not necessarily entail loss of structural integrity as the configuration of the neighboring stones can still offer a considerable degree of resistance against the destabilizing force. This in turn entails that placed riprap stability is not governed by individual riprap elements but rather that the unified structure formed due to interlocking of the ripraps stones as a whole resists the applied hydraulic loading. This behavior is comparable to the response of structural elements, such as a masonry structure acted on by external loading.

The qualitative and quantitative descriptions of the unique failure mechanism observed in toe supported placed ripraps further relate the fields of hydraulic and structural engineering. This provides a fresh perspective on design and construction of placed ripraps and hydraulic structures in general. Design approaches currently employed in hydraulic engineering generally place emphasis on the geometrical and flow boundary conditions, material characteristics and fluid properties. However, design methodologies taking into account the multilayered behavior of these structures are seldom encountered. Findings of the HydroCen study document the fact that stability of toe supported placed ripraps constructed on steep slopes is a predictable mechanism following the principles of an established structural theory. This leads to the possibility of incorporation of buckling as a failure mechanism within the design process, which can enhance the effectiveness of the process as numerous design parameters such as stone size and chute length, can be strategically designed to accommodate or impede the formation of buckling in ripraps.

This method of interrelating knowledge from different research disciplines should in general be applicable to every scientific branch. Perhaps the most significant takeaway from the results presented within the study evaluating buckling in placed ripraps could be that no research discipline is self-sufficient. In other words, drawing from gathered knowledge within different research areas can only strengthen and reinvigorate our scientific quest.

6.1.2 Significance of toe support on riprap stability (*M1, M2 and M4*)

The fundamental objective of experimental hydraulic research is to obtain accurate and realistic descriptions of behavior of structures and processes occurring within these structures as applicable to prototype scales. In order to obtain realistic portrayal of riprap stability under overtopping scenarios, it is of essence to incorporate, as far as possible, test conditions closely resembling those found in the prototype scale. The 2D deformation behavior in placed ripraps resembling column buckling was found in model placed ripraps provided with fixed toe supports (Figures 9 and 10). However, field survey of placed ripraps constructed on rockfill dams clearly demonstrated the fact that existing placed riprap structures are not provided with any form of systematized or well-designed toe supports (Figure 12). Incorporation of this finding into the experimental model studies in the lab gave rise to new results regarding riprap stability in general. In contrast to the 2D deformations observed in placed ripraps provided with toe support (***M1***), placed ripraps unsupported at the toe section (***M2***) were found to undergo sliding failure at a significantly lower overtopping magnitude (Figure 13).

Placed riprap stones experience minor degree of reorientations and displacements along the downstream chute direction following initial exposure to overtopping flows. Upon initial exposure to overtopping, the incremental hydraulic drag and lift forces and the resulting vibrations lead to rearrangements of the individual stones wherein the riprap structure undergoes compaction to fill the voids. Following these initial readjustments, the individual stones achieve a stable configuration leading to the formation of a unified riprap structure due to generation of interlocking forces between the individual stones. Upon further increment in overtopping magnitude, the riprap structure is exposed to higher destabilizing hydraulic forces. These are in part transferred on to the underlying filter layer as frictional forces. A part is also directed towards the riprap toe where the static frictional forces setup between the toe stones and the geotextile membrane laid on the horizontal platform increase in magnitude to counter the incremental hydrodynamic forces transferred towards the toe. Furthermore, initiation of riprap collapse marks the point of time at which the magnitude of the impacting hydrodynamic

forces exceed the limiting values of the static frictional forces between the toe stones and the horizontal platform and also the riprap-filer interface. This frictional yield results in displacements of the toe stones and following this event, the riprap structure in its entirety undergoes a progressive slide on the underlying filter layer, further forming a pile on the flume bottom.

Juxtaposition of these two disparate failure mechanisms in placed ripraps helps bring out the importance of toe support conditions in discerning the failure mechanism in placed ripraps. In case of a constrained toe structure as employed in ***M1*** (Figure 6), the riprap structure is likely to fail as a consequence of structural collapse or buckling as the toe support structure provides unlimited resistance stabilizing the toe, in turn eliminating the possibility of sliding of the riprap structure. Under such conditions, the riprap structure experiences some degree of compaction during initial stages of overtopping exposure and further, following the formation of a unified riprap structure, incremental overtopping flows give rise to development of progressive 2D deformation profiles in ripraps resembling the buckling process in a slender-long column. However, in case of an unrestrained toe, the placed riprap section slides along the steep slope as a result of limited frictional resistance offered at the toe section. Hence, findings from the HydroCen study demonstrates that the configuration of the toe section of placed riprap as a key factor influencing the overall failure mechanism. Further, Hiller et al. (2018) investigated 1D displacement of riprap stones in ***M1*** (Figure 13) and showed that compaction of the riprap structure at the downstream end leads to formation of a gap at the upstream crest of the riprap. However, this was not observed within ***M2*** (Figure 13) as the limited frictional forces setup at the interface between the toe stones and the horizontal platform do not allow for such a high degree of compaction to occur. The riprap structure experiences sliding failure due to toe yield before any major compaction or 2D deformation of the riprap structure could occur.

In contrast, failure mechanism in dumped ripraps was found to be similar between model setups ***M1*** and ***M2***. The riprap stones were found to undergo a surface erosion process where individual stones were eroded by the action of destabilizing turbulent flow forces. This contrasted with failure initiation in placed ripraps with unsupported toes (***M2***) wherein the riprap structure as a whole was found to undergo a slide. This difference in the failure mechanisms can be described as due to the absence of interlocking forces between individual riprap stones. Since dumped ripraps comprise of randomly arranged stones, individual stones are not interlocked with the adjacent elements. When the dumped riprap structure is exposed to overtopping flow forces, the individual stones counter the flow attack primarily through self-

weight of the individual elements and the bottom frictional forces generated at the riprap-filter interface. Failure initiation marks the instant at which the magnitude of the destabilizing hydrodynamic forces exceed the resultant of the stabilizing self-weight and the frictional forces. Hence, dumped riprap failure can be stated as the resultant of progressive unraveling erosion of individual riprap elements whereas placed riprap failure entails sudden slide of the entire riprap structure. This clearly documents the fact that toe support conditions can have significant influence on underlying failure mechanism in placed ripraps but dumped riprap failure mechanism is unaffected by toe support conditions.

This also provides an explanation for higher velocities measured for stone displacements in placed ripraps during failure as compared to dumped riprap stones. Placed ripraps experience an instantaneous slide following toe yield wherein the riprap structure moves down the slope as a unit. Whereas dumped riprap failure entails erosion of discreet riprap elements wherein individual stones suffer collisions with one another during the erosion process thereby resulting in loss of kinetic energy. Further, placed riprap failures were found to be initiated at higher overtopping magnitudes as compared with dumped ripraps. As a combined effect of these two causes, placed riprap stones travel on the slope at higher velocities than dumped riprap stones.

A brief summary of key findings regarding critical discharge magnitudes and failure mechanisms across model setups both for placed and dumped ripraps are presented in Table 10 for ease of reference. The critical overtopping discharge magnitudes for initiation of riprap collapse (q_c) were found to be q_c = 60. 10^{-3} m^3 s^{-1} and 40. 10^{-3} m^3 s^{-1} for placed and dumped riprap respectively within ***M2*** (Table 10). This in turn entails that placed ripraps unsupported at the toe offer 1.5 times higher stability, characterized by the critical overtopping magnitude as compared with dumped riprap. Past experimental studies conducted on placed riprap models provided with fixed toe supports such as Hiller et al. (2018), Peirson et al. (2008), Dornack (2001) and Larsen et al. (1986) have also demonstrated that placed ripraps offer higher stability as compared to dumped riprap, especially at steep slopes. Hiller et al. (2018) documented average critical overtopping magnitudes of q_c = 300. 10^{-3} m^3 s^{-1} and 40. 10^{-3} m^3 s^{-1} respectively for placed and dumped ripraps resulting in a ratio of average critical discharge values of 7.5. The fivefold reduction in placed riprap stability in terms of average critical overtopping discharge magnitude required to achieve placed riprap from q_c = 300. 10^{-3} m^3 s^{-1} within Hiller et al. (2018) to q_c = 60. 10^{-3} m^3 s^{-1} within the HydroCen study can be attributed to the absence of a toe support structure. However, dumped riprap stability can be stated as being unaffected by toe support conditions as the critical discharge for failure initiation remained constant at q_c

= 40. 10^{-3} m^3 s^{-1} between model setups. These findings further add to the earlier statement that toe support conditions can have considerable impacts on placed riprap stability and not on the stability aspects of dumped ripraps.

Table 10. Summary of critical discharges and failure mechanisms across model setups

Sl. no	Riprap type	Toe support condition	Model setup	Avg. Critical discharge (q_c) (. 10^{-3} m^3 s^{-1})	Failure mechanism
1	Placed	Fixed toe support	M1	300	2D buckling like deformations
2	Placed	Unsupported	M2	60	Sliding
3	Dumped	Fixed toe support	M1	40	Surface erosion
4	Dumped	Unsupported	M2	40	Surface erosion
5	Placed with dam	Unsupported	M4-A	30	Sliding
6	Placed with dam and internal toe	Unsupported	M4-B	45	Sliding
7	Dumped with dam	Unsupported	M4-A	17.5	Surface erosion
8	Dumped with dam and internal toe	Unsupported	M4-B	27.5	Surface erosion

Table 10 also presents results from the full dam (M4-A and B) studies conducted as part of the research activities aimed at obtaining a holistic picture of rockfill dam stability when subjected to extreme loading. A major trend can be observed within Table 10 with regards to stability of placed ripraps. The absence of toe support within M2 led to a fivefold reduction in critical discharge magnitude from q_c = 300. 10^{-3} m^3 s^{-1} to 60. 10^{-3} m^3 s^{-1}. Furthermore, coupling of the placed riprap structure with a full dam resulted in further reduction in critical discharge from q_c = 60. 10^{-3} m^3 s^{-1} to 30. 10^{-3} m^3 s^{-1}. This reduction could be attributed to introduction of throughflow within the model. The additional throughflow exiting the rockfill shoulder within M4-A would also be directed towards the riprap toe stones in addition to the overflow and the flow through the filter layer. This additional flow attack could lead to earlier yielding of the toe stones leading to ultimate riprap and dam failure.

Furthermore, the stabilizing effects offered by introduction of the internal toe within model setup M4-B have been outlined in detail within section 5.6.1. This in turn led to increase of the critical discharge magnitude from q_c = 30. 10^{-3} m^3 s^{-1} to 45. 10^{-3} m^3 s^{-1}. Similar trends in stability could be observed for dumped ripraps. Combining dumped riprap structures with full dams resulted in reduction of critical discharge levels from q_c = 40. 10^{-3} m^3 s^{-1} to 17.5. 10^{-3} m^3 s^{-1}. Furthermore, introduction of the internal toe within model setup M4-B for dumped ripraps led to increase of the critical discharge magnitude from q_c = 17.5. 10^{-3} m^3 s^{-1} to 27.5. 10^{-3} m^3 s^{-1}.

6.2 Flow through rockfill dams (*Objective 2*)

The present sub-section is intended at providing a broader perspective on the main results from research activities dealing with the hydraulic behavior of rockfill dams subjected to throughflow conditions.

6.2.1 Effects of toe configurations on throughflow

Considering the various phases involved in rockfill dam overtopping, it is evident that the first phase would be exposure of the dam shoulder to throughflow. Hence, to obtain a better understanding of response of rockfill dam shoulders comprised of uniform material subjected to throughflow, pertinent data sets accumulated as part of the IMPACT project were further analyzed as detailed in Section 5.5.4. Statistical evaluation of the data (Figures 17 and 18) gave rise to a general non-linear power law (Equation 19) describing the velocity-gradient relationship within the dam structures. This essentially signifies that flow through rockfill structures is a predictable process which can be characterized and quantified to form a general flow law. This further provides a description of the interaction between external hydraulic loading and the response of the dam structure.

Research outcomes from the HydroCen study are of significance also considering the fact that existing non-linear flow laws widely implemented in rockfill engineering applications were originally developed in the 1950's and the 1960's (Table 1) through small scale permeameter studies. Validity of these relationships were not tested in applications relating to real rockfill dam structures and especially at large scales. Findings from the HydroCen study address these concerns as data sets from model studies encompassing rockfill dam models of board ranging sizes of 0.6 m to 6 m in height and constructed with material of sizes d_{50} = 10.2 mm to 350 mm were evaluated to arrive at Equation (19). The performance of Equation (19) with respect to its

ability to predict experimental data was juxtaposed with existing relationships (Equations (6), (7) and (8)). Study outcome revealed higher correlation between predictions and observations for Equation (19) as compared with existing relationships.

Development of a sophisticated numerical model capable of simulating rockfill dam breach has been considered an uphill task owing to the complexity of the task at hand. Multitudes of external and intrinsic factors affect dam breach initiation and progression. Findings from the HydroCen study provides valuable information in this regard for implementation of non-linear throughflow characteristics of rockfill dams comprising of uniform material within these numerical models.

6.2.2 Effects of toe configurations on throughflow

Building on the results from the study, a new experimental program was devised to further our understanding of throughflow aspects of rockfill dams regarding effects of disparate toe configurations on throughflow development (Models **M3-A** to **D,** Figure 5). Widely implemented rockfill dam toe types such as the external, internal and combined toe configurations were investigated. Study outcomes provide quantitative and qualitative descriptions of throughflow development in rockfill dams coupled with different toe configurations as a function of throughflow magnitude (Figure 22).

Quantitative description of throughflow development in rockfill dams basing on experimental data is seldom found in international literature. Further, experimental corroboration of differences in hydraulic performance of disparate rockfill toe configurations has been rare. Findings from the HydroCen study add valuable knowledge to the international literature on behavior of rockfill dam structures exposed to throughflow. Investigation results enable effective engineering decision making with regards to ideal choice of rockfill dam toe design based on site-specific design restrictions. This facilitates rockfill dam design process and can further help strengthen the design both from economical and stability standpoints. Considering research applications, data sets accumulated as part of the experimental testing program could be further employed for validation of theoretical studies conducted in the past within the study discipline. Furthermore, the data sets could be valuable for calibration and validation of numerical models predicting throughflow behavior in rockfill embankments. Enhancement of capabilities of commercially available numerical seepage models could be of high interest for researches and also for agencies involved with rockfill dam design and safety assessment.

7 Towards the NVE guidelines for rockfill dams

Findings from the studies presented within this technical report establishes that toe conditions for placed ripraps plays a pivotal role in discerning the underlying failure mechanism and also, overall riprap stability. Dumped riprap stability was found to be unaffected by toe conditions. This finding has significant practical relevance, especially in light of the outcomes from the field survey which suggests that existing placed ripraps are unsupported at the toe. Further, inclusion of a toe structure with the rockfill dam also was found to have a considerable stabilizing effect on riprap in the physical models and in turn, overall rockfill dam stability. The following discussions presented within this section of the report take a look at the guidelines offered by the NVE with regards to design and construction of placed ripraps. The objective is to bring out comparative evaluations between findings from lab studies and the NVE recommendations.

Within Section 3.1 of this report, a brief discussion into the NVE guidelines for sizing of placed riprap elements was presented as Equation (2). Table 11 further presents the recommended design discharges for placed ripraps built on dams belonging to different consequence classes. By using these recommended design discharges within Equation (2), the minimum required sizing of riprap stones for placed ripraps built on the respective dam classes can be arrived at as presented in Table 11. Further, in order to achieve comparability of lab results with the NVE guidelines from Table 11, carrying out scaling of lab results to the prototype scale is necessary. This can be achieved employing the Stone related Froude number ($F_{S,C}$) (Equation 10). This method of scaling, only applicable to scaling of critical discharge values of the surface layer riprap stones works on the assumption that $F_{S,C}$ would be constant both at the laboratory and the prototype scale, considering fully turbulent flow. This technique has been used by several past experimental studies such as Hiller et al. (2019) for comparison of laboratory and prototype results. Hence, this yields to Equation (20):

$$Fs,c = \frac{q_m}{\sqrt{g{d_m}^3}} = \frac{q_p}{\sqrt{g{d_p}^3}} \tag{20}$$

where q_m and q_p stand for the critical discharge magnitudes at model and prototype scales respectively and d_m and d_p denote the median stone sizes at the model and prototype scales respectively. Further rearranging Equation (20) results in Equation (21):

$$q_p = q_m \sqrt{\frac{{d_p}^3}{{d_m}^3}} = q_m S_f \quad (21)$$

Using Equation (21), the critical discharge from the lab scale (q_m) could be scaled up to the prototype scale through a discharge scaling factor S_f (Table 11).

Table 11. Details of the NVE recommendations and the discharge scaling factors.

	Class 4	**Class 3**	**Class 2**
Design discharge (NVE) ($m^3 s^{-1} m^{-1}$)	0.7	0.5	0.3
D_{min} (NVE) (m)	0.64	0.49	0.33
Discharge scaling factor (-)	37.6	25.2	13.9

A total of 8 different riprap models were tested as part of the research activities conducted at NTNU, Trondheim. The different configurations were characterized by toe support conditions, inclusion of a rockfill dam shoulder structure and also, an internal toe structure. The results from the laboratory overtopping tests on these models were presented in Table 10. The critical discharge levels were further scaled to the prototype scale using Equation 21. The scaling was carried out for the three dam safety classes defined by the NVE (Table 11). The scaled discharge levels at the prototype scale are presented within Table 12.

As can be observed from Table 11, the scaled discharge values occupy a broad spectrum from 0.24 $m^3 s^{-1} m^{-1}$ to 11.29 $m^3 s^{-1} m^{-1}$. The intention of the analysis is to evaluate the discharges against the recommendations put forth by the NVE (Table 11). As a general observation, scaled discharges for all 3 dam classes from 7 out of the 8 tested models were found to exceed the NVE recommended design discharge values. Dumped ripraps with unsupported toes constructed on rockfill dam models were the only exception to this observation. To further bring out the essence of the comparison between the scaled discharge levels and the NVE guidelines, safety factors were computed as ratios of the scaled discharge levels and the NVE recommended design discharge magnitudes (Table 12). Also, the average safety factors for each of the 8 models have been presented within Table 12 and also plotted for easy visual observation as Figure 26.

Table 12. Details of scaling and safety factor computations.

Setup no	Riprap type	Toe support condition	Scaling from lab to prototype, q_p (m^3 s^{-1} m^{-1})			Safety factors SF (-)			
			Class 4	Class 3	Class 2	Class 4	Class 3	Class 2	Average
1	Placed	Fixed support	11.29	7.56	4.18	16.1	15.1	13.9	15.1
2	Placed	Unsupported	2.26	1.51	0.84	3.2	3.0	2.8	3.0
3	Dumped	Fixed support	1.50	1.01	0.56	2.1	2.0	1.9	2.0
4	Dumped	Unsupported	1.50	1.01	0.56	2.1	2.0	1.9	2.0
5	Placed with dam	Unsupported	1.13	0.76	0.42	1.6	1.5	1.4	1.5
6	Placed with dam and internal toe	Unsupported	1.69	1.13	0.63	2.4	2.3	2.1	2.3
7	Dumped with dam	Unsupported	0.66	0.44	0.24	0.9	0.9	0.8	0.9
8	Dumped with dam and internal toe	Unsupported	1.03	0.69	0.38	1.5	1.4	1.3	1.4

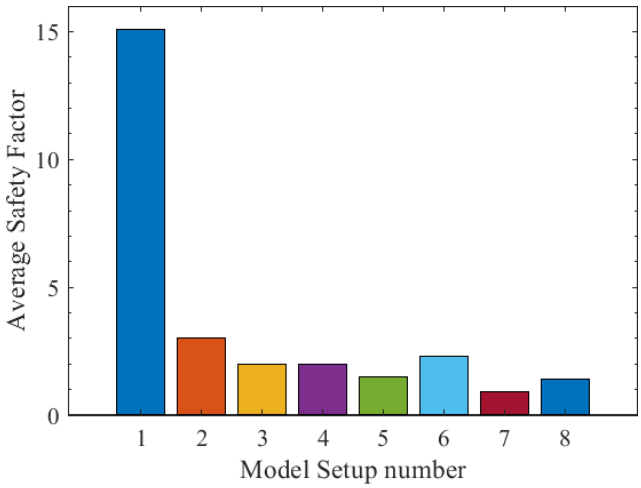

Figure 26. Average safety factors for different model setups.

From Table 12 and Figure 26, it can be observed that the safety factors range over a wide span of 0.9 to 15.1. The highest safety factor was computed for placed riprap models provided with fixed toe support. All configurations of placed riprap models tested were found to have safety factors of over 1.5. All tested dumped riprap configurations also nearly meet the NVE recommendations, apart from model setup 7 with a safety factor of 0.9. Some key conclusions could be drawn from these analyses:

1. All placed riprap models tested without the provision of fixed toe supports were found to meet the NVE guidelines with safety factors within the intervals 1.5 - 3. Considering that in practice, a safety factor is always assumed for design of critical infrastructure, the guidelines cannot be stated as being too conservative. This is even more applicable considering findings from the survey conducted to investigate toe support conditions for placed ripraps constructed on Norwegian rockfill dams. Model setups 5 and 6 appear to be the most commonly encountered rockfill dam structures in Norway. These models were found to have safety factors of 1.5 and 2.3 respectively. Hence, taking into account the critical nature of these structures with regards to protection against accidental overtopping events or sabotage, these safety factors could be considered as reasonable, particularly since safety factors on these critical discharges are not required by the regulations.

2. Taking a look at dumped ripraps, all the tested models were found to nearly meet the requirements of the NVE guidelines with safety factors of 0.9 - 2.0. placed riprap construction is resource intensive in terms of material requirements and manual and mechanical labor in comparison with dumped riprap construction, the efficacy of placed

riprap construction could be questioned. If the objective is to achieve acceptable degree of stability, even dumped ripraps, with slightly larger sizing compared to placed riprap, could meet the safety requirements against overtopping. Results from the HydroCen study reveal that there is a difference in stability between placed and dumped ripraps with placed ripraps offering higher stability. But with the currently adopted methods of construction, it appears that there is not a significant gain in stability achieved by construction of placed ripraps, especially considering the cost of construction.

3. The NVE, (2012) recommends design specifications for placed ripraps in general. However, protocols addressing specifics on the design aspects of toe support for the riprap structures are currently unavailable. The available references within the NVE recommendations pertinent to riprap toe stability state that it may be necessary to secure the lowermost part of the downstream slope and the abutments of rockfill dams with larger stones, or other reinforcing measures based on the dam cross-section and overtopping flow magnitude. It is also stated that rock foundation should provide good support against sliding of the toe stones. If the foundation should provide good support against sliding of the toe stones, one has to blast a trench or cast a foot, especially for foundations with inclinations larger than 10°. Although these statements point out key design considerations with regards to riprap design, design criteria for riprap toe support structures is currently not provided. But, from Table 12, it is apparent that placed ripraps provided with suitable toe support could potentially lead to significant increments in placed riprap and in turn, rockfill dam stability. However, this may be dependent on the height of the dam compared to the physical model. Still, to support for increased stability might be of value for cases where the stone size does not fulfill the criteria and could be counteracted with a toe support.

4. A similar argument could be made with regards to inclusion of internal rockfill dam toe structures. This was shown to considerably increase riprap and dam stability, irrespective of the riprap type. As of present, no reference to technical details regarding construction of rockfill dam toes can be found within NVE, (2012).

The research activities summarized within this technical report point to some key parameters which can be considered to have significant impact on overall rockfill dam stability. In all the tests conducted with full dam models covered with placed ripraps (M4), as is generally the case

for high consequence rockfill dams in Norway, failure was always found to initiate at the riprap layer. Furthermore, due to yielding of the toe stones leading to sliding of the whole structure. Further exposure of the underlying filter and shoulder to overtopping leads to erosion of the entire dam structure. Hence, toe sections for placed ripraps could be considered a critical location which can influence rockfill dam stability to a considerable extent. Hence, looking into arriving at well-defined toe stabilizing measures would be beneficial in augmenting placed riprap and in turn rockfill dam stability. Findings from Table 12 clearly point to the fact that inclusion of toe support for ripraps increases stability. However, Table 12 also indicates that the current practice without toe support fulfills the current guidelines, but then it must be considered at this can only be considered to apply for foundation condition that are comparable to the experimental setup, i.e. horizontal foundation. If the foundation slopes down away from the dam, toe support should be considered to increase the stability. Additionally, the shape of the riprap stones used in the physical model must be considered in any comparison to a real dam.

8 Further research activities

The experimental research works conducted at NTNU, Trondheim over the years have made valuable contributions with regards to obtaining better understanding of the behavior of rockfill dams subjected to extreme conditions. However, there is much progress to be made in the future to carry out further research within the frameworks laid by past studies. This section of the report is dedicated to outlining some of the potential further research activities that should be carried out in the coming years to further elaborate on the findings presented within this report.

8.1 Research with rockfill dams coupled with placed ripraps supported at the toe section.

The next step in developing the research findings from several riprap models investigated over the past years (Table 10) would be the inclusion of fixed riprap toe support with full dam structures. This would help address several relevant research questions associated with placed ripraps. First of all, it would help validate the findings from model M1 with regards to stability increments achieved with the inclusion of fixed toe support and measurements of the applied load. Furthermore, comparison of findings from models M2 and M4 have revealed that introduction of throughflow within the model greatly influenced riprap stability. Hence, the

proposed tests would give a holistic picture of all interactions taking place within the dam structure.

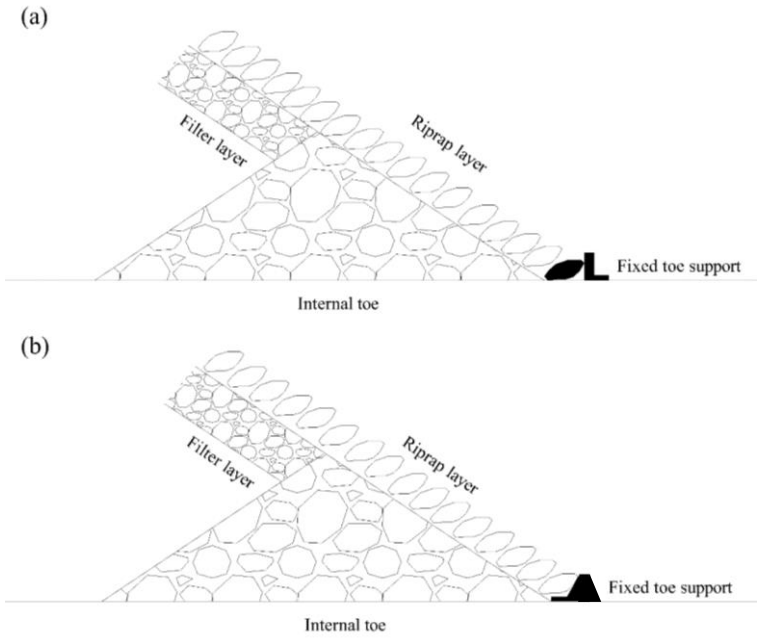

Figure 27. Rockfill dam model with placed riprap models coupled with fixed toe supports.

Fixed toe supports with load cells could be tested as part of the testing program. The most relevant configuration would be to add an 'L' shaped metallic toe support (Figure 27a), wherein the toe stone rests flat on the dam foundation and the subsequently placed stones are laid at incremental angles until an optimal angle of 60º is achieved. This is a practically applicable solutions as this would be suitable for installation with existing Norwegian placed ripraps that do not fulfill the stone criteria. However, the fixed toe support tested within M1 was of the form presented in Figure 27b, wherein the stones were placed at 60º inclination right from the toe support as the toe stone rests on a 60º angle provided by the metal surface. Although these two different support configurations perform similar functions, the inherent force transfer mechanisms would be different. At least one of those configurations a) or b) in Figure 27, should at least be tested. However, testing both of these two configurations would help in obtaining better understanding of the effects of these supports on riprap stability. Similar tests could also be conducted with dumped ripraps, but since previous studies have pointed out that toe support has negligible impact on dumped riprap stability or failure mechanism, these tests could be considered not imminent.

8.2. Evaluation of dynamic loading at riprap toe sections.

Results from the studies described within this technical report have clearly demonstrated the importance of toe support on riprap and rockfill dam stability. Looking further towards large scale implementation of such toe support for existing placed ripraps, a design criteria for such installations is of importance. The load generation patterns at the toe section of ripraps and in turn at the foundation would be highly dynamic owing to the nature of overflow forces. To have a better understanding of the load generation mechanisms at the foundation of ripraps would provide design criteria of importance for dimensioning of toe support structures. This is currently unavailable within international literature and also, within national dam safety guidelines.

As part of the experimental research conducted at NTNU, Trondheim, a series of overtopping tests were conducted on placed riprap models provided with load measuring pressure cells at the toe section (Figure 28). The accumulated data is yet to be analyzed as part of future research activities. The study objective would be to arrive at descriptions of the nature and the magnitude of flow forces generated at the toe section of placed ripraps as function of incremental overtopping exposure.

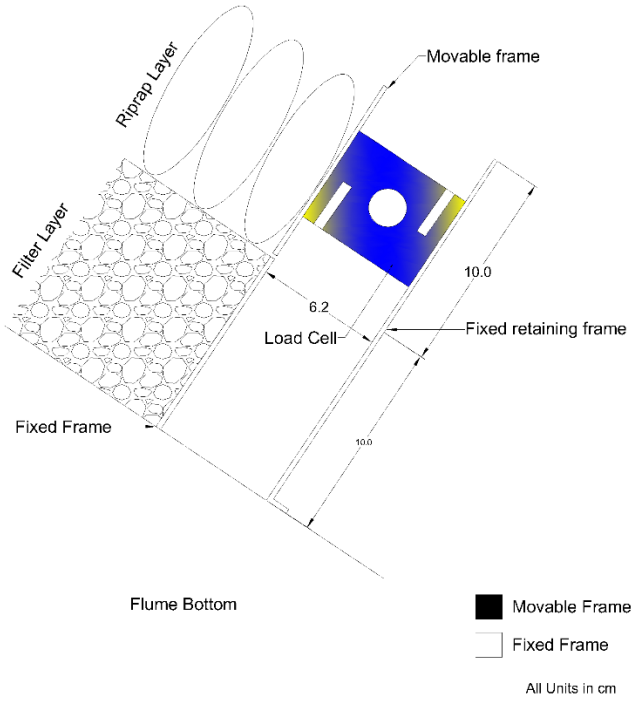

Figure 28. Model setup including load measurement cells at the toe section of placed ripraps.

8.3 Calibration of numerical tools to simulate flow through rockfill dams.

The experimental testing of rockfill dam models in laboratories is a time and resource demanding activity. Hence, recent research focus within the research discipline of hydraulic engineering is increasingly being placed on development, calibration and validation of numerical modeling tools. The ability to numerically model and in turn, predict the behavior of rockfill dams can greatly enhance ease of design of these structures. However, modeling of rockfill dam behavior under extreme throughflow and overflow scenarios is very challenging considering that the underlying processes involved are very intricate. Generation of good quality data from lab studies would be the only suitable way for further development of such models.

Data sets accumulated as part of M3 with regards to modeling of flow through rockfill dams to investigate the effects of different toe configurations on throughflow development are being further used as part of ongoing research. The aim of the investigation is to calibrate a widely used seepage model to predict flow through rockfill dams. Figures 29 and 230 present some of the outcomes from the study. The results appear to be promising with regards to the ability of the calibrated models to simulate throughflow development within the dam structures.

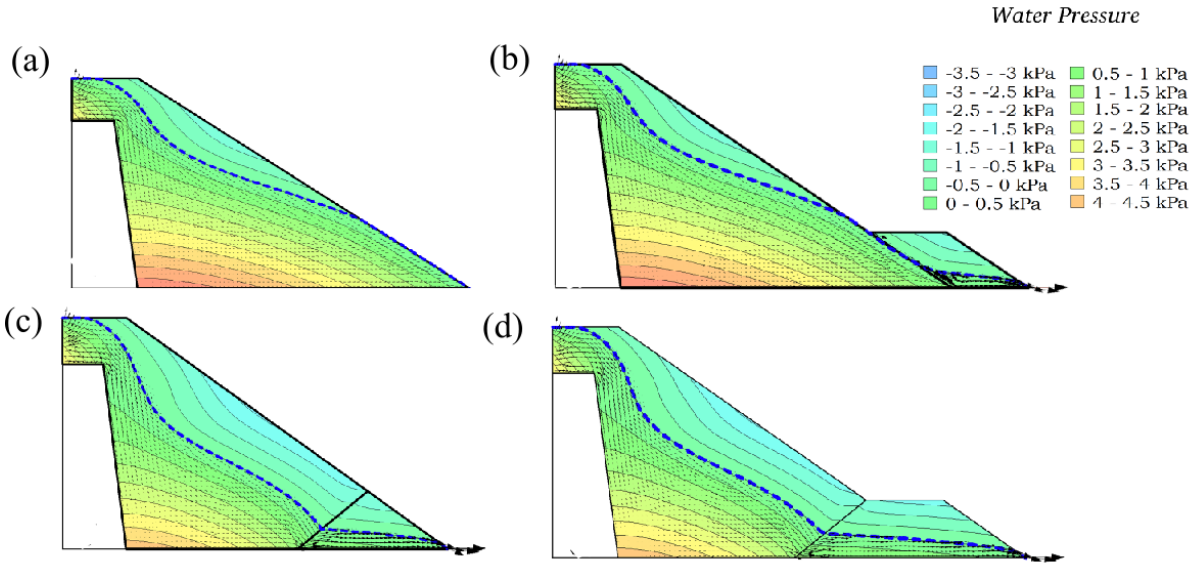

Figure 29. Simulation of flow through the different rockfill dam models. (Fig. Nils S Smith)

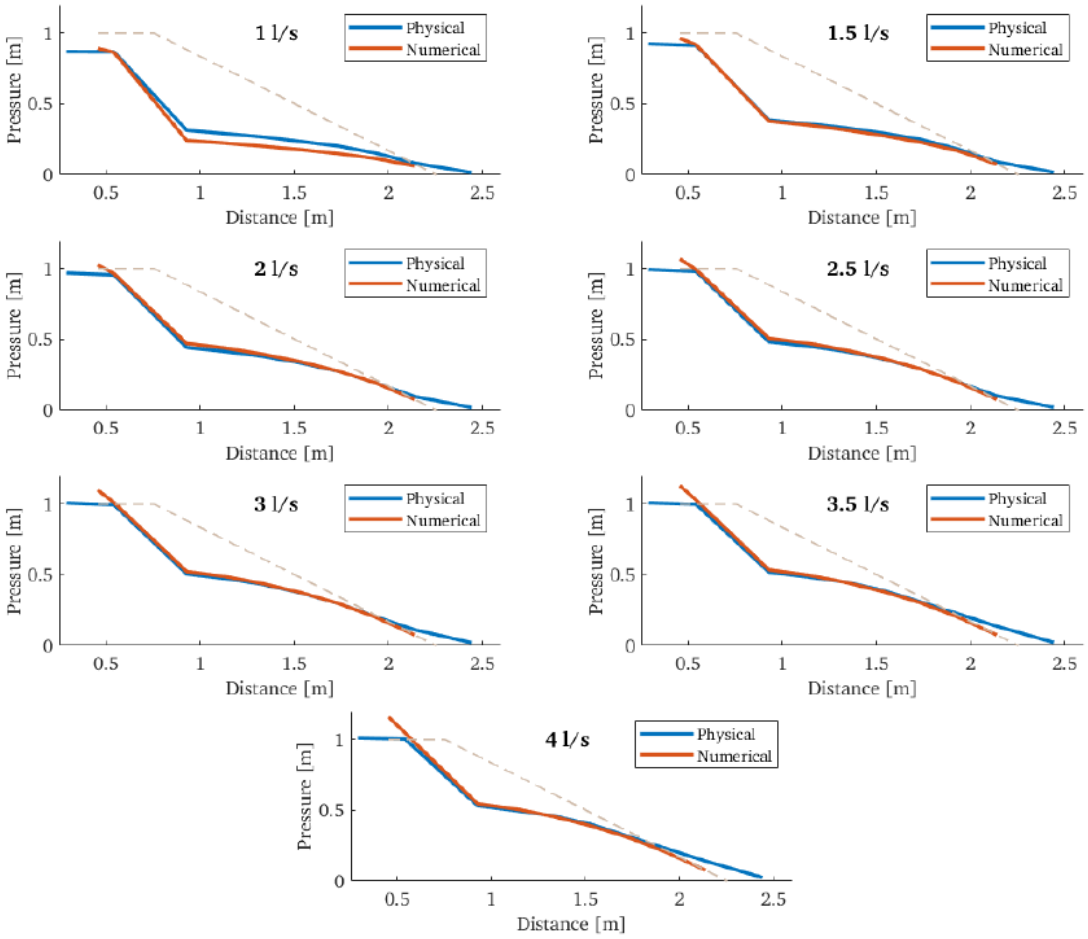

Figure 30. Comparison of physical observations with numerical predictions.

The models also were found to be capable of describing the effects of different toe configurations on throughflow development within the dams. Upon further refinement of the calibrations, the final outcomes from the study could be disseminated in the form of a technical publication.

8.4. Research on rockfill dam toes using numerical modeling

Investigation outcomes from M3 describe the effects various tested toe configurations can have on throughflow development within rockfill dams. To facilitate ease in constructing and carrying out the experimental studies, geometrically simple toe configurations such as equilaterally triangular and trapezoidal toe configurations were tested. This was since the idea behind the testing was to generate data sets for the calibration of numerical tools. But from a practical applicability standpoint, further refinement of the configurations would be necessary.

For instance, construction of a purely triangular toe would be practically very challenging due to the sharp nature of the tip of the toe.

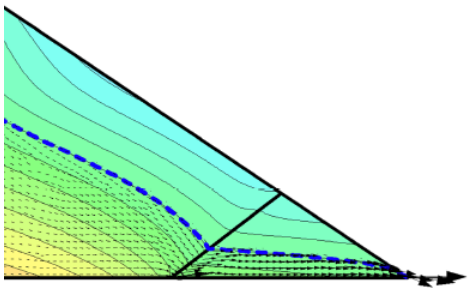

Figure 31. Depiction of the assumed triangular toe configuration.

Hence, arriving at toe configurations optimized both from hydraulic and practical applicability standpoints would be necessary. But, carryout out such elaborate tests in the laboratory would not be possible due to the highly resource intensive nature of experimental research with large models. Hence, the calibrated numerical model described in the earlier Section 8.3 could be put to use. Once the performance of the model is validated, it opens up possibilities for broad ranging numerical modeling of various toe configurations. A significant number of toe configurations can be tested for maximum throughflow and the performances can be ranked to arrive at ideal toe configurations considering hydraulic, practical and site-specific requirements.

It is also of interest to find appropriate numerical methods to model the erosion process. Calibrating such models to the experimental data will enable numerical experiments with dams of different heights and with different erosion protection downstream.

9 Concluding remarks

The aim of the research work, conducted in HydroCen and forming the basis for the PhD thesis of Ganesh H.R. Ravindra, has been to add to the state of the art on stability of rockfill dams exposed to extreme loading. Several experimental model studies, field surveys and statistical analysis were carried out. Research outcomes from the investigations present descriptions of hydraulic and structural behaviors of rockfill dams and or dam components under throughflow and or overtopping scenarios. These are further intended at facilitating development of design and construction methodologies thereby enhancing rockfill dam safety.

One of the primary findings from the HydroCen study is that toe supported placed ripraps constructed on steep slopes exposed to overtopping flows undergo buckling like 2D deformations, ultimately leading to riprap failure. A large-scale field survey of placed riprap built on nine Norwegian rockfill dams was conducted as part of the HydroCen study. The study helped document the fact that placed ripraps constructed on existing rockfill dams are not provided with well-defined toe support measures. Further, to achieve a more realistic picture of riprap stability, experimental overtopping tests were conducted on placed ripraps unsupported at the toe section. Study findings demonstrated sliding as the underlying failure mechanism in placed ripraps with unsupported toes. Placed ripraps with unrestrained toes on an average were found to suffer a fivefold reduction in stability, characterized by the critical overtopping magnitude as compared with placed ripraps provided with fixed toe supports. Furthermore, toe support conditions were found to have no effects on either the failure mechanism or the overall stability of dumped ripraps.

Throughflow data sets were accumulated from experimental studies conducted on homogeneous rockfill dams of sizes varying from 0.6 m to 6 m composed of uniform material as part of the IMPACT project. Subjecting the datasets to a statistical analysis, a general non-Darcy type power-law describing the non-linear relationship between throughflow velocities and gradient developments was derived. Further, experimental throughflow tests were conducted on 1:10 scale, 1 m high rockfill dam models coupled with different toe configurations as part of the HydroCen study. Investigation outcomes provide qualitative and quantitative descriptions of effects of internal, external and combined toe configurations on throughflow hydraulic properties.

The experimental research conducted as part of this research program to better understand placed riprap stability under overtopping conditions helps identify toe support conditions as an important parameter influencing overall placed riprap stability. This was also found to play a discerning role with regards to the underlying failure mechanism in placed ripraps. Coupling placed riprap structures with toe supports could result in significant stability gain and also lead to a predictable buckling like failure mode.

These findings are of particular significance considering outcomes from the field survey which suggests that existing placed ripraps are unsupported at the toe. Placed riprap construction is a more resource intensive activity as compared with dumped riprap construction. Further, multitude of rockfill dams are poised to be upgraded in the near future. Hence, arriving at

efficient design and construction methodologies to provide toe supports for placed ripraps could lead to large stability and economic gains. The planned research activities focusing on placed riprap stability will be aimed at addressing these issues.

Further, research works conducted as part of the HydroCen study investigating flow through rockfill dams improves our understanding of the interaction between throughflow and rockfill dams. The study also presents findings regarding the effects of disparate toe configurations on throughflow development. Ability to predict the response of rockfill dams when subjected to extreme throughflow conditions facilitates development of numerical modelling tools for dam breach predictions. Enhancement of capabilities of commercially available numerical seepage models could be of high interest for researches and also for agencies involved with rockfill dam design and safety assessment. Data sets collected as part of the various research works presented aim at supplementing development, calibration and validation of such numerical modelling tools as part of future investigations.

Bibliography

Abt, S R, & Thornton, C. I. (2014). Riprap Design for Overtopping – Man Do I Need a Martini! *World Environment and Water Resources Congress 2014*, *1936*, 1191–1198.

Abt, Steven R., Thornton, C. I., Scholl, B. A., & Bender, T. R. (2013). Evaluation of overtopping riprap design relationships. *Journal of the American Water Resources Association*, *49*(4), 923–937.

Abt, Steven R, Terry L, J., & Members, A. (1991). Riprap Design for Overtopping Flow. *Journal of Hydraulic Engineering*, *119*, 959–972.

Chang, H. H. (1998). Riprap Stability on Steep Slopes. In *International Journal of Sediment Research* (Vol. 13, pp. 40–49).

Cruz, P. T., Materon, B., & Freitas, M. (2009). *Concrete Face Rockfill Dams*. CRC Press.

Cruz, P. T., Materon, B., & Freitas, M. (2010). *Concrete Face Rockfill Dams*. CRC Press, Taylor and Francis Group.

Dornack, S. (2001). Uberstrombare Damme-Beitrag zur Bemessung von Deckwerken aus Bruchsteinen/ Overtopping dams-Design criteria for riprap. *PhD Thesis, Technische Universitat Dresden*.

EBL Kompetanse, A. (2003). *Stability and Breaching of Dams Report on Sub-Project 1 Shear Strength of Rockfill and Stability of Dam Slopes*.

EBL Kompetanse, A. (2006). *Stability and breaching of embankment dams, Report on Sub-project 2: Stability of downstream shell and dam toe during large through-flow*.

EBL Kompetanse, A. (2007). *Stability and Breaching of Embankment Dams Report on Sub-Project 3 (SP3) Breaching of Embankment dams*.

Engelund, F. (1953). On the laminar and turbulent flows of groundwater through homogeneous sand. *Trans. Dan. Acad. Tech. Sci., 3*, 1–105.

Escande, L. (1953). Experiments Concerning The Infiltration Of Water Through A Rock Mass. *Proceedings of the Minnesota International Hydro Convention*.

Ferdos, F., & Dargahi, B. (2016a). A study of turbulent flow in large-scale porous media at

high Reynolds numbers. Part I: numerical validation. *Journal of Hydraulic Research*, *54*(6), 663–677.

Ferdos, F., & Dargahi, B. (2016b). A study of turbulent flow in large-scale porous media at high Reynolds numbers. Part II: flow physics. *Journal of Hydraulic Research*, *54*(6), 678–691.

Ferdos, F., Worman, A., & Ekstrom, I. (2015). Hydraulic Conductivity of Coarse Rockfill used in Hydraulic Structures. *Transport in Porous Media*, *108*, 367–391.

Foster, M., Fell, R., & Spannagle, M. (2000). The statistics of embankment dam failures and accidents. *Canadian Geotechnical Journal*, *37*(1992), 1000–1024.

Frizeii, K. H., Ruff, J. F., & Mishra, S. (1998). Simplified Design Guidelines for Riprap Subjected To Overtopping Flow. *In Proceedings of the Annual Conference of the Assoc. Of State Dam Safety Officials.*, 301–312.

Garcia, D. (2011). A fast all-in-one method for automated post-processing of PIV data. *Experiments in Fluids*, *50*, 1247–1259.

Garga, V. K., Hansen, D., & Townsend, D. R. (1995). Mechanisms of massive failure for flowthrough rockfill embankments. *Canadian Geotechnical Journal*, *32*(6), 927–938.

Hansen, D., Garga, V. K., & Townsend, D. R. (1995a). Flowthrough Rockfill Embankments: Behavior in Subzero Temperatures. *Journal of Cold Regions Engineering*, *9*(December), 195–218.

Hansen, D., Garga, V. K., & Townsend, D. R. (1995b). Selection and application of a one-dimensional non-Darcy flow equation for two-dimensional flow through rockfill embankments. *Canadian Geotechnical Journal*, *32*(2), 223–232.

Hansen, D., & Roshanfekr, A. (2012). Assessment of Potential for Seepage-Induced Unraveling Failure of Flow-Through Rockfill Dams. *International Journal of Geomechanics*, *12*(5), 560–573.

Hansen, D., Zhao, W. Z., & Han, S. Y. (2005). Hydraulic performance and stability of coarse rockfill deposits. *Proceedings of the Institution of Civil Engineers, WM4*, 163–175.

Hiller, Priska H. (2017). Riprap design on the downstream slopes of rockfill dams,. *Doctoral Thesis, Norwegian University of Science and Technology, Trondheim*.

Hiller, Priska H, Aberle, J., & Lia, L. (2018). Displacements as failure origin of placed riprap on steep slopes. *Journal of Hydraulic Research*, *56*(2), 141–155.

Hiller, Priska H, Lia, L., & Aberle, J. (2019). Field and model tests of riprap on steep slopes exposed to overtopping. *Journal of Applied Water Engineering and Research*, *7*(2), 103–117.

Hiller, Priska Helene. (2016). *Kartlegging av plastring på nedstrøms skråning av fyllingsdammer*.

Hyllestad, E. (2007). *Retningslinjer for fyllingsdammer. Presentasjon under EBLs vårmøte 23.5.2007: Norges vassdrags- og energidirektorat.*

ICOLD. (1995). Dam Failures - statistical analysis. *Bulletin 99*, 73.

ICOLD. (2019). *World Register of Dams*.

Isbash, S. (1936). Construction of Dams by Depositing Rock in Running Water. *International Congress on Large Dams*.

Izbash, S. V. (1931). O filtracii v krupnozernistom materiale. *Izv. Nauchno Issled. Inst. Gidro-Tekh. (NILG)*.

Javadi, N., & Mahdi, T.-F. (2014a). Experimental investigation into rockfill dam failure initiation by overtopping. *Natural Hazards*, *74*, 623–637.

Javadi, N., & Mahdi, T. F. (2014b). Experimental investigation into rockfill dam failure initiation by overtopping. *Natural Hazards*, *74*(2), 623–637.

Khan, D., & Ahmad, Z. (2011). Stabilization of Angular-Shaped Riprap under Overtopping Flows. *World Academy of Science, Engineering and Technology, International Journal of Civil, Environmental, Structural, Construction and Architectural Enfineering*, *5*(11), 550–554.

Kiplesund, G. H., Ravindra, G. H. R., Rokstad, M. M., & Sigtryggsdottir, F. G. (2020). Effects of toe configuration on throughflow hydraulic properties of rockfill dams. *Journal of Applied Water Engineering and Research (Submitted)*.

Kjellesvig, H. M. (2002). *Stability and Failure Mechanisms of Dams, Data Report No. 1*.

Kjetil, V., Løvoll, A., Höeg, K., Morris, M., Hanson, G. J., & Hassan, M. A. (2004). Physical modeling of breach formation: Large scale field tests. *Preceedings Of Dam Safety*, 1–16.

Kobayashi, N., & Jacobs, B. K. (1985). Riprap Stability Under Wave Action. *Journal of Waterway, Port, Coastal, and Ocean Engineering*, *111*(3), 552–566.

Larese, A., Rossi, R., Oñate, E., Toledo, M. Á., Morán, R., & Campos, H. (2015). Numerical and Experimental Study of Overtopping and Failure of Rockfill Dams. *International Journal of Geomechanics*, *15*(4), 04014060.

Larsen, P., Bernhart, H. H., Schenk, E., Blinde, A., Brauns, J., & Degen, F. P. (1986). Uberstrombare Damme, Hochwasserentlastung uber Dammscharten/ Overtoppable dams, spillways over dam notches. *Unpublished Report Prepared for Regierungsprasidium Karlsruhe, Universita*.

Leps, T M. (1973). Flow through rockfill. *John Wiley and Sons*, 87–107.

Leps, Thomas M. (1975). Flow through rockfill: In Embankment-dam Engineering. In P. SJ & H. RC (Eds.), *John Wiley and Sons INC., Pub., NY, 1973, 22P* (Vol 12, No).

Lia, L., Vartdal, E. A., Skoglund, M., & Campos, H. E. (2013). Riprap protection of downstream slopes of rockfill dams-a measure to increase safety in an unpredictable future climate. *European Club Symposium of the International Comission on Large Dams*.

Marulanda, A., & Pinto, N. L. de S. (2000). Recent experience on design, construction, and performance of CFRD dams. In *Concrete Face Rockfill Dams* (pp. 279–299). Barry Cooke.

Midttømme, G. H., Isomäki, E., Meyer, A. E., & Bartsch, M. (2012). Regulations and guidelines for dam safety in Finland , Norway and Sweden. *ICOLD, European Club*.

Moran, R. (2015). Review of embankment dam protections and a design methodology for downstream rockfill toes. *Dam Protections against Overtopping and Accidental Leakage - Proceedings of the 1st International Seminar on Dam Protections Against Overtopping and Accidental Leakage*, 25–39.

Morán, R, & Toledo, M. A. (2011). Reserarch into protection of rockfill dams from overtopping using rockfill downstream toes. *Canadian Journal of Civil Engineering*, *38 (12)*(April), 1314–1326.

Moran, Rafael. (2015). Review of embankment dam protections and a design methodology for downstream rockfill toes. *Dam Protections against Overtopping and Accidental Leakage - Proceedings of the 1st International Seminar on Dam Protections Against Overtopping*

and Accidental Leakage, 25–39.

Morán, Rafael, Toledo, M. Á., Larese, A., & Monteiro-alves, R. (2019). *A procedure to design toe protections for rock fi ll dams against extreme through- fl ows*. *195*(May), 400–412.

Morris, M. W., & Park, H. (2007). Breach formation : Field test and laboratory experiments Formation d ' une brèche dans une barrage : Test sur le terrain et expériences en laboratoire. *Journal of Hyd. Research*, *45*(September 2011), 9–17.

NVE. (2012). Veileder for fyllingsdammer. *Norwegian Water Resources and Energy Directorate*, 21–25.

OED. (2009). *Forskrift om sikkerhet ved vassdragsanlegg (Damsikkerhetsforskriften). Oljeog energidepartementet.*

Olivier, H. (1967). Through and Overflow Rockfill Dams-New Design Techniques. *Proceedings of the Institution of Civil Engineers*, 433–471.

Parkins, A. K. (1963). Rockfill dams with inbuilt spillways. *Water Res. Edn. Aust., Bulletin No.6*.

Parkins, A. K. (1966). Rockfill structures subjected to water flow. *Journal of Soil Mech. Found. Div. ASCE*.

Peirson, W L, Figlus, J., Pelles, S. E., & Cox, R. J. (2008). Placed rock as protection against erosion by flow down steep slopes. *Journal of Hydraulic Engineering*, *134*(9), 1370–1375.

Peirson, William L, Jens, F., Steven E, P., & Ronald J, C. (2008). Placed Rock as Protection against Erosion by Flow down Steep Slopes. *Journal of Hydraulic Engineering*, *134*, 1370–1375.

Ravindra, G. H. R., Gronz, O., Dost, B., & Sigtryggsdottir, F. G. (2020). Failure mechanism in placed riprap on steep slope with unsupported toe. *Engineering Structures (In Review)*.

Ravindra, G. H. R., Sigtryggsdottir, F. G., Asbølmo, M. F., & Lia, L. (2019). Toe support conditions for placed ripraps on rockfill dams- A field survey. *Vann*, *3*.

Ravindra, G. H. R., Sigtryggsdottir, F. G., & Høydal, Ø. A. (2019). Non-linear flow through rockfill embankments. *Journal of Applied Water Engineering and Research*.

Ravindra, G. H. R., Sigtryggsdottir, F. G., & Lia, L. (2018a). Evaluation of Design Criteria for

Downstream Riprap of Rockfill Dams. *Proceedings of the 26th Congress on Large Dams*.

Ravindra, G. H. R., Sigtryggsdottir, F. G., & Lia, L. (2020). Buckling analogy for 2D deformation of placed ripraps exposed to overtopping. *Journal of Hydraulic Research*.

Ravindra, G. H. R., Sigtryggsdottir, F. G., & Lia, L. (2018b). Protection of embankment dam toe and abutments under overtopping conditions. *3rd International Conference on Protection against Overtopping, UK, June*.

Salahi, M.-B., AsI, M. S., & Parvizi, M. (2015). Nonlinear Flow through a Packed-Column Experiment. *Journal of Hydraulic Engineering, 20(9):0401*.

Sand, K. (2002). *Stabiliy and Failure Mechanisms of Dams, Sub Project No.2*.

Scheidegger, A. E. (1963). The physics of flow through porous media. *University of Toronto Press, Toronto, Canada*.

Siddiqua, S., Blatz, J. A., & Privat, N. C. (2011). Evaluating Turbulent Flow in Large Rockfill. *Journal of Hydraulic Engineering, 137*, 1462–1469.

Siddiqua, S., Blatz, J. A., & Privat, N. C. (2013). Evaluating the behaviour of instrumented prototype rockfill dams. *Canadian Geotechnical Journal, 50*, 298–310.

Sidiropoulou, M. G. (2007). Determination of Forchheimer equation coefficients a and b. *Hydrol Processes, 21(4)*, 534–554.

Siebel, R. (2007). Experimental investigations on the stability of riprap layers on overtoppable earthdams. *Environmental Fluid Mechanics, 7*(6), 455–467.

Sigtryggsdóttir, F. G., Snæbjörnsson, J. T., Grande, L., & Sigbjörnsson, R. (2016). Interrelations in multi-source geohazard monitoring for safety management of infrastructure systems. *Structure and Infrastructure Engineering, 12*(3), 327–355.

Solvik, O. (1991). Throughflow and stability problems in rockfill dams exposed to exceptional loads. *Sixteenth International Congress on Large Dams*, 333–343.

Sommer, P. (1997). Uberstrombare Deckwerke/ Overtoppable erosion protections. *Unpublished Report No. DFG-Forschungsbericht La 529/8-1, Universita*.

Soni, J. P., Islam, N., & Basak, P. (1978). An experimental evaluation of non-Darcian flow in porous media. *Journal of Hydrology, 38*(3–4), 231–241. https://doi.org/10.1016/0022-1694(78)90070-7

Thielicke, W. (2014). The flapping flight of birds Summary and Conclusions. *PhD Thesis, Rijksuniversiteit Groningen*.

Thielicke, W, & Stamhuis, E. . (2014). PIVlab - Time-Resolved Digital Particle Image Velocimetry Tool for MATLAB (version: 2.02). *Published under the BSD License, Programmed with MATLAB 7.0.246 (2014): R14*.

Thielicke, William, & Stamhuis, E. J. (2014). *PIVlab – Towards User-friendly , Affordable and Accurate Digital Particle Image Velocimetry in MATLAB*.

Thornton, C. I., Abt, S. R., Scholl, B. N., & Bender, T. R. (2014). Enhanced Stone Sizing for Overtopping Flow. *Journal of Hydraulic Engineering*, *140*(4), 06014005–.

Toledo, M. Á., & Morera, L. (2015). Design of overtopping-resistant rockfill dams. *Dam Protections against Overtopping and Accidental Leakage-2015*, 133–141.

Townsend, R. D., Garga, V., & Hansen, D. (1991). Finite difference modelling of the variation in piezometric head within a rockfill embankment. *Canadian Journal of Civil Engineering*, *18*(2), 254–263.

Venkataraman, P., & Rama Mohan Rao, P. (1998). Darcian, transitional and turbulent flow through porous media. *Journal of Hydraulic Engineering*, *124*, 840–846.

Wang, C. M., & Wang, C. Y. (2004). *Exact solutions for buckling of structural members* (Volume 6). CRC Press.

Wilkins, J. K. (1955). Flow of water through rockfill and its application to design of dams. *New Zealand Engineering*, *01*, 382–387.

Wilkins, J. K. (1963). *The stability of overtopped rockfill dams*.

Worman, A. (1993). Seepage induced mass wasting on coarse soil slopes. *Journal of Hydraulic Engineering*, *119*(10), 1155–1168.

Zech, Y., & Soares-Frazao, S. (2007). Dam-break flow experiments and real-case data. A database from th European Impact research. *Journal of Hydrauli Research*, *45*, 5–7.

Zingg, T. (1935). *Beitrag Zur Schotteranalyse, Doctoral Thesis, ETH Zurich*.

NVE

Norwegian Water Resources and Energy Directorate

MIDDELTHUNS GATE 29
P.O. BOX 5091 MAJORSTUEN
N-0301 OSLO
NORWAY
TELEPHONE: (+47) 22 95 95 95

www.nve.no